Tuning Polymeric Latex Functionality via The Miniemulsion Technique



Dissertation
Zur Erlangung des Doktorgrades Dr. Rer. Nat.
der Falkutät für Naturwissenschaften
der Universität Ulm

vorgelegt von
Daniel Crespy
aus Rennes, Frankreich
Ulm, 2006

Amtierender Dekan: Prof. Dr. K.-D. Spindler

1. Gutachter: Prof. Dr. K. Landfester

2. Gutachter: Prof. Dr. N. Hüsing

Tag der Promotion: 1 Dezember 2006

Universität Ulm, Fakultät für Naturwissenschaften, 2006

Table of contents

1. INTRODUCTION……...…7

2. THEORETICAL SECTION…….....……..…11

2.1. Heterophase polymerizations……...……...12

2.1.1. The different types of polymerization…….12

2.1.1.1. Chain-growth polymerization……...……...12

2.1.1.2. Step-growth polymerization…….....13

2.1.2. Polymerizations in dispersion…….13

2.1.3. The Ouzo effect and the solvent displacement technique……...…16

2.1.4. The miniemulsion polymerization……..16

2.1.4.1. Principle of the miniemulsion polymerization technique……..……..16

2.1.4.2. Stability of the miniemulsion..…..……...…18

2.2. The free-radical polymerization in miniemulsion……..…19

2.2.1. Free-radical polymerization in direct miniemulsion……...19

2.2.2. Free-radical polymerization in inverse miniemulsion…….19

2.2.3. Copolymerization in heterophase systems……..20

2.3. Anionic miniemulsion polymerization……...22

2.3.1. Anionic miniemulsion polymerizations……..……22

2.3.2. Anionic heterophase polymerization of lactams…….23

2.4. Miniemulsion polycondensation and polyaddition……...23

2.4.1. Step-growth polymerizations in miniemulsion……...23

2.4.2. Interfacial polycondensation in miniemulsion……....24

3. RELEVANT METHODS FOR CHARACTERIZATION…….26

3.1. Light Scattering……27

3.2. Electron microscopy (TEM, SEM)…….28

3.2.1. The scanning electron microscope……..28

3.2.2. The transmission electron microscope……30

4. RESULTS AND DISCUSSION…….31
4.1. Free-radical polymerization in miniemulsion……...32
4.1.1. Free-radical polymerization in direct miniemulsion ……..32
4.1.1.1. Free-radical polymerization in direct miniemulsion in the presence of a solvent in the dispersed phase…….…32
4.1.1.2. Free-radical polymerization in the presence of metal complexes in direct miniemulsion…….……38
4.1.1.3. Free-radical polymerization initiated by borohydrides in direct miniemulsion…...…46
4.1.1.4. Free-radical copolymerization with a surfactant in direct miniemulsion…….....50
4.1.2. Free-radical polymerization in inverse miniemulsion…….....59
4.1.2.1. Miniemulsion polymerization at high temperature……..59
4.1.2.2. Synthesis of nanocapsules via inverse free-radical miniemulsion polymerization…..69
4.2. Anionic polymerization of lactams in miniemulsion and synthesis of polyamide latexes……...…70
4.2.1. Anionic polymerization of ε-caprolactam……...71
4.2.2. Synthesis of polyamide 6 nanoparticles and nanocapsules via two miniemulsion/ solvent displacement techniques…….……..79
4.3. Polycondensation in miniemulsion systems……...…89
4.3.1. Polyamide latexes in miniemulsion polycondensation……...89
4.3.1.1. Tentative synthesis of polyamide latexes in direct miniemulsion at low temperature……....89
4.3.1.2. Tentative synthesis of polyamide latexes at low temperature in an inverse system....90
4.3.1.3. Tentative synthesis of polyamide latexes at higher temperature…….91
4.3.2. Polyurea and polyurethane latexes in miniemulsion polycondensation…….92

5. CONCLUSION AND PERSPECTIVES…….117

6. EXPERIMENTAL PART……122

6.1. Miniemulsion free-radical polymerization……..123
6.1.1. Free-radical polymerization in direct miniemulsion…….123
6.1.1.1. Free-radical polymerization in direct miniemulsion in the presence of a solvent in the disperse phase…….…123

6.1.1.2. Free-radical polymerization in the presence of metal complexes in direct miniemulsion……...123
6.1.1.3. Free-radical polymerization initiated by borohydrides in direct miniemulsion…….124
6.1.1.4. Free-radical copolymerization with a surfactant in direct miniemulsion……...125
6.1.2. Free-radical polymerization in inverse miniemulsion……...125
6.1.2.1. Miniemulsion polymerization at high temperature……125
6.1.2.2. Synthesis of capsules with hydrophilic liquid core via radical miniemulsion polymerization……126
6.2. Anionic polymerization of lactams in miniemulsion and synthesis of polyamide latexes…….127
6.2.1. Anionic polymerization of ε-caprolactam……127
6.2.2. Synthesis of polyamide 6 nanoparticles and nanocapsules via two miniemulsion/ solvent displacement hybrid techniques……...……..129
6.3. Polycondensation in miniemulsion……...130
6.3.1. Polyamide latexes in miniemulsion polycondensation……130
6.3.1.1. Tentative synthesis of stable polyamide latexes by direct miniemulsion polycondensation at low temperature……..…131
6.3.1.2. Tentative synthesis of stable polyamide latexes by inverse miniemulsion polycondensation at low temperature ……131
6.3.1.3. Tentative synthesis of stable polyamide latexes by miniemulsion polycondensation at higher temperature ……132
6.3.2. Polyurea and polyurethane latexes in miniemulsion polycondensation……...132

7. APPENDIX……135

7.1. Methods……...136
7.2. Abbreviations……..…140
7.3. Symbols……...…142

ACKNOWLEDGEMENTS…….143

REFERENCES……..147

ZUSAMMENFASSUNG UND AUSBLICK……...……158

1. Introduction

There was no "before" the beginning of our universe, because once upon a time there was no time.

John D. Barrow (1952 - /)
American professor in the department of Applied Mathematics & Theoretical Physics, Cambridge University.

A lot of efforts, either in academic or industrial research, are focusing on the design of new polymers with superior properties compared to the old ones, or the improvement of known polymers or processes. Industrially, the first possibility involves strong investments to start creating some niches, which eventually become new markets. The second possibility needs less investment but serious profits are generated only through huge mass production. Heterophase polymerization is well established in the plastics industry since it benefits of interesting advantages such as the good heat exchange with the surrounding medium and the decrease of the viscosity compared to the bulk process. In the brilliant review "90 Years of Polymer Latexes and Heterophase Polymerization: More vital than ever" [**Ant**_2003], Tauer and Antonietti deal with what they call "the most obvious candidates with blockbuster character". Among them, there are the "dispersions of engineering plastics". In the different dispersion polymerization techniques, the miniemulsion technique is the most promising one. Indeed, the miniemulsion droplets realize the concept of exceptionally stable nanoreactors. The miniemulsion is hence naturally inscribed in the growing field of the nanoscience but also has the potential to provide suitable materials for drug-delivery systems. Active research related to the miniemulsion technique is currently exponentially sustained [**SCO**_2005]. Despite the recent advances in the miniemulsion technique concerning miniemulsion of inorganic particles and dyes, almost every document concerning miniemulsion still deals with the synthesis of polymer latexes and the trend is even the increase of this proportion [**ISI**_2005]. Among the reported polymerizations, free-radical polymerization is the most used technique. Controlled radical polymerization in miniemulsion has become recently a significant topic for miniemulsion. Especially, the RAFT (Radical Addition Fragmentation Transfer) [**DeB**_2000] and the controlled radical polymerizations by the nitroxides [**Lans**_2000] play an important role. Finally, non-radical polymerizations in miniemulsion are seldom reported and they concern mainly the polyaddition and the anionic polymerization. The work on polyurethane latexes in miniemulsion initiated by Landfester found a significant echo [**Tia**_2001]. The causes may be the versatility of the technique and the industrial importance of the polymer. Ganachaud underlined in a recent publication that although the miniemulsion was applied for the synthesis of polycondensate, there was no literature concerning the synthesis of polyamide in miniemulsion [**Gan**_2005]. The polyamides, and especially those belonging to the nylon family are competitive materials, which are used since long time in the everyday life.

Finally, the proportion of research articles dealing with encapsulation via the miniemulsion process increased a lot in recent time [**ISI2**_2005]. It is indicative of the current trend where

more complex materials such as hybrid or composite latexes are synthesized. It is therefore very important to sustain active research in miniemulsion polymerization to create new nano-objects with different structures via known synthesis. A perfect nano-object would be a highly functional object (thus of high added value), which is industrially convenient to produce via an environmentally responsible process.

We deliver in this thesis some contributions to help obtaining these materials in miniemulsion. Our purpose was to show the polyvalence of the miniemulsion technique for the synthesis of nanomaterials with very different reaction conditions. This wide range of reaction conditions includes different types of polymerization; namely radical, anionic, and condensation polymerizations; and the use of high temperatures and unconventional initiators. We showed that such a wide range of polymerizations can be easily performed in miniemulsion whereas no other dispersion processes are as polyvalent.

We investigated unconventional free-radical polymerizations in direct and inverse miniemulsions. First, we showed that the morphology of the final latex can be easily controlled by the ratio of monomer to hydrophobic solvent in direct miniemulsion for a given system. Secondly, hybrid metal/ polymer latexes were synthesized in direct miniemulsion. We encapsulated efficiently hydrophobic metal complexes in polystyrene particles matrix in an one-pot process. These hybrid particles were then deposited on silicon substrates as ordered monolayer, and were subsequently submitted to plasma-etching. The plasma-etching allowed the simultaneous removal of the polystyrene and the reduction of the metal complex to yield ordered metal clusters on the surface. The distance between the metal clusters was controlled by the diameter of the metal/ polymer particles. Thirdly, we also synthesized polymer particles with borohydrides salts as new radical initiators. They are as cheap as typically used azo-initiators but have a lower temperature for comparable conversion. As a fourth topic, we copolymerized styrene and divinylbenzene with a polymerizable surfactant or surfmer in direct miniemulsion. The surfmer remained on the particles after dialysis, showing that the surfmer was efficiently grafted onto the polystyrene particles.

Fifth, we studied miniemulsion free-radical polymerization at high temperature (>100 °C). High temperature involves a faster polymerization and lower the cycle time of the industrial polymerization processes, and therefore the cost of these systems. Whereas other heterophase polymerizations involve strong diffusion of species during their process, diffusion in miniemulsion polymerization with dispersed phase-soluble initiator is very limited. We could show that the addition of a second stabilizer in miniemulsion at high temperature allow the system to be stable for very long time.

We present a method to make nanocapsules with a simple vinyl monomer in inverse miniemulsion. The polymeric shell is able to encapsulate hydrophilic compounds, which is extremely seldom reported in the literature.

Then we also investigated the synthesis of nylons in miniemulsion with the goal of combining the versatility of the miniemulsion technique with the good properties of the nylon material.

The potential of the anionic polymerization of lactams in miniemulsion was shown, and especially the synthesis of the most produced synthetic polyamide; nylon 6. We synthesized the first nylon 6 nanoparticles via two methods: a standard inverse miniemulsion procedure and a miniemulsion/ solvent displacement technique. The first method led to polyamide 6 nanoparticles with less structural irregularities than the one produced in bulk. The second method led to polyamide/ polyvinyl alcohol core-shell particles.

Finally, we report on the synthesis of polyurethane, polyurea and polythiourea via interfacial polycondensation in miniemulison. Particles and capsules could be synthesized depending on the experimental conditions. Polyurea capsules were subsequently used as nanoreactors for the reduction of silver nitrate in silver nanoparticles in the hydrophilic core of the capsules.

2. Theoretical section

When you take stuff from one writer it is plagiarism; but when you take it from many writers, it is research.

Wilson Mizner (1876-1933)
American author.

2.1. Heterophase polymerizations

2.1.1. The different types of polymerization

Polymerizations are classified in two major classes depending on their mechanism: the step-growth polymerizations and the chain-growth polymerizations [**Odi**_1991]. The latter mechanism is responsible for the production of major commodity and technical polymers such as polyethylene, polypropylene, polystyrene, poly(vinyl chloride) and poly(methyl methacrylate). The step-growth polymerization is used to produce polyesters, polyamide, polyurethane, polysiloxanes and polycarbonates. But more importantly, most of the natural polymers are synthesized via the step-growth mechanism.

2.1.1.1. Chain-growth polymerization

In chain-growth polymerization, one monomer is added to the growing chain at a time. Chain-growth polymerization comprises free-radical, anionic, cationic and living radical polymerizations. The resulting polymer has different properties depending on their polymerization technique. Thus, it is possible to obtain polymer chains with controlled molecular weight and polydispersity by the so-called living polymerizations as shown in Figure 1. Cationic and anionic polymerizations give usually good control on the molecular weight. Nevertheless, they are limited to certain monomers and the experimental conditions are demanding. Current macromolecular research hence focuses on the controlled radical polymerizations, which have the advantages of the living technique with mild experimental conditions. The most investigated controlled radical polymerization techniques are for the moment the ATRP (Atom Transfer Radical Polymerization), the RAFT (Radical Addition Fragmentation Transfer) and the NMP (Nitroxides Mediated Polymerization) [**Mat**_2000].

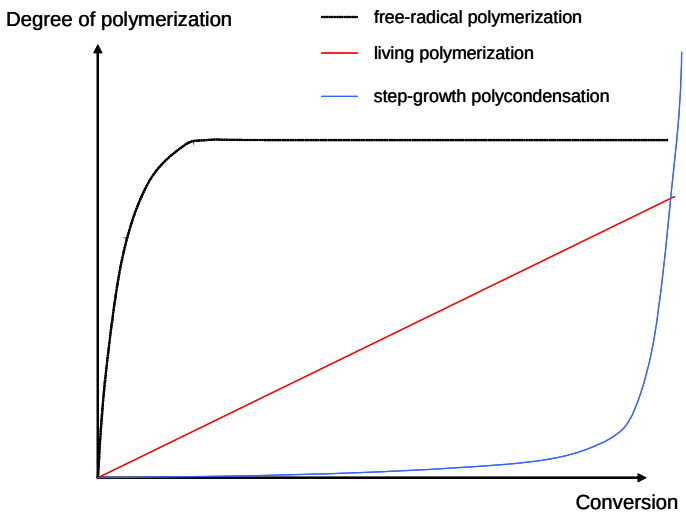

Figure 1. Typical aspects of the degree of polymerization versus conversion curves for different polymerization techniques.

2.1.1.2. Step-growth polymerization

In step-growth polymerizations, two reactants with distinct or same degree of polymerization combine to form their respective polymer. Step-growth polymerizations are either called polycondensation or polyaddition respectively depending on the formation or not of molecules other than the polymer as polymer is formed. Similarly to the chain-growth polymerization, researchers developed different techniques to obtain controlled polycondensation [**Voi**_2000].

2.1.2. Polymerizations in dispersion

Heterophase polymerizations are described as processes resulting in finely dispersed polymer particles in a continuous phase [**Ant**_2003]. The heterophase involves the coexistence of different phases separated by interfacial static or dynamic boundaries depending on the process. Among these combinations of phases, only the combination gas in gas cannot be made. However, the material forming the dispersed phase should be in majority insoluble or immiscible in the continuous phase. It is then possible to perform reactions in the heterophase system, especially polymerizations. Heterophase polymerizations occur when a monomer partially or completely building the dispersed phase is polymerized in a heterophase system. The most important groups of heterophase polymerizations comprise the suspension, dispersion, precipitation, emulsion, microemulsion and miniemulsion polymerizations. All these processes are differentiated by their mechanisms of polymerization and their mechanisms of stability. They require different dispersing techniques and yield a final product

with different sizes as shown in Table 1. Let us notice that the amount of surfactant in Table 1 is given in wt.% compared to the dispersed phase. A microemulsion system is created when a certain amount of surfactant or surfactant/ cosurfactant mixture is used to form a spontaneous thermodynamically stable emulsion. Such systems require a high amount of surfactant and thus lead to an interfacial tension between the two liquid phases close to zero. In the microemulsion polymerization, the initiation does not occur in the same time in all microdroplets leading to a final state containing polymer particles in coexistence with empty micelles. However, a microemulsion with discrete droplets is realistic only for low fraction volume of the dispersed phase. In the macroemulsion polymerization process, empty or monomer-swollen micelles and big monomer droplets with diameter d ~ 1-10 μm are present in the initial state. The initiator is dissolved in the continuous phase and thus reacts with the monomer molecules dissolved in the continuous phase, building oligoradicals. In most of the macroemulsion polymerization systems, the nucleation mechanism is the so-called micellar nucleation. Because the surface offered by the micelles is much larger than the surface offered by the monomer droplets, the oligoradical migrates into the micelles in majority. The monomer diffuses through the continuous phase from the reservoir droplets to the micelles. The polymer growth inside the micelles finally leads to the particles. The miniemulsion and the suspension polymerization processes form almost a 1:1 copy from the initial droplets to the polymer particles. The essential difference between the two techniques is the size of the droplets, the shearing process used but also the fact that the initiator can be only in the dispersed phase in the case of suspension polymerization [**Lan**_2001]. In miniemulsion polymerization, the initiator can be in the dispersed phase or the continuous phase. Finally, the dispersion process is a particular system since on the contrary to the other processes, the initial state is homogeneous. Indeed, the monomer is soluble in the continuous phase and micron-sized aggregates are only formed during the polymerization.

Table 1. Characteristics of some dispersion polymerization processes.

Process	Shearing and stabilization	Initiator locus	State of the system	
			Initial	Final
Microemulsion polymerization	weak shearing before polymerization surfactant >10 wt.%	dispersed or continuous phase	micelles d~5-10 nm	particles d~5-50 nm + micelles d~5-10 nm
	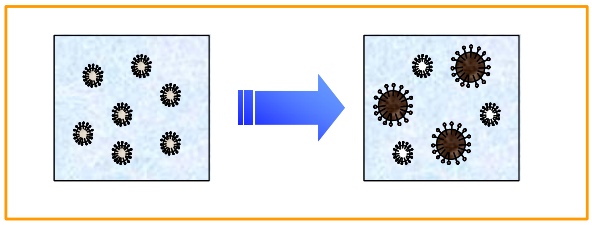			
Macroemulsion polymerization	mechanical agitation during polymerization surfactant, stabilizer	continuous phase	reservoir droplets d~1-10 μm + micelles d~5-10 nm	particles d~50-1000 nm
	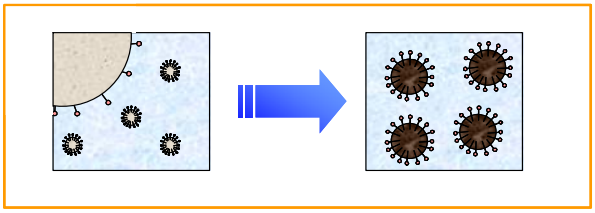			
Suspension polymerization	mechanical agitation during polymerization stabilizer	dispersed phase	~ same states droplets, particles d~10-100 μm	
	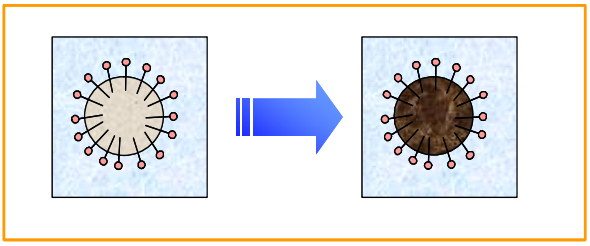			
Miniemulsion polymerization	sonicator, homogenizer before polymerization	dispersed or continuous phase	same states droplets, particles d~50-500 nm	
	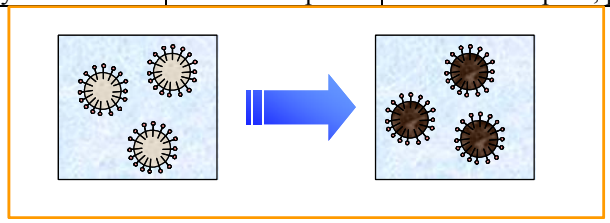			
Dispersion polymerization	mechanical agitation during polymerization stabilizer	continuous phase	homogeneous state	Particles d~1-5 μm
	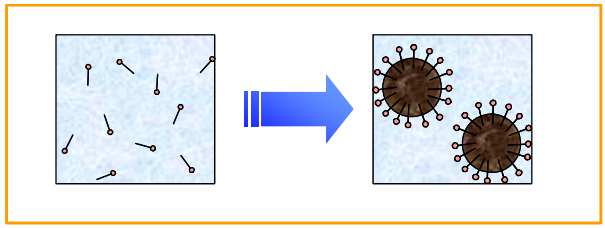			

2.1.3. The Ouzo effect and the solvent displacement technique

Polymer latexes can be also done using the so-called Ouzo effect. The preparation of such latexes is performed by spontaneous droplet formation followed by polymer synthesis or precipitation [**Gan**_2005]. In practice, spontaneous emulsification in water is done upon pouring a solution of oil and hydrophilic solvent in a large amount of water. Upon mixing with water, the oil droplets are nucleated because of the supersaturation of the oil. The oil diffuses to the other droplets yielding a decrease of the supersaturation. No further nucleation occurs and an emulsion is obtained as shown in Figure 2. The solid content obtained with the Ouzo effect is very low and is often increased by subsequent evaporation of the solvents.

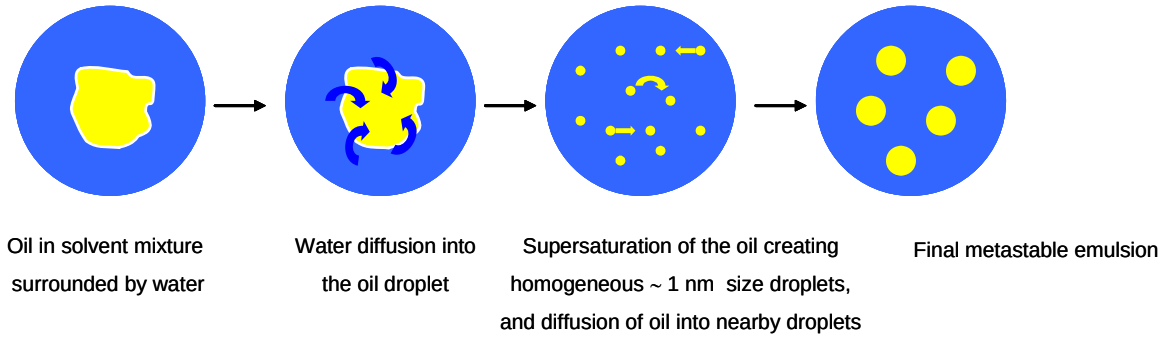

Figure 2. Principle of the Ouzo effect [**Gan**_2005].

In the case of the solvent displacement technique, both bimodal and spinodal decomposition can be observed depending on the concentrations. In the special case of the Ouzo effect, only bimodal decomposition occurs by bringing the composition between the bimodal and spinodal lines in a phase diagram.

2.1.4. The miniemulsion polymerization

2.1.4.1. Principle of the miniemulsion polymerization technique

A miniemulsion polymerization is performed upon shearing a mixture containing two immiscible liquid phases, one containing or being the monomer, a surfactant and an osmotic pressure agent. Droplets with sizes ranging from 30 to 500 nm are obtained, which can be subsequently polymerized without significant change in their identity and number as shown in Figure 3. The system is called a “direct miniemulsion” if the dispersed phase is hydrophobic and an “inverse miniemulsion” if the dispersed phase is hydrophilic. Some parrticular

miniemulsion polymerization systems can allow a fluorophilic monomer to be dispersed in a fluorophobic continuous phase or vice-versa. The droplet size is easily tuned by varying the amount and the type of the surfactant as shown in Figure 4 [**Bec**_2000].

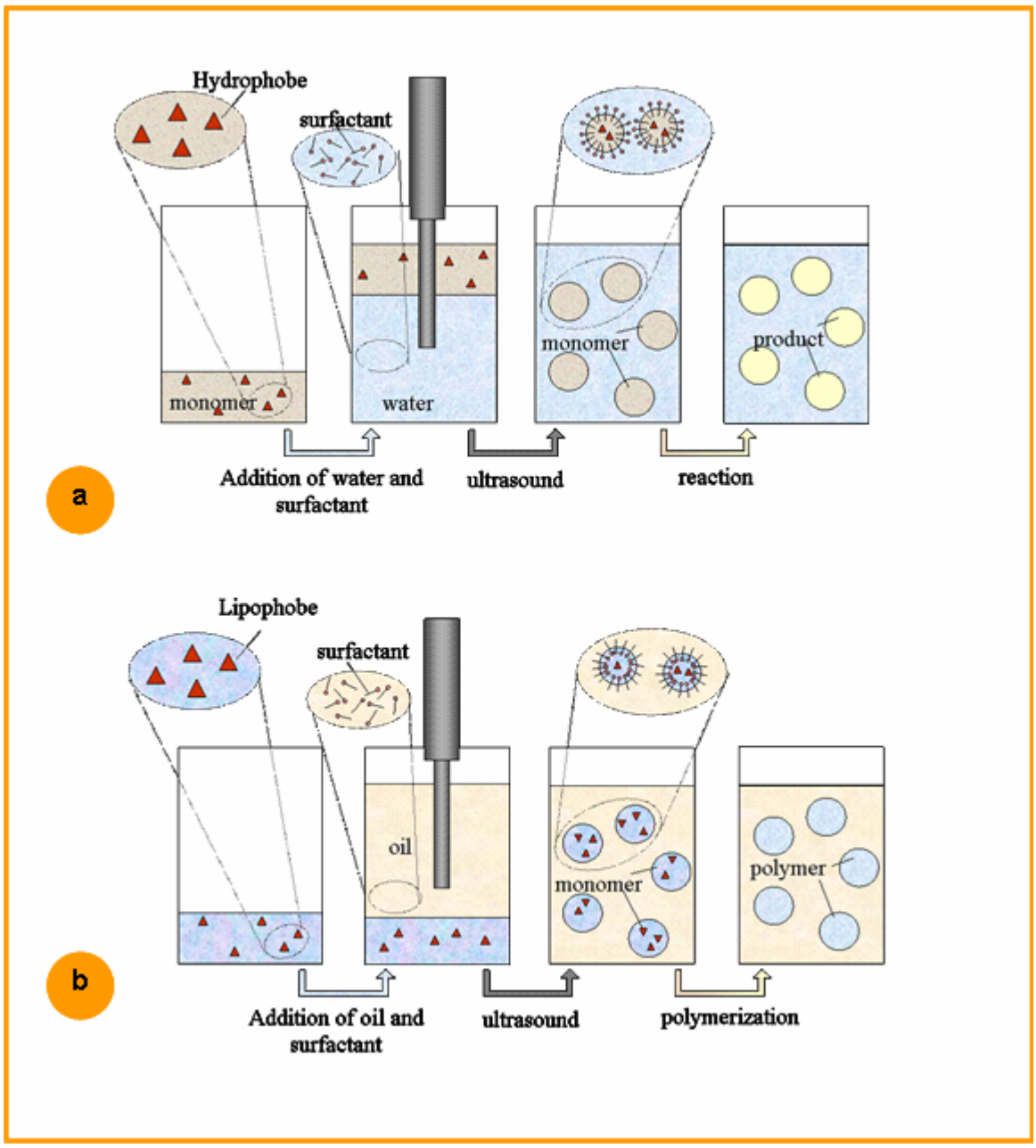

Figure 3, a-b. Principle of the miniemulsion polymerizations, **a** direct miniemulsion, **b** inverse miniemulsion.

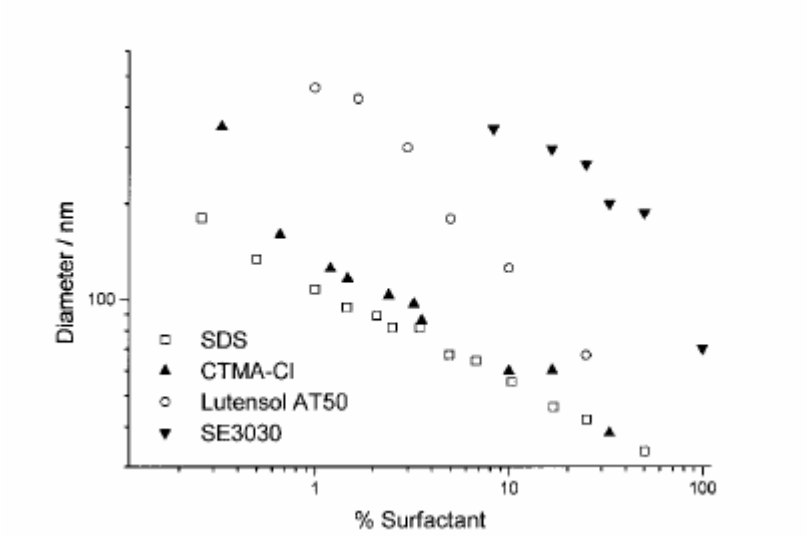

Figure 4. Variation of the particle size with the amount and type of the surfactant in miniemulsion polymerization of styrene. Figure taken from reference [**Bec**_2000].

2.1.4.2. Stability of the miniemulsion

The size of the droplets is given by the rate of collision involving the ultrasound or high-pressure homogeneization fission and the droplet´s fusion. Upon such conditions, the minimum size of droplets is performed for a certain amount of stabilizer. Miniemulsion are then stabilized against collisions between the droplets by the use of stabilizers, which can be surfactants [**Lan**_2001], polymeric stabilizers [**Kim**_2003], or inorganic stabilizers [**Tia2**_2001]. The miniemulsions are additionally stabilized against Ostwald ripening by the addition of an osmotic pressure agent [**Lan2**_2000], [**Sch**_2005]. The role of the osmotic pressure agent is to compensate an off-balance of the osmotic pressure as shown in Figure 5. Consequently, the osmotic pressure agent should have a very low solubility in the continuous phase to be efficient. A convenient name for the osmotic pressure agent is hydrophobe or ultrahydrophobe in direct miniemulsions and lipophobe in inverse miniemulsions.

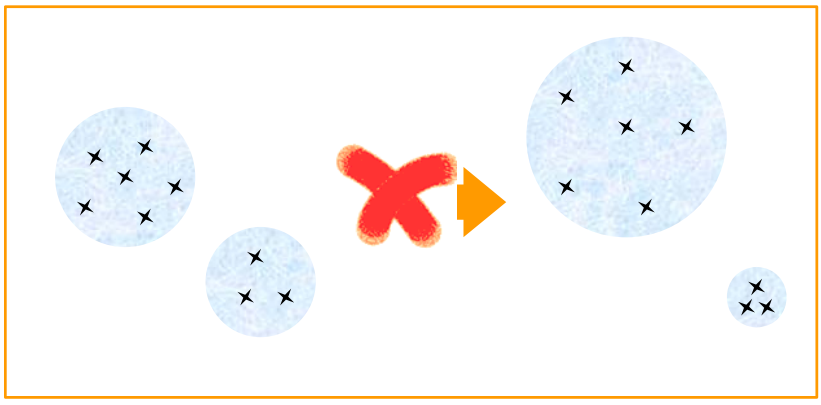

Figure 5. The addition of the osmotic pressure agent suppresses the growth of the droplets by Ostwald ripening.

Usually, the growth of the minidroplets takes place on a much greater time scale compared to the polymerization time. This means that the miniemulsion provides a situation very close to 1:1 copy of the monomer droplets to the polymer particles as proved by a small angle neutron scattering (SANS) experiment [**Lan**_1999].

Hence, compared to the other heterophase techniques, the miniemulsion is a very stable system, which offers an incomparable flexibility to create polymeric nanoparticles. In fact, the initiation can be realized either in the dispersed phase or in the continuous phase. And maybe more importantly, the miniemulsion stability should not be seriously affected by the temperature since transport processes do not occur between the droplets.

2.2. The free-radical polymerization in miniemulsion

2.2.1. Free-radical polymerization in direct miniemulsion

A cornucopia of documents was addressed to the mode of nucleation of the miniemulsion droplets. It was concluded that, if the miniemulsion is efficiently stabilized against Ostwald ripening, the predominant nucleation is the droplet nucleation. Bechthold and Landfester showed that the maximum reaction speed is strongly dependent on the particle size if the initiator is soluble in the continuous phase [**Bec2**_2000]; i.e. the droplets are polymerized faster when they are smaller. The miniemulsions with large droplets have a reaction profile similar to the macroemulsion, whereas the reaction profile of the miniemulsion with small droplets was similar to a microemulsion kinetics. Miniemulsions with intermediate particle sizes display a mixture of the two mechanisms.

A lot of hydrophobic monomers can be polymerized in direct miniemulsion. However, most of the papers are related to the polymerization of styrene, (meth)acrylates, or vinyl acetate for industrial reasons. Because of the mechanism of the miniemulsion polymerization, it was even possible to polymerize very hydrophobic monomers such as fluorinated monomers without the use of carrier materials [**Lan**_2002]. Moreover, polymerization of styrene in non-aqueous direct miniemulsion systems were also successfully performed [**Lan3**_2000].

2.2.2. Free-radical polymerization in inverse miniemulsion

Radical polymerizations can also be performed in inverse miniemulsion systems. Hydrophilic monomers such as hydroxyethyl(meth)acrylate, acrylic acid or acrylamide, are miniemulsified

in a non-polar media and then subsequently polymerized [**Lan3**_2000]. The non-ionic amphiphilic poly(ethylene-*co*-butylene-*b*-ethylene oxide) was found to be a suitable surfactants to stabilize efficiently the miniemulsion droplets.

2.2.3. Copolymerization in heterophase systems

The copolymer composition and structure can be predicted by the copolymer equation, which is dependent on the monomer reactivity ratios. But it has to be reminded that monomer reactivity ratios are generally, but not always, independent of the reaction medium in radical copolymerization [**Odi**_1991]. Wu and Schork investigated the direct macroemulsion and miniemulsion copolymerization of two monomers with different monomer reactivity ratios and water solubility. It was found that the miniemulsion obeyed the integrated Mayo-Lewis equations whereas the macroemulsion system did not [**WuX**_2000]. Because of the difference of the solubility of the two monomers, the comonomer feed composition at the reaction site in macroemulsion (micelle) is different from that in the bulk of the reaction system.

Willert et al. investigated the copolymerization of the polar monomer acrylamide, and one non-polar monomer (styrene, methyl methacrylate) in direct and inverse miniemulsion [**Wil**_2002]. The locus of initiation has a preponderant significance on the structure of the final copolymers. The lowest extent of homopolymers and of blockiness for the AAm/MMA copolymer occurred when the initiation was done in the continuous phase in an inverse system. For the AAm/styrene copolymer, the best results were obtained with an interfacial initiation in inverse miniemulsion (see Figure 6). It can be concluded that the copolymer structure is highly dependent on the reaction medium and on the type of initiation. The classical copolymerization equation is insufficient to predict correctly the copolymer composition. Thus, a good model should take into account the surface tension forces and the respective polarity of the monomers and the polymers [**Kuc**_2005].

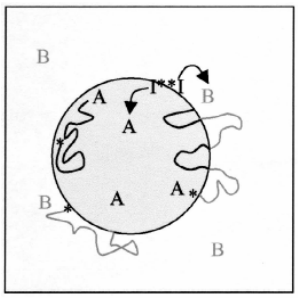

Figure 6. Miniemulsion copolymerization with an interfacial initiation. A is the monomer in the dispersed phase, B the monomer in the continuous phase and I-I the surface active initiator. Figure taken form reference [**Wil**_2002].

Surfactants play a very important role in the stabilization of colloids during polymerization processes and later during the storage. In the last decades, polymerizable surfactants have attracted much attention. Efficient polymerizable surfactants, so called surfmers (surfactant + monomer), are covalently bonded onto the latex particle they stabilize [**Guy**_1994], [**Guy**_1996], [**Asu**_1998]. The properties of the resulting latexes such as resistance to freeze-thaw cycles or electrolyte addition [**Ott**_1995], [**Coc**_1997] are significantly improved. When the latex is used for film formation, the surfmer does not migrate to the interfaces. Thus the adhesion properties of the film are not lowered as it happens if using a conventional surfactant which is physically adsorbed onto the surface of the particle.

In emulsion polymerization, some amount of the surfmer may be buried inside the final latex due to the mechanism of the polymerization [**Duf**_2003]. According to Schoonbrood and al. [**Sch**_1997], a surfmer behaves in emulsion polymerization in an optimum way if it is not reactive at the beginning and more reactive towards the end of the reaction. It involves that the copolymerization parameter of the surfmer and the monomer is a key factor in the control of the latex stability. In fact, in the beginning of an emulsion polymerization, big monomer droplets cohabit with micelles. If the surfactant is fast polymerized, there would be the formation of poly(surfmer) molecules in the continuous phase, which are not suitable for the stabilization of the system. Secondly, the corona of the micelles would be polymerized before the monomer could diffuse from the big reservoir droplets to the micelles. The micelles are then less swellable by the monomer and the surfactants can be buried into the forming particles leading to unstable latexes. This problem can be avoided by performing a miniemulsion polymerization, where the surfmer molecules are situated on the surface of the

droplets already at the beginning of polymerization. These droplets do not change during the polymerisation because the diffusion processes are negligible and therefore, the surfactant stabilize the system at any time of the reaction. Boisson et al. studied the miniemulsion polymerization of styrene and methyl methacrylate with the polymerizable surfactant vinylbenzosulfoccinic acid sodium salt. Stable latexes were obtained with either 2,2´-azoisobutyronitrile (AIBN) or potassium persulfate (KPS) as initiator [**Boi**_2001]. It was estimated by surface tension measurements that 50 to 75% of the surfactants remained fixed onto the surface of the particles. Latexes polymerized with KPS were found to be more stable toward electrolytes and freeze-thaw tests. The authors explained the increase in stability by a gain of steric stabilization when KPS was the initiator, completing the electrostatic stabilization given by the sulfonate group of the surfactant.

Guyot et al. carried out a miniemulsion polymerization of MMA and styrene with the polymerizable surfactants produced from the reaction between succinic anhydride and either hydroxypropylmethacrylate, or hydroxyethylmethacrylate [**Guy**_2003]. The pure surfmers showed a poor surface activity according to surface tension measurements. Thus, a mixture of the surfmer with sodium dodecyl sulfate (SDS) was used to stabilize the miniemulsion droplets. The surfmers employed are highly soluble in water; therefore some surfmers remained in the water phase and were not polymerized. The grafting efficiency of the surfmer increases when the SDS amount in the mixture of surfactants was higher. The prepared latexes exhibited a good resistance to freeze-thaw tests.

Another group [**Pic**_2005] successfully used a mono-fluoroalkyl maleate as a surfmer to stabilize miniemulsion copolymerization of styrene and n-butyl methacrylate. The size of the particles could be controlled by the concentration of the surfmer. The authors blended the synthesized particles with a styrene-butadiene copolymer latex to produce the composite films. These films show more hydrophobic properties compared to the films made of pure styrene-butadiene latexes.

2.3. Anionic miniemulsion polymerization

2.3.1. Anionic miniemulsion polymerizations

Anionic miniemulsion polymerizations are a rather unconventional class of heterophase polymerizations. They led to a good control of the polymer architecture with a narrow polydispersity in the molecular weight. Some investigations were done on the ionic

polymerization of cyclosiloxanes in aqueous miniemulsion [**Bar**_2001], [**Bar2**_2001]. The same process was used to anionically polymerize alkylcyanoacrylates [**Lim**_2003], and glycidyl ethers [**Mai**_2000]. In all these ionic polymerization processes in miniemulsion, water was the continuous phase, with most of the time using the reactive counterion of an inisurf (both initiator and surfactant) to initiate the polymerization. However, these processes are limited to very reactive monomers and/ or give quite low molecular weight products.

2.3.2. Anionic heterophase polymerization of lactams

There is only a very limited number of investigations about heterophase anionic polymerization of less reactive monomers such as lactams initiated by strong bases, e.g. sodium and potassium hydride. Because of the use of the strong bases, the water is not suitable for such polymerizations. Thus, efficient anionic polymerizations initiated by strong bases are theoretically restricted to the dispersion process, the direct heterophase systems with polar aprotic continuous phase and the inverse systems with aprotic continuous phase. 2-pyrrolidone [**Cos**_1981], and ε-caprolactam [**Ric**_2002] were polymerized in suspension processes using strong bases, leading to polymer microparticles. Polyisobutylene oil and NaH were respectively the continuous phase and the initiator for the ε-caprolactam polymerization.

2.4. Miniemulsion polycondensation and polyaddition

2.4.1. Step-growth polymerizations in miniemulsion

Miniemulsion, suspension and dispersion polymerizations are particularly suitable processes among the heterophase systems to perform polycondensation and polyaddition due to the non-micellar nucleation process. In the dispersion polymerization process, the particles are formed during the polymerization, in the case of miniemulsion and suspension polymerization, the droplets themselves the loci of reaction become particles. Whereas the suspension and dispersion polymerization processes can only lead to micron sized particles, the miniemulsion process allows one to produce stable particles in the nanometer size range, typically resulting in particles with a diameter of between 50 and 500 nm. Moreover, the miniemulsion technique provides a complete control on the particle size since the size keeps constant during the polymerization since coalescence and Ostwald ripening are effectively avoided.

In the case of performing a non-radical polymerization in miniemulsion, several papers have been recently reported in the literature. Miniemulsion droplets consisting of a mixture of epoxides and diamines, dithiols, or bisphenols in water were polymerized to obtain epoxy particles [**Lan**_2000]. Minami et al. prepared epoxy particles having one void via polyaddition in miniemulsion [**Min**_2005]. They found that the presence of a pre-dissolved amount of polystyrene in the dispersed phase promote the phase separation of the epoxy resin, which tends to adsorb to the interface of the droplets. High molecular weight hydrophobic polyurethanes could be prepared in direct miniemulsion, dispersing the diisocyanate and the diol in water in the presence of an organo-tin catalyst [**Bar**_2003]. Li et al. synthesized poly(n-butyl methacrylate)/ polyurethane latexes in direct miniemulsion. The n-butyl methacrylate was radically polymerized in the presence of an polyurethane pre-polymer, which was subsequently cross-linked with a hydrophobic chain extender [**LiM**_2005]. Finally, it was shown that polyesters could be obtained in a polycondensation reaction in miniemulsion, reacting a hydrophobic diol and diacid dispersed in the presence of water [**Bar2**_2003].

2.4.2. Interfacial polycondensation in miniemulsion

It is also interesting to use the very large surface offered by the miniemulsion droplets to perform an interfacial polycondensation. The principle consists in reacting one hydrophilic monomer contained in the dispersed phase and one hydrophobic monomer contained in the continuous phase. The method can eventually be used to encapsulate different compounds. Torini et al. investigated the synthesis of polyurethane latexes by reacting the relatively stable isophorone diisocyanate with 1,6-hexanediol in direct miniemulsion [**Tor**_2005]. In a similar manner, Takasu et al. produced a polyurea shell around a styrene liquid core by interfacial polycondensation [**Tak**_2005]. The styrene was subsequently radically polymerized to give core-shell particles.

Thus, the miniemulsion technique has an unique ability to allow the synthesis of polymer nanoparticles via non-radical methods. These still exotic synthesis produce usually well-defined materials in an environmentally responsible process (when performed in a direct system). The information about the synthesis described in the literature up to now, are displayed in the Table 2. Finally, Taira et al. described very recently the trap and release of oligo-nucleotide using pH-responsive amphoteric particles prepared by interfacial polymerization in a W/O miniemulsion system [**Tai**_2006].

Table 2. Non-radical miniemulsion polymerizations.

Method	Polymer class	Monomers	Morphology	Reference
Polyaddition/ polycondensation	Epoxy	hydrophobic diamines or diols or dithiols + diepoxides	particles	[**Lan**_2000], [**Kaw**_2001]
		hydrophobic diepoxides and diamines	capsules	[**Mar**_2002] [**Min**_2005]
		hydrophobic diepoxides and hydrophilic diamine (lysine)	particles	[**Tai**_2005]
	Polyurethane	hydrophobic diols and diisocyanates	particles	[**Tia**_2001], [**Bar**_2003]
		hydrophobic urethane prepolymer and hydrophobic diol	particles	[**LiC**_2005]
		hybrid: hydrophobic urethane prepolymer and –OH of HEMA/ BMA copolymer	particles	[**LiM**_2005]
		hydrophobic diol and diisocyanate	capsules	[**Tor**_2005]
	Polyurea	hydrophobic diamines and diisocynates	shell in core-shell particles	[**Tak**_2005]
	Polyester	hydrophobic diacids and hydrophobic diols	particles	[**Bar2**_2003]
	Polysiloxane	hybrid: hydrophobic diisocyanate and siloxanediol	particles	[**Lan**_2005]
	Polyamide	hydrophilic diamine and hydrophobic diacyl chloride	shell in core-shell particles	[**Bou**_2005]
Anionic	Polyacrylate	butylcyanoacrylate	particles	[**Lim**_2003]
	Polyether	glycidyl ether	particles	[**Mai**_2000]
	Polysiloxane	octamethylcyclotetrasiloxane	particles	[**Bar**_2001] [**Bar2**_2001]
Cationic	Styrenics	p-methoxystyrene	particles	[**Cau**_2002] [**Cau**_2005] [**Cau**_2004]
	Polysiloxane	2,4,6,8-tetramethylcyclotetrasiloxane	particles	[**Pal**_2006]
Metal-catalyzed	Polyolefin	ethylene	particles	[**Tom**_2000]
		ethylene/ hexadecene/ octene	particles	[**Sou**_2002]
		5-acetyl-2-norbornene[**Che**_2005] dicyclopentadiene [**Que**_2005] norbornene [**Que**_2005] [**Cla**_2001], [**Que2**_2005] cyclooctadiene [**Que2**_2005]	particles	[**Che**_2005] [**Que**_2005] [**Cla**_2001] [**Que2**_2005]
	Polyketone	Ethylene/ CO	particles	[**Hel**_2002]
Enzymatic	Polyester	pentadecanolide	particles	[**Tad**_2003]
Oxidative	Semi-conductor polymer	aniline	particles	[**Mar**_2003]
		pyrrole	particles	[**Ham**_2005]
		pyrrole	shell in core-shell particles	[**Cho**_2005]

3. Relevant methods for characterization

It is only when they go wrong that machines remind you how powerful they are.

Clive James (1939 - /)
Australian author.

3.1. Light Scattering

The light scattering techniques are highly employed for the characterization of polymers and colloids as reviewed by Aseyev and the references herein [**Ase**]. The phenomenon of light scattering happens because the molecules investigated are polarized by the electrical field of the passing light ray and because they have a dimension comparable to or smaller than that of the wavelength of the light. For very small molecules, the effect is extremely weak. In fact, the strength of the scattering does not depend simply on the amount of the solute present, but is stronger for the same weight of solute portioned into large molecules than if it is portioned into small ones. Thus scattering can determine the molecular weight and is particularly suited to applications to large molecules such as polymers. Static light scattering (SLS) focuses on the study of the magnitude of the average scattered intensity whereas dynamic light scattering (DLS) deals with the time behavior of fluctuations of the scattered intensity.

The particles inside a dispersion are animated by the Brownian motion. Because of this phenomenon, the phases of each scattered waves fluctuate in time. Therefore, the intensity of the scattered wave fluctuates also randomly. The photomultiplier registers the number of photons that hit the detector during different intervals of time, which are called "channel width" as shown in Figure 7. The value of the diffusion coefficient of small particles is bigger than that of big particles and thus the signal changes more. It is hence possible to find a correlation between the coefficient of diffusion and the fluctuation in time of the scattered intensity. The autocorrelation function of the intensity is calculated and can be plotted versus the channel width. The average diffusion coefficient of the particle and its standard deviation are extracted from the fitting of this curve. Finally, the use of the Stokes-Einstein equation gives the hydrodynamic diameter and its standard deviation:

$$D = \frac{kT}{6\pi\eta R}$$

D: diffusion coefficient [$m^2.s^{-1}$] η : dynamic visocisty [$kg.s^{-1}.m^{-1}$]

T : temperature [K] R : hydrodynamic radius [m]

k : Boltzmann´s constant = $1.3806503 \times 10^{-23}$ m^2 kg s^{-2} K^{-1}

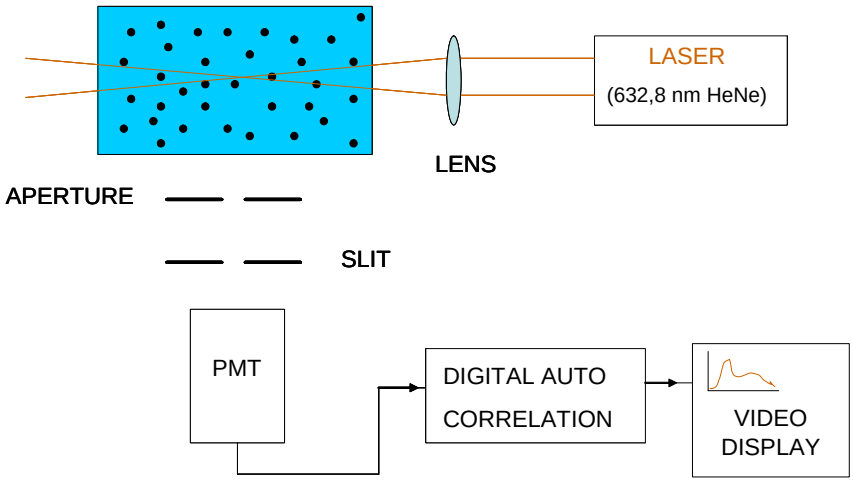

Figure 7. Schematic presentation of a typical dynamic light scattering machine. Illustration based on a figure of the particle sizer Nicomp model 370, PSS Santa Barbara, CA.

3.2. Electron microscopy (TEM, SEM)

"It is a miracle that by now the difficulties have been solved to an extent that so many scientific disciplines today can reap benefits". In this manner ends the Nobel Lecture of Ruska about electron microscopy made some twenty years ago [**Rus**_1986]. Still now, materials scientists and biologists use extensively electron microscopy, which became a routine technique. Currently, some machines are able to reach an amazing Angström resolution. We describe shortly here two analytical methods employed in this thesis: the scanning electron microscope (SEM) and the transmission electron microscope (TEM).

3.2.1. The scanning electron microscope

In a typical scanning electron microscope (SEM) configuration (Figure 8), the electrons are emitted by a cathode filament. The electrons are then attracted towards the anode, which causes their acceleration. The electron beam, which has typically an energy between a few keV to 50 keV, is focused by two successive condenser lenses into a beam with a spot size around 5 nm. The beam passes through an objective lens and strikes the surface of the sample as shown in Figure 8. The electrons are inelastically scattered by the atoms of the sample. The primary beam spreads and fills a teardrop-shaped volume, called interaction volume, which has a depth between 1 and 5 µm. Interactions in this region give an emission of electrons that

are detected to produce an image (see Figure 9). X-rays are also produced and may be detected in SEM equipped for energy dispersive X-ray spectroscopy. The electron-matter interaction leads to an accumulation of charges at the surface. These charges are evacuated to the mass if the sample is conductive. In the case of an insulative material, the accumulation of charges deforms the electron beam and modifies its effective energy. Thus, a thin layer of a conductive material (gold, gold-palladium, carbon) is deposited on non-conductive samples.

The secondary electrons come from the near surface region and hence the contrast depends on the surface area exposed to the primary beam. This area increases when the surface becomes steeper. The image is then representative on the topology of the sample. However, it may be difficult to distinguish between voids and the relief in the sample if only the secondary electrons are used. In addition to the secondary electrons, backscattered electrons (elastically scattered primary electrons) can also be detected. The topological contrast given by the backscattered electrons is inferior to the one given by the secondary electrons. In fact, they are scattered from fairly deep within the sample because they have a higher energy. However, the emission of the backscattered electrons is proportional to the square root of the atomic number of the atoms of the sample. It is then possible to obtain images with a contrast in composition.

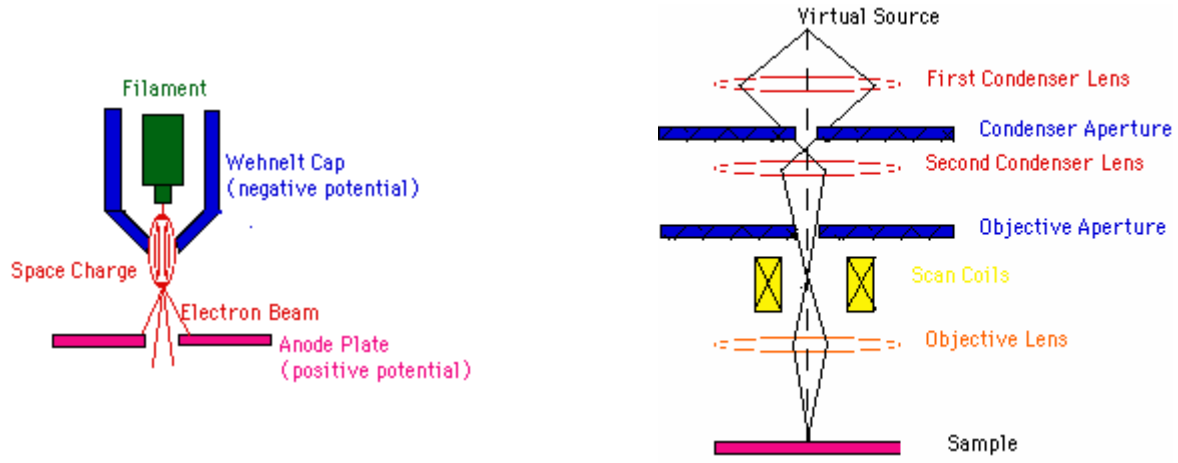

Figure 8. Schematics of the SEM principle. Figures taken from an online document of the University of Nebraska Lincoln [**UNL**].

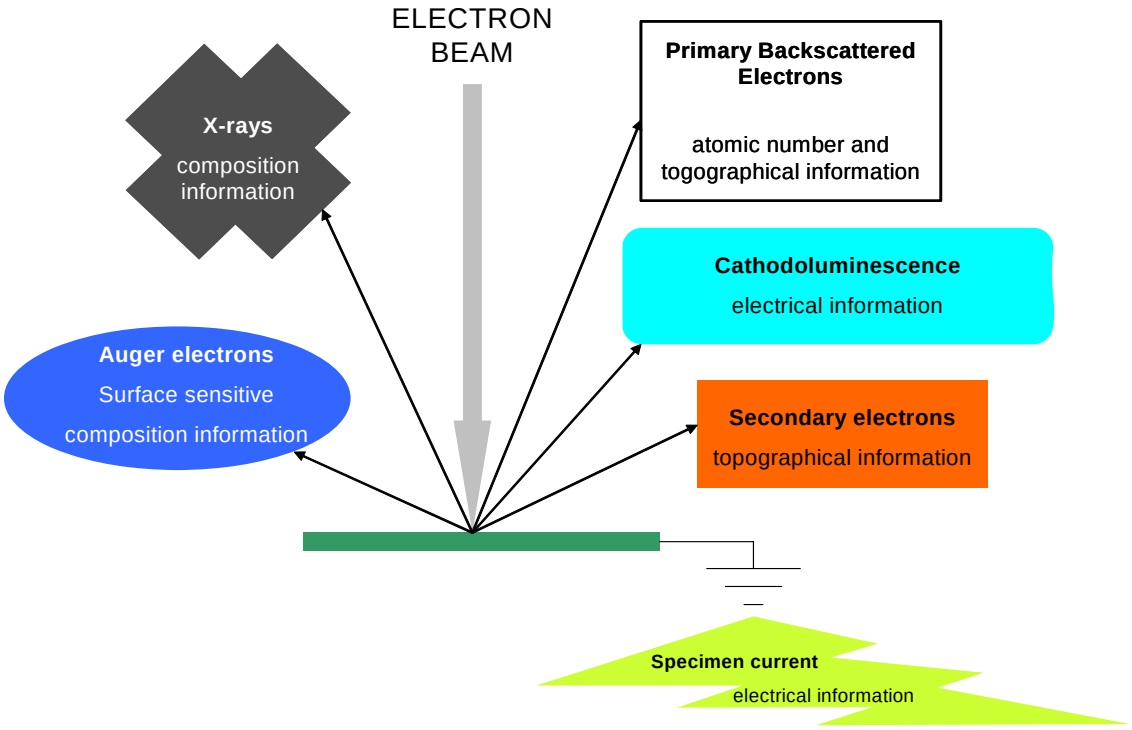

Figure 9. Signals and information generated by the interaction between the electron beam and the sample. Figure based on an online document from the university of Rennes [**CME**].

3.3.2. The transmission electron microscope

The principle of the TEM measurements is the same as for the SEM. The difference is that the transmitted electrons are analyzed in TEM. Darker areas of the image are produced when fewer electrons were transmitted through (thicker or denser areas). For instance, it is then possible to distinguish capsules from particle morphologies since electrons are better transmitted through the core than through the shell of a capsule.

4. Results and Discussion

Clouds may be identified with the moon.
Valleys are at variance with mountains.
The reality is universal and blessed.
It is either one or two.

Mumon-Ekai (1183~1260)
Great Zen master during the Sô dynasty in China.

4.1. Free-radical polymerization in miniemulsion

Free-radical polymerization is the most investigated procedure in the literature dealing with the miniemulsion technique. However, there is still a huge scope for the current research, which can be condensed in the three following topics:

- to produce latexes with a lower cycle time
- to produce latexes with superior properties
- to produce latexes with an environmentally responsible process.

We want to show that free-radical polymerization applied in miniemulsion processes can be performed in order to reach these objectives.

4.1.1. Free-radical polymerization in direct miniemulsion

4.1.1.1. Free-radical polymerization in direct miniemulsion in the presence of a solvent in the dispersed phase

Free-radical polymerization of styrene or divinylbenzene was performed in direct miniemulsions in the presence of either toluene or octane in the dispersed phase. The monomers, either styrene or divinylbenzene, are soluble in the solvents toluene and octane. Polystyrene is soluble in toluene whereas phase separation occurs between polystyrene and octane even if the octane can swell the polymer to a certain content. Poly(divinylbenzene) is a cross-linked polymer and swells both in toluene and in octane with a better swelling capacity in toluene. The conversion of the monomer was not hindered by the presence of the solvent inside the dispersed phase since all conversions were found to be superior to 99% by thermogravimetry analysis. We investigated the influence of the ratios of the monomer to the hydrophobic solvent in the dispersed phase on the morphologies of the latexes formed by TEM. The characteristics of the different prepared miniemulsions are shown in Table 3 and the morphologies are presented in Figure 10, 11, 12, and 13. A desired morphology of the particles can be achieved simply by varying the ratio of monomer to solvent. Let us notice that octane, as a good solvent for the monomer and bad solvent for the polymer, was found to be suitable to create nanocapsules whereas previous studies used the longer alkyl chain component hexadecane [**Tia2**_2001], which is more difficult to remove for eventual further film-formation for instance.

Table 3. Characteristics of the direct miniemulsions prepared with hydrophobic solvent in the dispersed phase.

Entry	Monomer		Solvent		Hydrodynamic diameter (nm)
	Nature	Amount (g)	Nature	Amount (g)	
DC308	DVB	0.5	Toluene	1	81
DC309	DVB	0.5	Octane	1	117
DC310	S	0.5	Toluene	1	114
DC311	S	0.5	Octane	1	94 (48%) 36 (52%)
DC312	DVB	0.2	Toluene	1.3	122
DC313	DVB	0.2	Octane	1.3	102 (42%) 908 (58%)
DC314	S	0.2	Toluene	1.3	75 (25%) 174 (75%)
DC315	S	0.2	Octane	1.3	59 (6%) 314 (94%)
DC316	DVB	0.35	Toluene	1.15	85
DC317	DVB	0.35	Octane	1.15	66 (45%) 208 (55%)
DC318	S	0.35	Toluene	1.15	67
DC319	S	0.35	Octane	1.15	55 (25%) 292 (75%)
DC320	DVB	1	Toluene	0.5	240
DC321	DVB	1	Octane	0.5	175 (34%) 552 (20%) 908 (46%)
DC322	S	1	Toluene	0.5	80
DC323	S	1	Octane	0.5	60 (35%) 150 (65%)
DC253	DVB 6	6	X		106
DC295	DVB	5	X		109
	S	1			
DC296	DVB	3	X		97
	S	3			
DC297	DVB	1	X		92
	S	5			

The styrene/ toluene dispersed phase has always a monomodal distribution (DC310, DC322, DC318) except for the small ratio styrene/ toluene in the dispersed phase (DC314). However, as shown in Table 3, the DLS does not detect always a monomodal distribution for the particles. The styrene/ octane system has always bimodal distribution of diameters (DC311, DC315, DC319, and DC323). This is due to demixing between the polymer and the octane in the droplets. The octane has a little swelling ability toward the polymer but phase separation occurs anyway because of the insufficient solubility of the polymer in octane.

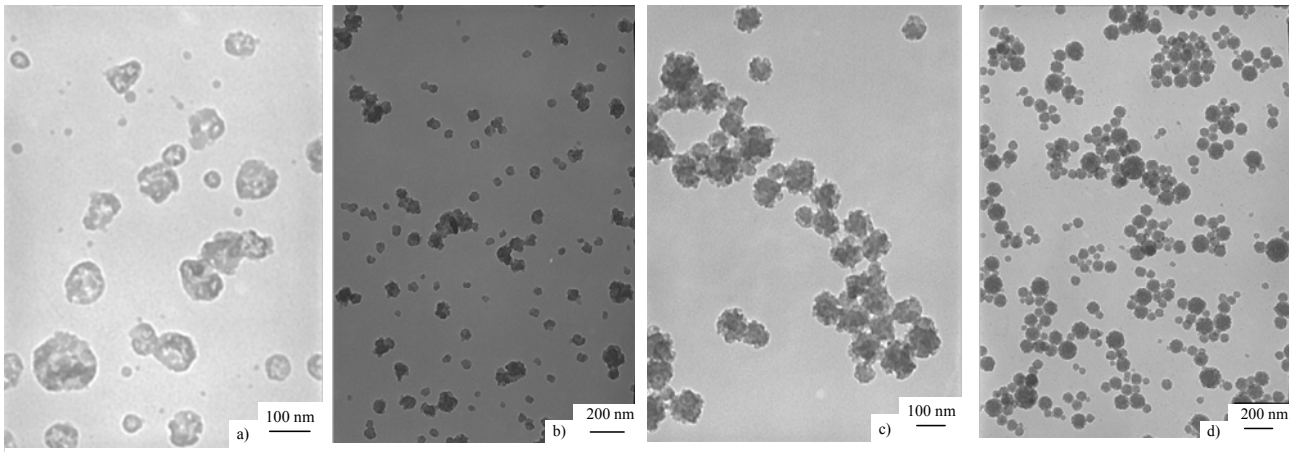

DVB/ toluene	13/87	23/77	33/67	67/33

Figure 10. TEM micrographs of samples prepared with increasing ratios DVB/ toluene wt.%/ wt.%. **a**: sample DC312, **b**: sample DC316, **c**: sample DC308, **d**: sample DC320.

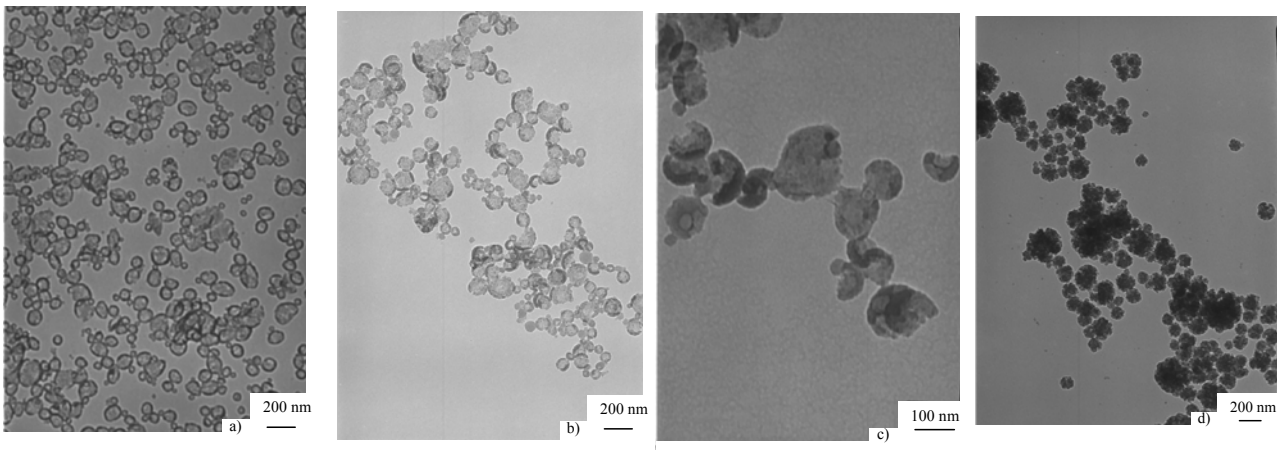

DVB/ octane	13/87	23/77	33/67	67/33

Figure 11. TEM micrographs of samples prepared with increasing ratios DVB/ octane wt.%/ wt.%. **a**: sample DC313, **b**: sample DC317, **c**: sample DC309, **d**: sample DC321.

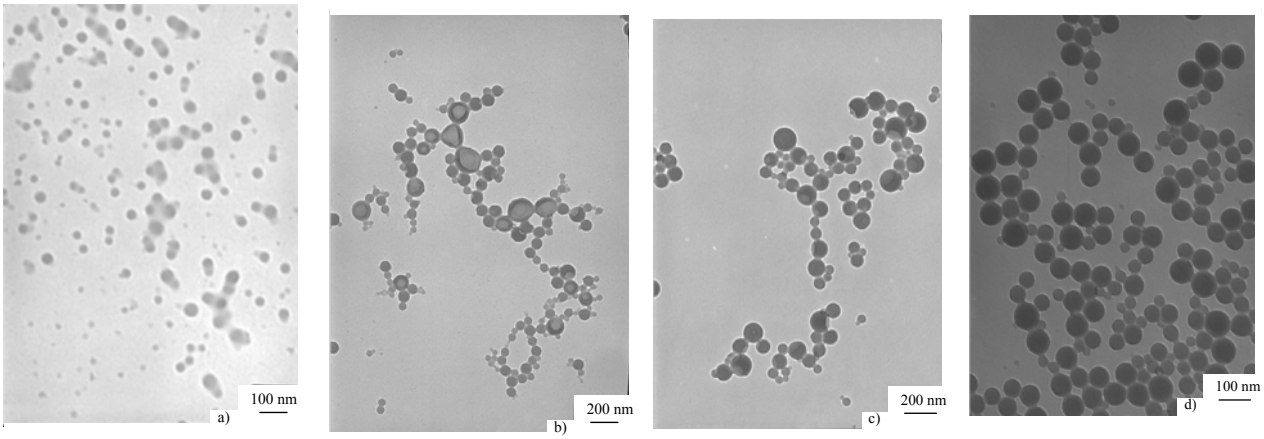

styrene/ octane	13/87	23/77	33/67	67/33

Figure 12. TEM micrographs of samples prepared with increasing ratios styrene/ octane wt.%/ wt.%. **a**: sample DC315, **b**: sample DC319, **c**: sample DC311, **d**: sample DC323.

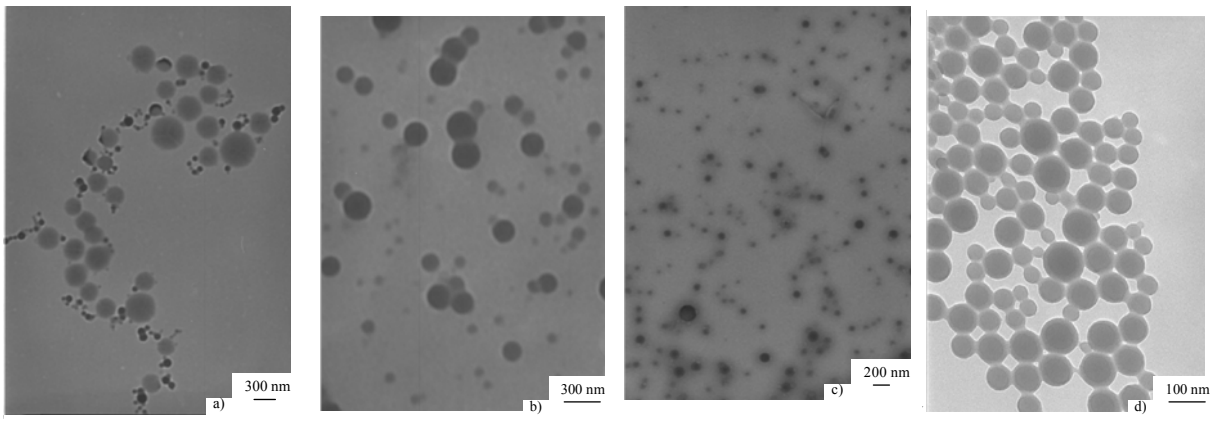

styrene/ toluene	13/87	23/77	33/67	67/33

Figure 13. TEM micrographs of samples prepared with increasing ratios styrene/ toluene wt.%/ wt.%. **a**: sample DC314, **b**: sample DC318, **c**: sample DC310, **d**: sample DC322.

The morphology of the particles was investigated with TEM measurements. The morphology of the particles in the system DVB/ toluene (Figure 10) and DVB/ octane (Figure 11) as dispersed phase were very similar. The main difference is that the capsules and the particles in the system DVB/ toluene (samples DC312, DC316, DC308, DC320) present a rougher surface than the ones in the system DVB/ octane (DC313, DC317, DC309, DC321). Due to the poor solubility of the polymer in the solvent, the capsules are created by the precipitation

of the polymer at the interface of the droplets. Very smooth capsule morphology is formed with a ratio DVB/ octane of 13/87 wt.% as the dispersed phase (sample DC313). Such capsules possesses also a thin wall of 22 nm as determined by TEM. On the other hand, the systems styrene/ octane (Figure 12, samples DC315, DC319, DC311, DC323) and styrene/ toluene (Figure 13, samples DC314, DC318, DC310, DC322) have more differences. Capsules are created for the system styrene/ octane with the medium ratios styrene/ octane 23/77 (sample DC319) and 33/67 wt.% (sample 311). Lower (sample 315) and higher ratios (sample 323) lead to particle morphology. We believe that the particle morphology observed at high ratio styrene/ octane is due to an engulfing of the polystyrene particles in the octane droplets. Besides, the content of polystyrene in the system with low ratio styrene/ octane is very low and may be insufficient to allow the efficient precipitation of the polymer. The system styrene/ toluene as dispersed phase gave always a smooth particle morphology (samples DC314, DC318, DC310, DC322). In this case no distinct phase separation occurs and the polymer is homogeneously distributed in the droplets because of the better solubility of the polymer in the solvent.

We investigated further the system to know if the rough surface observed in the particles containing poly(divinylbenzene) above were due to the polymer itself or due to the use of a hydrophobic solvent in the dispersed phase. Therefore, we carried out miniemulsion polymerization with different ratios styrene/ divinylbenzene without any solvent in the dispersed phase. As shown in Table 4, the amount of divinylbenzene does not affect significantly the hydrodynamic diameter (see samples DC253, DC295, DC296, DC297). The morphology observed is always a particle morphology. No capsule formation is expected since there is no non-solvent for the polymer to allow a phase separation in the droplet. However, the amount of divinylbenzene in the monomer mixture has a strong influence on the roughness of the particles. As shown in Figure 14, once the ratio wt./wt. of DVB/ styrene is superior to a certain value, comprised between 0.16 and 0.5, the surfaces of the particles are rougher. Crosslinking is known to induce a non-spherical shape for particles if the amount of crosslinker is sufficient. Interfacial forces tend to minimize the interfacial energy and hence keep the shape of the particles spherical whereas elastic forces induced by crosslinking can induce a slight modification of the shape. The observations show that if the content of divinylbenzene in the styrene/ divinylbenzene mixture is sufficiently high, the elastic forces induced by crosslinking prevail on the interfacial forces, and hence the particles are not completely spherical. They keep a general sphere-shape but with a roughness on the surface.

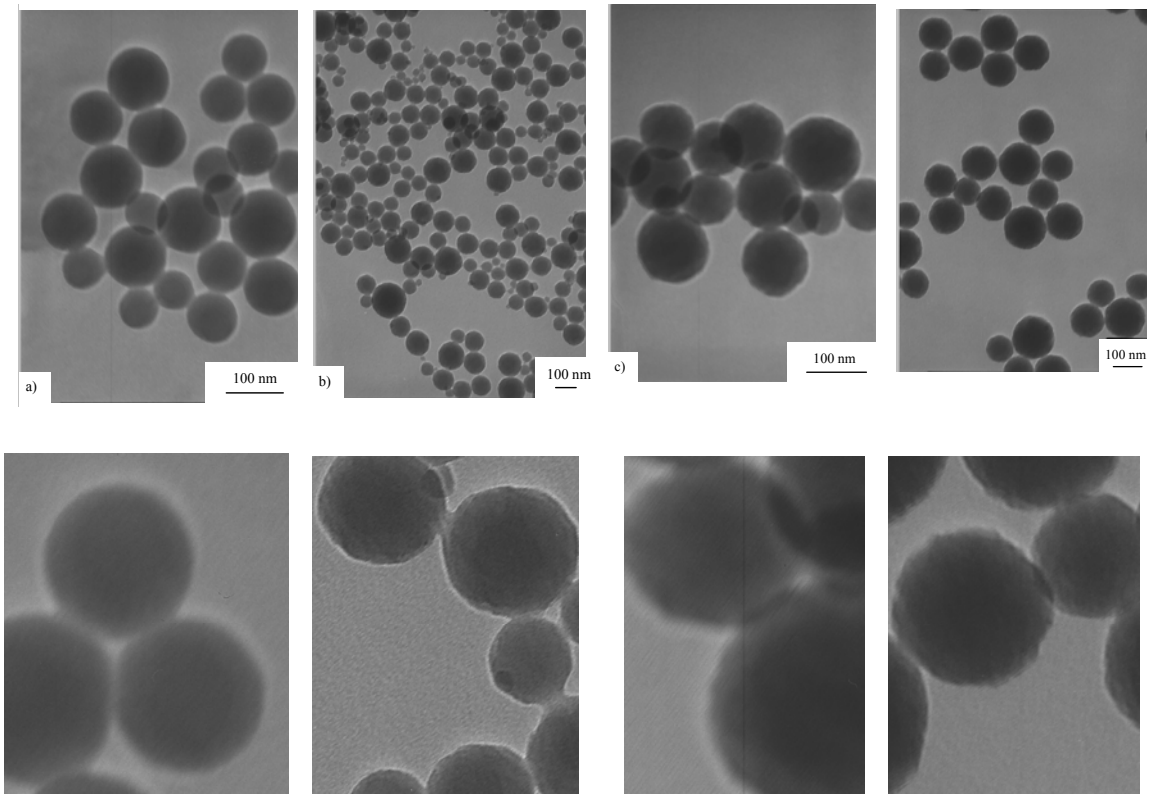

DVB/ styrene	80/20	50/50	20/80	100/0

Figure 14. TEM micrographs of samples prepared with different ratios divinylbenzene/ styrene wt.%/wt.%. **a**: sample DC297, **b**: DC296, **c**: DC295, **d**: DC253. Micrographs below are zooms of the micrographs above and are presented to underline the change in the roughness of the particles.

Thus, it is possible to tune the morphology of the particles synthesized in direct miniemulsion simply by the addition of a hydrophobic solvent present in the droplet. Different morphologies are created, depending on the solubility of the polymer in the hydrophobic solvent and on the ratio monomer to solvent. Polymeric caspules are formed if a non-solvent for the polymer is present in the dispersed phase in large amount. Particles are formed if the dispersed phase before polymerization is composed of the monomer only, or of a mixture of the monomer and a good solvent for the polymer, or of a mixture of monomer and a small amount of non-solvent for the polymer. It is also possible to tune the roughness of the particle surface by the addition of a crosslinker to the monomer mixture.

4.1.1.2. Free-radical polymerization in the presence of metal complexes in direct miniemulsion

Hybrid or composite latexes contain inorganic and organic parts and hence benefit of the good properties of both materials. For further applications, sometimes one component, the inorganic or the organic part, is removed from the material. For instance silica particles can be used as template to deposit polymeric shell around it. Then the silica can be chemically eliminated giving polymeric hollow capsules. In this case the organic part is kept. The inorganic part can be also kept for further applications. Thus, it was shown in past time that unconventional lithography could be performed by plasma-etching self-assembled monolayers of metal-loaded micelles [**Sel**_1999]. The material was constituted of gold nanoparticles embedded in diblock PS-*b*-P2VP copolymer micelles in toluene. The more hydrophilic P2VP is in contact with the gold nanoparticles whereas the PS part ensures the steric stabilization of the nanoparticles in the continuous phase. The metal containing micelles were deposited on silicon surfaces in an ordered array. They were then submitted to plasma-etching to remove the organic part and the process gave ordered arrays of gold nanoparticles on silicon surfaces. These arrays served as masks for reactive ion etching because of the better resistance of the gold compared to the silicon. The silicon around the nanoparticles could be removed, leading to the formation of silicon nanopillars. In this system, the interparticle distance could be varied from 30 to 140 nm by using different lengths of the blocks in the diblock copolymers. The height of the clusters could be varied between 1 to 15 nm. Despite the good properties of the process, it suffers from a certain number of important drawbacks. First, the PS-*b*-P2VP micelles are synthesized by anionic polymerization, which is a demanding and expensive process. Secondly, the micelles are dispersed in a non-environmentally friendly organic solvent (toluene). Thirdly, the micelles are soft materials, which have the tendency to move on the surface during the plasma-etching. Fourthly, the metal-loaded micelles have also the tendency to sediment and are not stable for long period of time. Finally, the distance between the metal clusters can be varied only in a narrow range, i.e. between 30 and 140 nm.

We propose to improve significantly the method with the use of metal-loaded latexes made by miniemulsion instead of using micelles. First, the metal-loaded particles can be synthesized by the easy-handled free-radical polymerization in miniemulsion. Secondly, the particles are dispersed in water instead of a non-environmentally friendly organic solvent. Thirdly, we can synthesize hard polymer particles, i.e. with a high glass transition temperature, that would be less mobile than the micelles during the etching process. Fourthly, the miniemulsion

technique provides very stable latexes for a long period of time due to the efficient stabilization against both coalescence and Ostwald ripening (discussed in the theoretical part). And finally, the miniemulsion particle diameter and hence the distance between the metal clusters can be varied in a very wide range, between 50 and 500 nm. The upper limit of the inter-cluster distance cannot be attained with the micellar technique (140 nm was the maximum interparticle distance). Thus, we propose to synthesize metal loaded particles in miniemulsion. Two main different approaches can be identified: the synthesis of particles containing a metal complex as precursor material and the synthesis of the particles containing the pure metal. In the first approach, the metal cluster is formed during the plasma-etching process by reduction of the metal complex. The latexes are then deposited on silicon substrates, and the organic part is plasma-etched with a simultaneous reduction of the metal complex. The nanoparticles arrays serve as masks for reactive ion etching as shown in Figure 15.

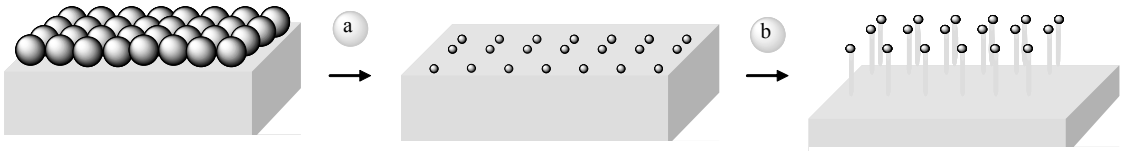

Figure 15. Schematics for the production of silicon nanopillars. **a**: plasma-etching of metal/ polymer hybrid latex, the polymer is etched and the metal complex is reduced; **b**: the metal nanoparticles are used as a mask to remove silicon by electron beam lithography.

For the second approach, one or several metal nanoparticles are already present in the latexes before the plasma etching as shown in Figure 16.

We present here a collaborative work between the department of Macromolecular Chemistry and the department of Solid State Physics on the use of miniemulsion latexes for lithography techniques. The two approaches described above were investigated: the particles containing metal complex and particles containing the metal. For the first approach, platinum (II) acetylacetonate/ polystyrene hybrid particles were synthesized, whereas polyurea capsules containing silver nanoparticles (synthesis presented in part 6.3. of this thesis), and silver/ polyvinylpyrroldione hybrid particles (synthesis presented in part 6.1. of this thesis) were synthesized for the second approach. The results concerning the polyvinylpyrrolidone and the polyurea are reported in the following parts: chapter 4.1.2.1. and chapter 4.3.2. respectively of this thesis. We describe here the results obtained with the first approach.

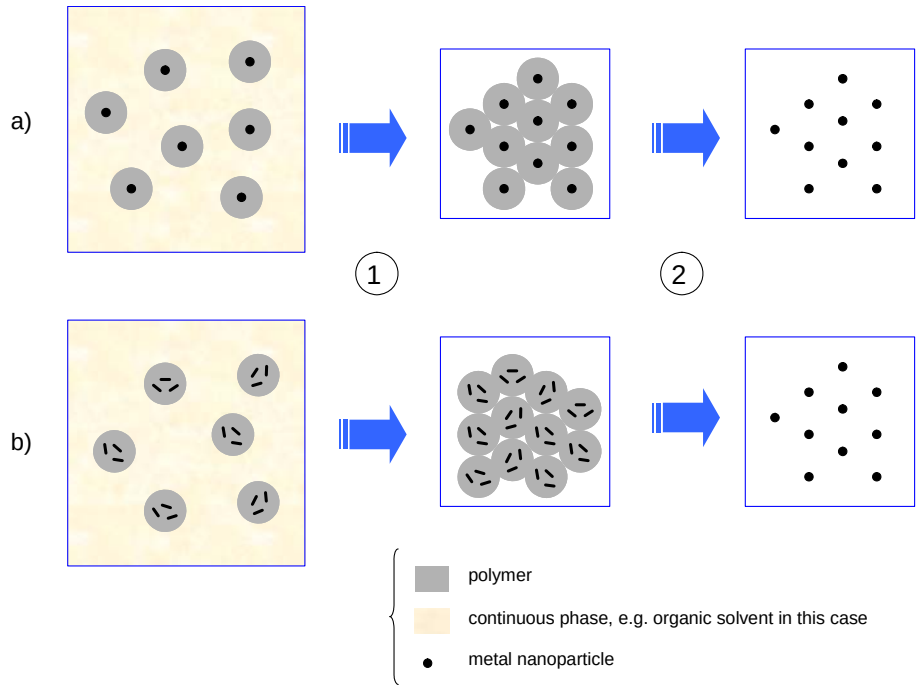

Figure 16. Process to make well-ordered metal clusters; **a**: with one single metal nanoparticle per polymer particle, **b**: with several metal nanoparticles per polymer particles, which combine to one metal nanoparticle. The process is composed of 1) the deposition of the latex on a surface and 2) the plasma etching of the polymer.

Synthesis of the metal complex/ polymer latexes

Direct miniemulsion polymerization of styrene was performed in the presence of different metal complexes. The metal complex were chosen with the following criteria: they should be hydrophobic and soluble in styrene but not in water; they should not be sensitive towards the water; they should be commercially available for further eventual scale-up processes; and finally the reduced form of the metal complex, i.e. the zero valent metal, should be well resistant to reactive ion etching. Suitable complexes were namely the platinum (II) acetylacetonate, the nickel (II) cyclohexylbutyrate and the nickel (II) naphtenate shown in Figure 17.

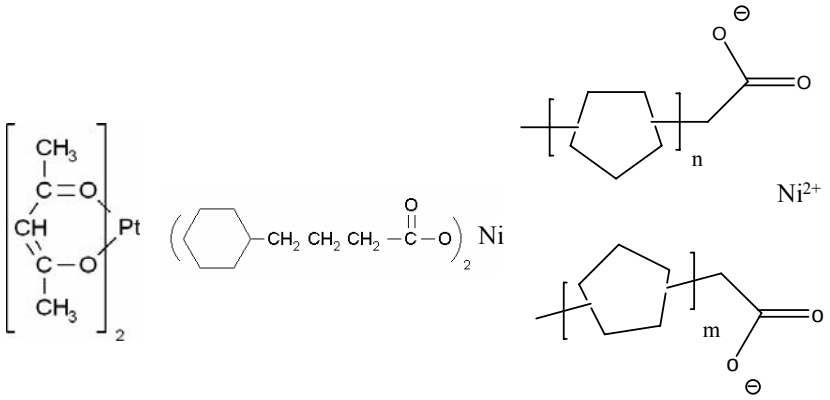

Figure 17. Scheme of the hydrophobic complexes platinum (II) acetylacetonate, nickel (II) cyclohexanebutyrate and nickel (II) naphtenate.

The characteristics of the latexes are summarized in Table 4. The metal complex was dissolved in the dispersed phase with an amount varying from 10 to 50 mg. The first observation concerning the synthesized latexes is that the conversions of the polymerizations were found always to be superior to 99% by thermogravimetric analysis. Different particle sizes could be obtained varying from nm (sample DC709) to 154 nm (sample DC725). The particles prepared with a mixture of SDS and Lutensol AT-50 (sample DC716) or a mixture of SDS and PVP (DC717) have a larger particle size, respectively 108 nm and 139 nm, than the sample DC711 prepared with the same amount of the sole SDS (88 nm). Miniemulsions with different surfactants, and different surfactant amounts were performed with the objective to form latexes containing metal complexes with a low polydispersity in size. In fact, a low polydispersity may facilitate the self-assembly of the particles in a large area and may allow that the distance between the metal clusters will be constant. Several stabilizer and amount of stabilizer were tested. The standard deviation calculated for the hydrodynamic diameter in % for all samples, except sample DC725, with styrene as dispersed phase and platinum (II) acetylacetonate were found to be very similar and comprised between 19 and 25%. The sample DC725, prepared with a medium amount of surfactant (~ 2.4 wt.% compared to the dispersed phase) presents a standard deviation for the hydrodynamic diameter as low as 10%. However, samples prepared with toluene or heptane in the dispersed phase have a higher standard deviation. Samples prepared with the nickel complexes have also higher standard deviation. Sample DC724 contains acrylic acid as the monomer to study the influence of the carboxylic group on the deposition of the latex on the silicon substrate. Because these functional groups are located on the surface of the latex, they may have an influence on the self-assembly of the particles during the drying process.

Table 4. Characteristics of the hybrid latexes.

Entry	monomer/ solvent		hexadecane (mg)	AIBN (mg)	metal complex (mg)	Surfactant		particle size *	
	nature	amount (g)				nature	amount (mg)	diameter (nm)	σ (nm/ %)
platinum (II) acetylacetonate/ polystyrene hybrid latexes									
DC709	S	1.5	60	40	25	SDS	16.5	79	17/ 21
DC711	S	1.5	60	40	40	SDS	10	88	22/ 25
DC716	S	1.5	60	40	40	SDS	5	108	26/24
						Lutensol AT-50	5		
DC717	S	1.5	60	40	40	SDS	5	139	27/ 19
						PVP	5		
DC718	S	0.04	15	2	10	SDS	2.5	150	104/ 69
	toluene	0.35							
DC720	S	0.075	15	3	10	SDS	2.5	118	40/ 34
	toluene	0.4							
DC721	S	0.4	15	10	10	hexadecyltrimethyl ammonium bromide	2.5	119	28/ 24
DC724	S	1.4	60	40	40	SDS	15	190	41/ 22
	AA	0.1							
DC725	S	1.5	60	40	40	SDS	3.8	154	16/ 10
poly(divinylbenzene)/ platinum (II) acetylacetonate hybrid latex									
DC719	DVB	0.05	15	5	7	SDS	18	201	97/ 48
	heptane	1.3							
polystyrene/ nickel (II) cyclohexanebutyrate hybrid latex									
DC722	S	1.5	60	40	0.12	SDS	15	131	48/ 37
polystyrene/ nickel (II) naphtenate hybrid latex									
DC723	S	0.75	60	40	0.75	SDS	15	209	109/ 53

* determined by dynamic light scattering

Monolayer formation

Dip-coating at 45° and dropping were tried as techniques to obtain a monolayer of particles on silicon substrates. The best method was found to be the simple dropping of the latex on the substrate. The optimal dilution of the latexes to get a monolayer of particles was 1/20 wt./wt. latex/water. As shown in Figure 18, regular arrays of nanoparticles can be built on the silicon substrate. SEM investigations with a lower magnification showed that an ordered assembly of the particles is facilitated when acrylic acid is added to the miniemulsion (sample DC724). These SEM micrographs revealed also that the platinum complex is homogeneously distributed. In fact, a non homogeneous structure would have resulted in some darker spots due to the zones with high concentration of platinum since the emission of the backscattered electrons is proportional to the square root of the atomic number of the atoms of the sample.

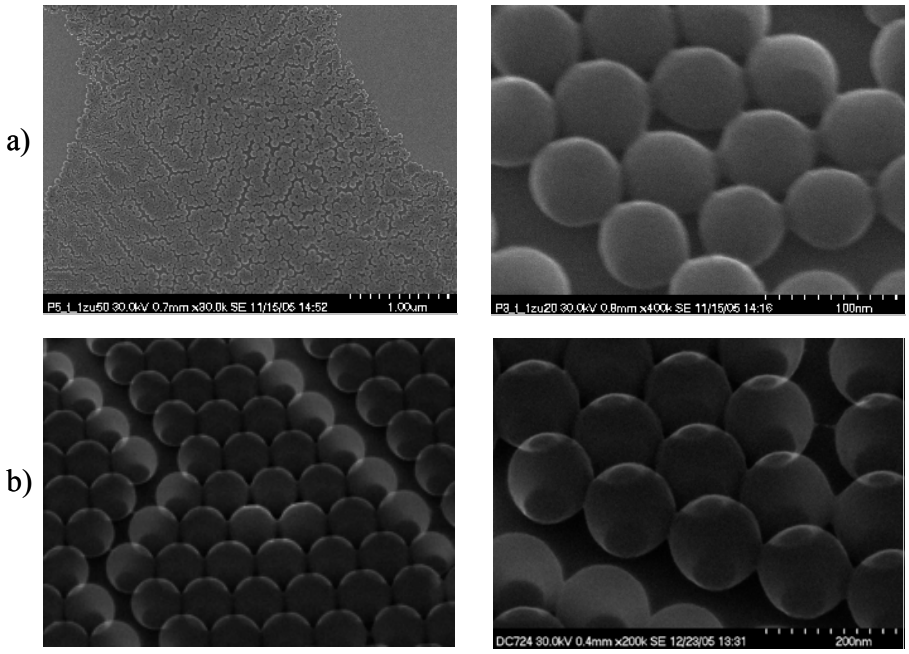

Figure 18. Monolayer formation upon dropping the diluted latex on a silicon substrate. **a**: polystyrene latex DC709 with 0.8 wt.% of platinum compared to the polymer, **b**: poly(styrene-*co*-acrylic acid) DC724 containing acrylic acid with 1.3 wt.% of platinum compared to the polymer.

Plasma-etching of the particles

Then in a next step, plasma-etching was achieved with oxygen or/ and hydrogen on the monolayer of particles as shown in Figure 19. The best combination was found to be first etching with oxygen then with hydrogen because etching with oxygen is more aggressive toward the polymer.

Figure 19 shows that the metal complex is reduced in one spot. The metal is formed through the reduction of the metal complex by the plasma-etching. The spot is either composed of several aggregated nanoparticles (Figure 19a, b, c) or one nanoparticle (Figure 19d). One nanoparticle per spot is obtained when the sample is submitted to an annealing at 600 °C. The melting point of bulk platinum is normally 1772 °C at atmospheric pressure but small nanoparticles are known to have a lower melting point due to their size. Three important facts correlates the principle shown in Figure 15, i.e. the fact that all the metal complex is reduced in one spot in the center of the former particle. First, it is observed that the polymer particles shrink during the plasma-etching process. Secondly, the distance between the metal spots are equal to the diameter of the former metal complex/ polymer particles. Thirdly, the diameter of the platinum spot is lower than the theoretical one. These facts show that the particles do not move during the plasma-etching, that the metal spot is created in the center of the former particles and finally that the metal spots do not coalesce with other metal spots from other particles.

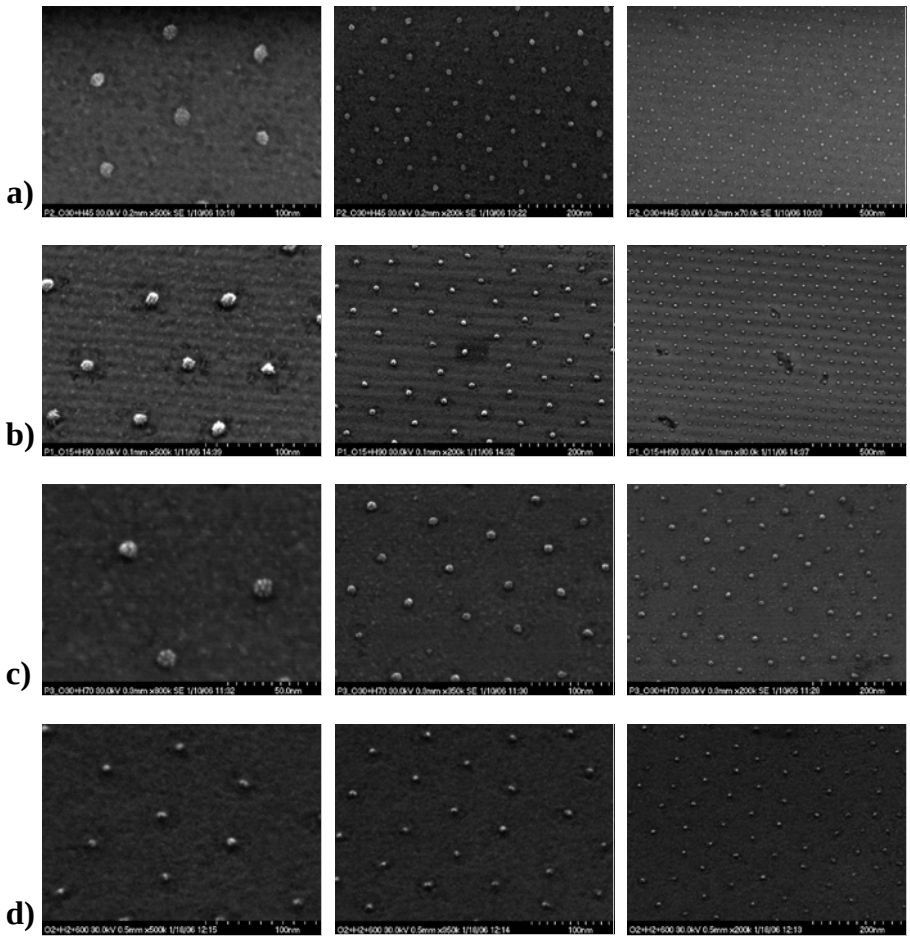

Figure 19. SEM micrographs of the plasma-etched platinum (II) acetylacetonate/ polystyrene particles under three different conditions. **a**: O_2 30 min, H_2 45 min; **b**: O_2 15 min, H_2: 90 min, **c**: O_2: 30 min, H_2: 70 min, **d**: O_2, H_2 and annealing at 600 °C for 30min.

Formation of the nanopillars

The ordered metal nanoparticles on silicon substrate were used as masks for further reactive ion etching. By the latter process, it is possible to remove the upper layer of the silicon substrate while the metal nanoparticles remain intact due to their high resistance to the ion etching. The longer the etching, the deeper the silicon is removed and hence silicon nanopillars can be formed with metal nanoparticles on the top of the pillars as shown in Figure 20. SEM micrographs show that the nanopillars keep a straight line in height. The regularity of the array of the nanopillars is kept during the process since it is similar to the regularity of the metal nanoparticles.

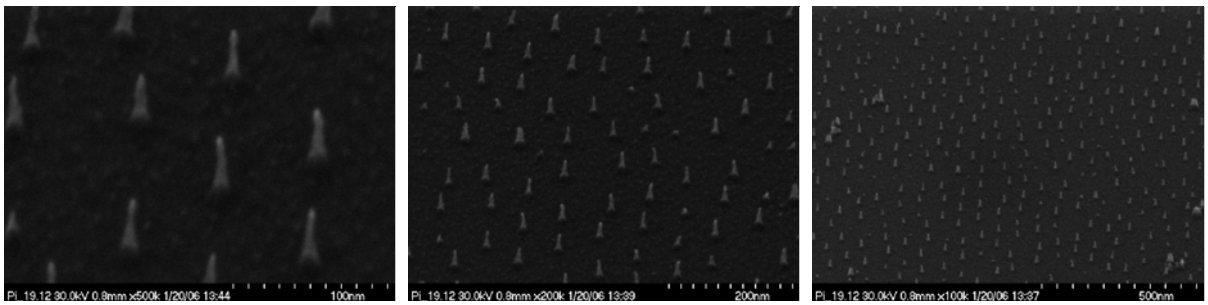

Figure 20. SEM micrographs of silicon nanopillars made by Reactive Ion Etching with etched particles as masks. The metal clusters are still visible on the top of the nanopillars.

Thus, hydrophobic metal complexes can be encapsulated in a polymer particle matrix via direct miniemulsion polymerization. In the presence of platinum (II) acetylacetonate the smaller polydispersity in size was observed for a medium amount of SDS surfactant. The particles can be assembled in one ordered monolayer on silicon substrate simply upon drying of a diluted latex. When plasma-etching is carried out on these metal complex/ polystyrene particles, the polystyrene is removed and the metal complex is reduced to its metal to one spot located in the center of the former particles. Ordered array of metal nanoparticles are created where the distance between the metal spots is controlled by the diameter of the hybrid particles. The ordered nanoparticles are subsequently used as a mask for reactive ion etching. The latter process gives rise to silicon nanopillars.

In further experiments, it should be possible to control the diameter of the polymer particles with the miniemulsion technique. It would be also interesting to control in a wider range the amount of metal complex inside the particles. A more suitable method of latex deposition on surfaces should be applied to maximize the area where the particles assemble in ordered array on the substrate [**Bur**_1997], [**Goe**_1998]. Finally, the described technique could be applied

for different metal complex, especially to form ordered arrays of the very interesting Fe/Co or Fe/Pt nanoparticles.

4.1.1.3. Free-radical polymerization initiated by borohydrides in direct miniemulsion

Despite the fact that metal borohydrides are widely used in inorganic chemistry and organic chemistry as efficient reducing agents, they are seldom used in the polymer chemistry field. Several groups studied the polymerization of non-vinyl monomer by lanthanide complexes of borohydrides. Recently, the ability of sodium borohydride to initiate the free-radical polymerization of styrene in a direct emulsion polymerization process was demonstrated [**Jan**_2004]. Yields of about 30% were obtained, whereas a combination of this new initiator with iodomethane or iodoethane gave satisfactory yields of 99+%. The iodo-compound played hence a significant role as chain-transfer agent to increase the reactivity of the radicals produced. The borohydride salts as initiators are interesting because they are relatively cheap. Besides, it may be possible to use them both as initiator and as reducing agent in a tandem reaction. There is an increasing interest in tandem or "one-pot" synthesis, which allows complex materials to be easily synthesized. The main advantage of such synthesis is the decrease of the separation steps, hence a lowering of the cost of production and of energy consumption.

Thus, we decided to use the borohydride compounds to polymerize monomers in miniemulsion processes. We checked the reactivity of different borohydride salts, namely lithium, sodium and potassium borohydride. The nature and quantity of the chain-transfer agent was changed, whereas we kept constant the surfactant, namely SDS, and the amount of the surfactant and the continuous phase. The nature of the continuous phase was varied thanks to the addition of different carrier solvent soluble in the water continuous phase to study its influence on the conversion. The best results were considered to be the experiments that gave the higher yields. Alternatively, the polydispersity index of the molecular weight of the resulting polymer was also carefully checked since we thought the polymerization could proceed via a quasi-living radical mechanism.

Characteristics of the polymerization

We carried out experiments with different monomers; styrene, MMA (entry B1 of Table 5) and vinyl acetate as monomers (entry B2). We studied then the influence of different chain transfer agent on the yield: iodomethane, perfluorhexyl iodide (entry B9), iodoform (entry B10), iodoacetonitrile (entry B14), iodophenol (entry B11), iodoaniline (entry B12), N-

bromosuccinimide (entry B13) and indium (III) chloride (entries B15 and B16). N-bromosuccinimide was tried because it is known to be an efficient thermal iniferter [**Zho**_2005]. Iniferters are initiators for radical polymerization. The usual different steps of a radical polymerization in the presence of an iniferter are: initiation, propagation, primary radical termination, and transfer to initiator. The polymerization can be a controlled radical polymerization if the end groups of the polymer synthesized with a suitable iniferter serve further as a polymeric iniferter. We thought N-bromosuccinimide could be then a suitable transfer agent for our system. Indium (III) chloride was chosen because it is known to form active species with sodium borohydride [**Ran**_2003].

Experiments were performed with the lithium (entry B6), the sodium, and the potassium borohydride (entry B5) as initiators of the polymerization. As shown in the Table 5, only styrene was polymerized efficiently by borohydrides initiators whereas the borohydride system is insufficiently reactive toward vinyl acetate and MMA to polymerize these monomers. We test different chain-transfer or radical reactive compounds, mainly iodo-compounds, to increase the conversion. Only the iodomethane was found suitable. This is again due to the better reactivity of the iodomethane than of the others compounds. Even iodoacetonitrile, which is reactive in polymerizations via degenerative iodine transfer [**Mat**_1995] was found not to be suitable. Jang et al. performed the emulsion polymerization of styrene in the presence of the carrier solvent: triethylene glycol dimethylether (triglyme). Experiments performed with different carrier solvents such as dioxane, diglyme, triethylene glycol monomethyl ether, diisopropylamine and N-methylpyrrolidone (21 wt.% compared to the overall continuous phase) showed that the conversion was not better with carrier solvent than without in our miniemulsion system. In fact, on the contrary to the emulsion polymerization mechanism, the miniemulsion polymerization operates via droplet nucleation and thus there is no need to increase the solubility of the active species in the continuous phase. Different borohydrides were tested and they can be classified by order of increased yield: KBH_4>$NaBH_4$>$LiBH_4$ (see Table 8). This classification is the inverse of the traditional classification of the activity of the borohydrides, which correlates to the order of increased reactivity for reduction reactions of organic compounds: $LiBH_4$<$NaBH_4$<KBH_4. For instance, lithium borohydride reduce esters of relatively active carboxylic acids while sodium borohydride do not. This is solely a polarizing effect of the metal ion.

Table 5. Characteristics of the miniemulsion polymerizations initiated by borohydrides salts.

Entry	Monomer	Chain transfer agent	Initiator	Yield (%)
Influence of the monomer				
B1	MMA	iodomethane	$NaBH_4$	7.1
B2	vinyl acetate	iodomethane	$LiBH_4$	13.9
B3	vinyl acetate	perfluorhexyl iodide	$LiBH_4$	5.1
B4	styrene	iodomethane	$NaBH_4$	83.7
Influence of the chain-transfer agent				
B5	styrene	iodomethane	KBH_4	90.4
B6	styrene	iodomethane	$LiBH_4$	40.5
B7	styrene	iodomethane/5	$NaBH_4$/5	38.1
B8	styrene	iodomethane/2	$NaBH_4$	30.1
B9	styrene	perfluorhexyl iodide	$NaBH_4$	27.4
B10	styrene	iodoform	$NaBH_4$	36.2
B11	styrene	iodophenol	$NaBH_4$	36.1
B12	styrene	iodoaniline	$NaBH_4$	17.7
B13	styrene	N-bromosuccinimide	$NaBH_4$	17.2
B14	styrene	iodoacetonitrile	$NaBH_4$	8.6
B15	styrene	indium (III) chloride: 5,5.10-4 mol^{-1}	$NaBH_4$	unstable miniemulsions
B16	styrene	indium (III) chloride: 4,5.10-5 mol^{-1}	$NaBH_4$	1.8

Stability of the droplets

Every miniemulsions prepared with organic transfer agent were stable. Thanks to the good stability of the system, monodispersed polystyrene latexes could be obtained as shown in Figure 21. However, the miniemulsion of sample B15 was unstable, probably because of the large quantity of the trivalent salt indium (III) chloride in the continuous phase. The concentration of indium salt is superior to the critical coagulation concentration of the droplets and thus the salt destabilizes the miniemulsion droplets.

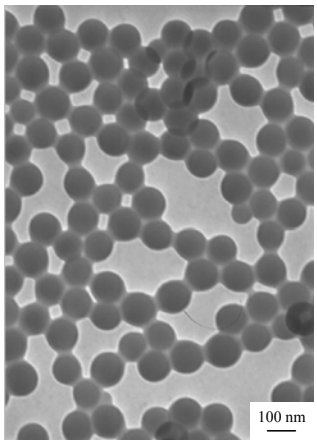

Figure 21. TEM micrographs of the sample B4.

Molecular weight and molecular weight polydispersity of the polymer

If some iodo-coumpounds are added to a monomer, controlled radical polymerization can occur via a degenerative iodine transfer mechanism. This approach was also tested successfully in miniemulsion [**Lans**_1999]. Nevertheless, the authors found that the polymerization was better controlled, and consequently the polydispersity of the molecular weight decreases, when the initiation takes place in the droplet and not in the continuous phase. As shown in Figure 22, the polymerization with borohydrides did not occur as a quasi-living or controlled radical polymerization. In fact, one important consequence of a living radical system is that the plot of the molecular weight versus the conversion should be linear. This is not the case in our system but we observe an increase in the molecular weight during time, which is also contradictory to a pure free-radical polymerization mechanism. As a consequence of this non perfect living radical mechanism, the polydispersity of the molecular weight of the samples was found to be high as determined by GPC (see Table 6). In our case the polydispersity of the molecular weight is always much larger than 2, which is typical for a free-radical polymerization process. Therefore, we confirmed the results of Jang et al. done in emulsion [**Jan**_2004], who showed that the use of sodium borohydride as initiator and iodomethane as transfer agent lead to a broad molecular weight distribution. We obtained also similar molecular weight for the same concentration of initiator and iodomethane. The very low molecular weight and the low yield measured for the sample B12 is similar to the molecular weight and the yield measured by Jang et al. with dodecyl mercaptan as transfer agent. This indication shows that the iodoaniline is not an efficient transfer agent in miniemulsion. The iodoaniline behaves in a similar manner than for the dodecyl mercaptan in the emulsion system of Jang et al. The molecular weight of the sample B9 is also low.

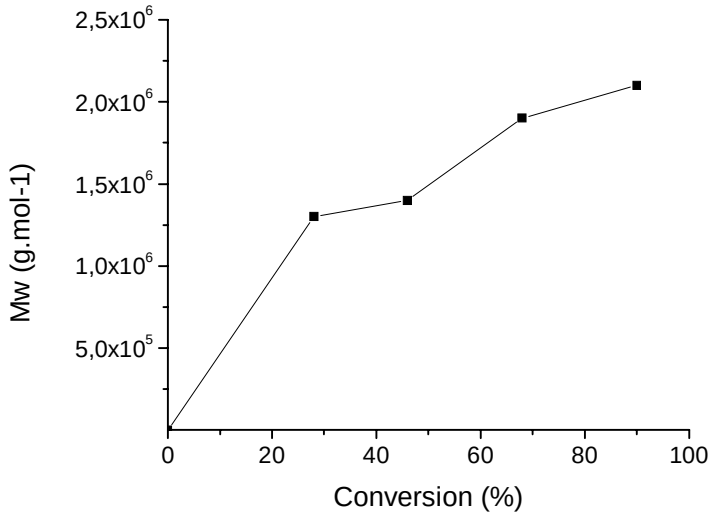

Figure 22. Mass average molecular weight of the polystyrene versus the conversion for sample B5.

Table 6. Molecular weight of the polystyrene made by radical polymerization initiated with borohydrides.

Entry	$M_n \cdot 10^{-5}$ (g·mol^{-1})	$M_w \cdot 10^{-6}$ (g·mol^{-1})	Polydispersity
B4	3.4	1.9	5.6
B5	4.6	2.1	4.5
B6	2.2	1.3	6.0
B7	3.9	1.8	4.6
B8	1.3	1.3	9.9
B9	0.14	0.28	1.9
B10	0.01	0.059	5.6
B12	5.2	1.5	2.8

We showed that sodium and potassium borohydrides are suitable initiators for free-radical miniemulsion polymerizations. With these initiators, satisfactory yields are obtained (>90%) if they are in the presence of iodomethane as a transfer agent. Polymer particles are obtained with high molecular weight and a broad molecular weight distribution.

4.1.1.4. Free-radical copolymerization with a surfactant in direct miniemulsion

In the present work, we studied the behaviour of one anionic polymerizable polyethylene-polypropylene based surfactants, the Tego XP-1008, which structure is shown in Figure 23, in

miniemulsion polymerization. First, we examined the influence of the amount of polymerizable surfactant on the polymerization yield, average particle size and molecular weight of the resulting latexes. Additionally, the effect of monomer composition was studied. The anionic Tego XP-1008 could be used in order to obtain stable miniemulsions. The polymerization was initiated inside the droplets by using the oil-soluble initiator AIBN. The characteristic data of the latexes stabilized by the Tego XP-1008 are summarized in Table 7.

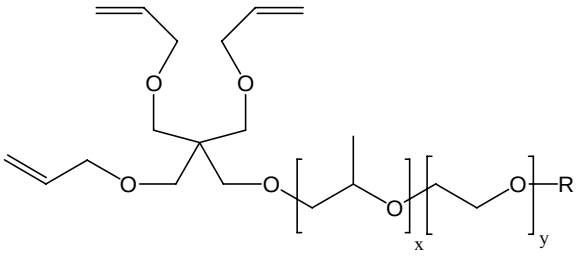

Figure 23. Structure of the anionic polymerizable surfactant Tego XP-1008 with R = phosphate.

Table 7. Characteristics of the miniemulsion latexes in the presence of Tego XP-1008.

Sample	Surfactant (wt.%) *	Initiator	Monomer (s) (g)		Diameter (nm)**	Surface tension ($mN \cdot m^{-1}$)	Solid content (%)	M_w ($g \cdot mol^{-1}$)
			Nature	Mass (g)				
1	0.6	AIBN	S	6	200	68	17	44 790
2	1.1	AIBN	S	6	166	67	19	47 810
3	1.2	AIBN	S	6	150	68	20	59 450
4	2.25	AIBN	S	6	126	65	20	93 570
5	2.8	AIBN	S	6	112	67	20	84 670
6	3.9	AIBN	S	6	109	66	20	91 590
7	5.3	AIBN	S	6	98	66	19	85 740
8	7.8	AIBN	S	6	86	65	19	85 840
9	10.4	AIBN	S	6	88	62	18	104 100
10	2.9	AIBN	S	3	129	67	15	69 880
			BA	3				
11	4.5	AIBN	S	3	112	65	20	73 260
			BA	3				
12	2.9 (SDS)	AIBN	S	3	76	69	20	95 660
			BA	3				
13	4.5 (SDS)	AIBN	S	3	66	68	19	95 020
			BA	3				
14	1.1	KPS	S	6	151	68	20	52 260

* amount related to the dispersed phase; ** diameter determined by DLS measurements

Characteristics of the surfmer Tego XP-1008

The CMC was determined using the Du Noüy ring method. The CMC was calculated to be $4.9 \cdot 10^{-5}$ mol·l^{-1} at 23 °C as shown in Figure 24. The value of the CMC is low as expected for a polymeric surfactant.

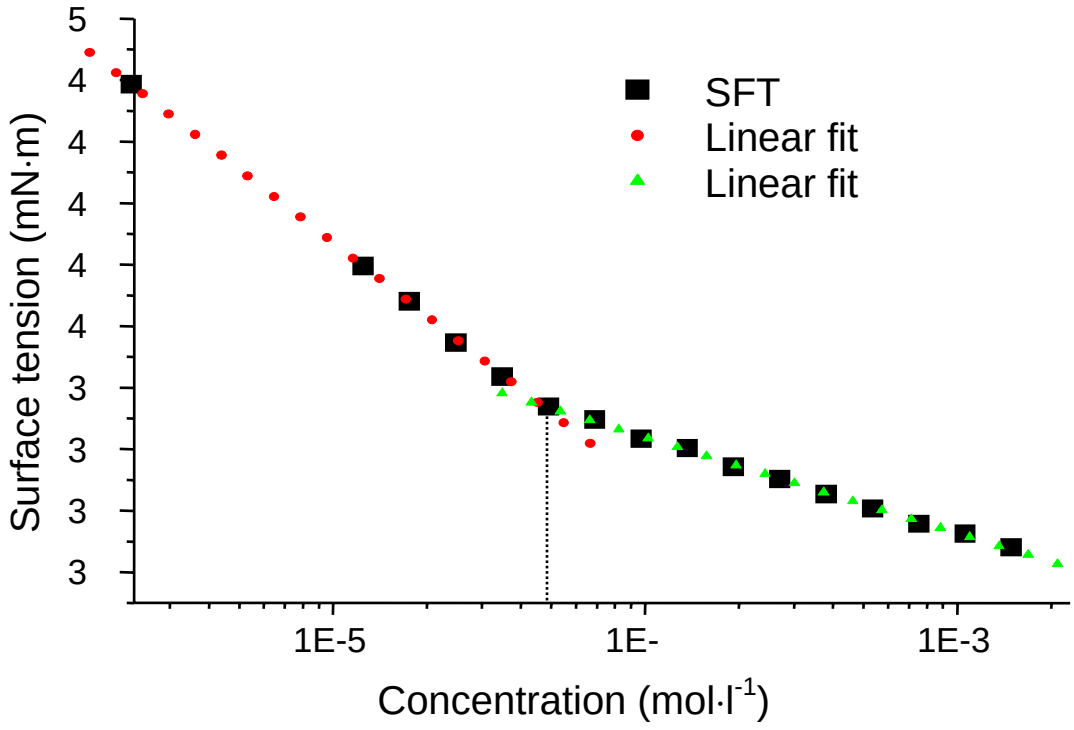

Figure 24. Plot of the surface tension versus the concentration of surfactant added in the solution.

Polymerization in the presence of the surfmer Tego XP-1008

According to the solid content measurements, high conversions were obtained after the polymerizations, indicating that the polymerizable surfactants do not interfere negatively with the radical polymerization reaction.

Stable particles with a diameter of 200 nm could be obtained by using only 0.6 wt% of surfactant. This diameter is almost twice as large as the diameter obtained by SDS which can be explained with a lower hydrophobicity of the PPO chain compared to the $C_{12}H_{25}$-chain. With increasing surfactant amount, the particle size decreases as expected.

The log-log plot of the hydrodynamic diameters versus the concentration of surfactant (Figure 25) indicates that the size of the particles decreases quasi-linearly with the amount of surfactant employed in the miniemulsion polymerization. This behavior is similar to the one

observed with conventional surfactants [**Lan**_2003]. However the particles are larger than in the case of other ionic surfactants like SDS or CTMA-Cl. This can be attributed to the nature of the surfactant where on the PEO-PPO chain, one phosphate group is located. GPC measurements listed in the Table 7 show that the molecular weight is quite low, but slightly increasing with increasing surfactant concentration from M_w = 50 000 to 100 000 g·mol^{-1}. The quite high surface tension of the latexes obtained with Tego XP-1008 (see Table 7) is independent on the amount of surfactant. This indicates a low concentration of molecular surfactant dissolved in the continuous phase, which is due to the grafting of the surfactant onto the polymer particles.

Also copolymer particles consisting of styrene and butyl acrylate can successfully be stabilized (samples 10 and 11). Here, the particle size is slightly larger compared to the pure styrene stabilized with the same surfactant (Tego XP-1008), and much smaller than the comparable SDS stabilized samples (sample 12 and 13).

The use of hydrophilic KPS as initiator does not influence the particle size which clearly speaks for a true miniemulsion process where the particle size should be independent of the locus of initiation (sample 14).

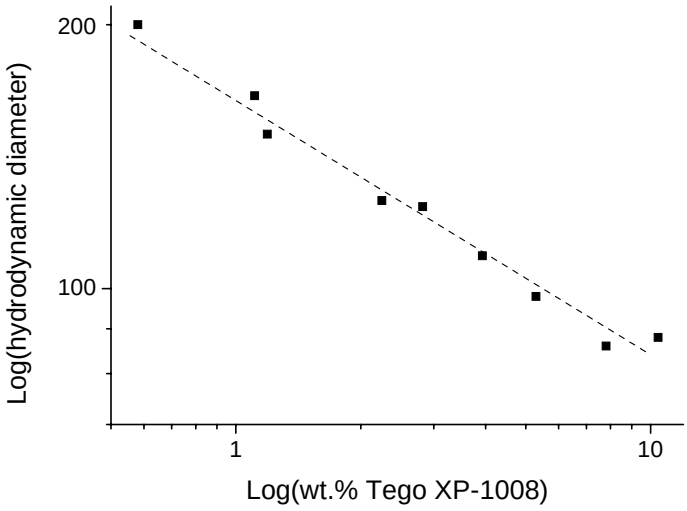

Figure 25. Evolution of the hydrodynamic diameter in function of the amount of Tego XP-1008.

Stability of the miniemulsions

In the case of using Tego XP-1008, the use either of AIBN or KPS as initiator leads to the stable particles with no significant change in the particle size. Photon correlation spectroscopy was also applied to study the behaviour of the latexes synthesized with Tego XP-1008 toward

the addition of NaCl solutions (Figure 26). The measurements were performed at several concentrations of the salt solutions, allowing us to find the critical coagulation concentration (CCC) of the latex by dichotomy. For latexes stabilized with Tego XP-1008 the CCC values were found by extrapolation of the curves presented in Figure 26: CCC = 0.25 $mol \cdot l^{-1}$ and 0.28 $mol \cdot l^{-1}$ for sample 4 and 5.

In addition, all latexes show high stability during dialysis experiments, which is expected from the surfactant covalently bonded to the particles.

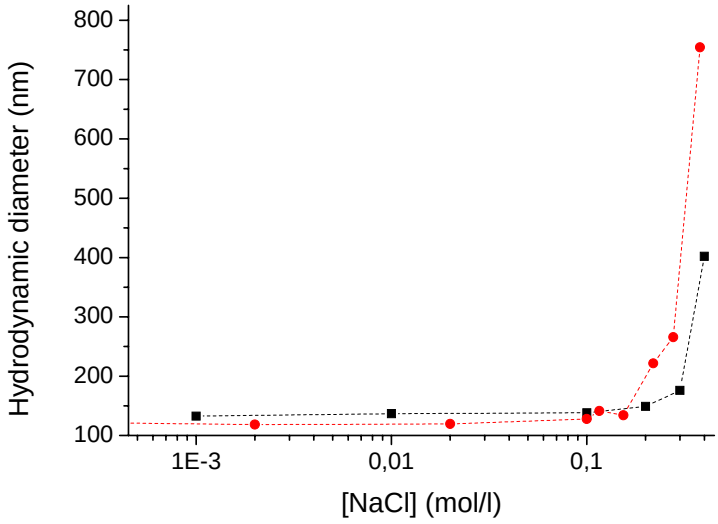

Figure 26. Evolution of the hydrodynamic diameter of latex 4 (black dot) and 5 (red dot) upon addition of electrolyte (Tego XP-1008 used as surfactant).

Grafting of the polymerizable surfactant onto the particles

^{1}H NMR spectroscopy was carried out on the latexes to check the reactivity of the double bonds of the surfmer towards the polymerization as shown in Figure 27. It could be shown that the double bonds of the surfactant are completely converted in all the samples.

Furthermore, XPS measurements were conducted on the latex particles obtained with Tego XP-1008 in order to investigate the grafting efficiency of the surfmer onto the particle surfaces. We performed XPS on three different samples: one not dialysed reference sample prepared with SDS as a surfactant, and two dialysed latex samples, i.e. sample 2 (low concentration of surfmer) and sample 5 (high concentration of surfmer). Unfortunately, the phosphor atom of the surfmer could not be seen with accuracy for the sample 2. Nevertheless, results shown in Figure 28 provide information on the oxygen atom content, which is more present in the surfmer. In fact, oxygen is contained in the oligo(ethylene oxide) and oligo(propylene oxide) parts. As expected for a successful grafting of the surfmer onto the particles, sample 5 has a higher oxygen content than sample 2. Both samples contain more

oxygen than the non-dialysed sample prepared with SDS, which contains four atoms of oxygen in its molecule. This means that a high amount of surfmer is still on the particles despite the repeated dialysis.

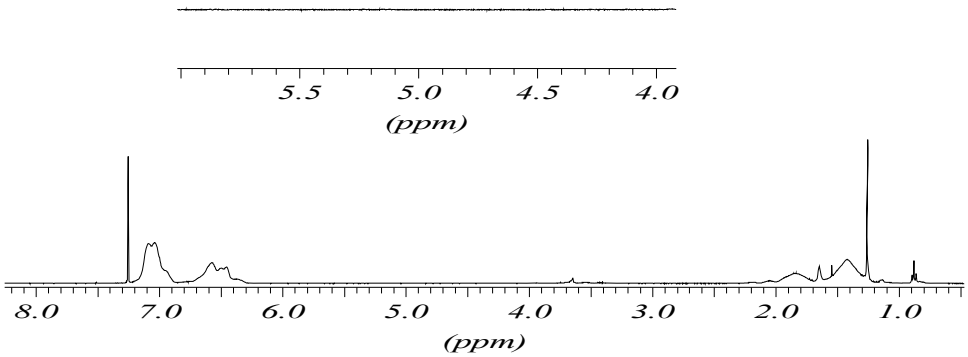

Figure 27. Typical proton NMR spectrum of dialyzed polystyrene latexes synthesized with Tego XP-1008. We can observe that the double bonds of the surfactant are converted.

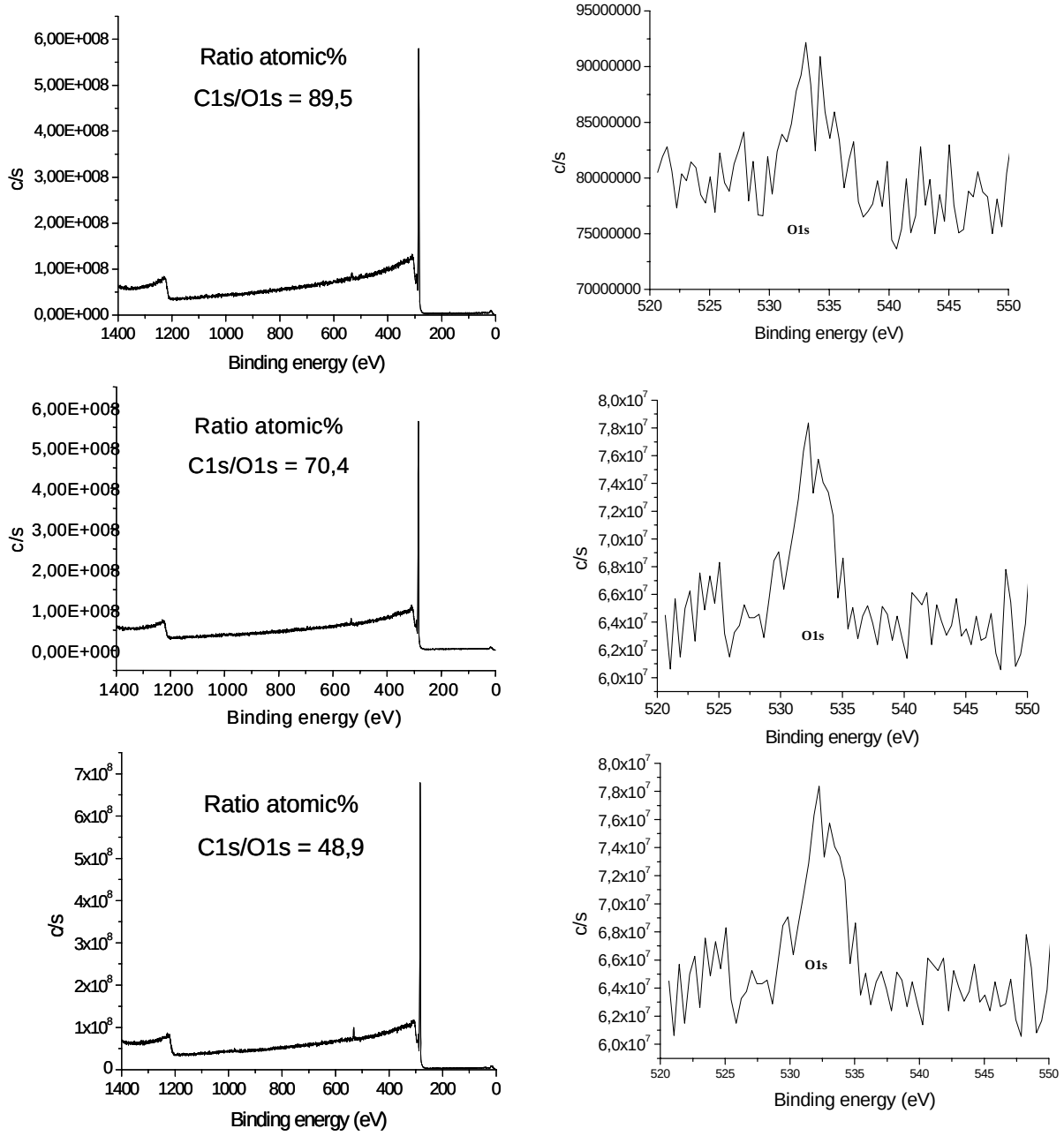

Figure 28. a-f XPS spectra of the polymers, ratio atomic % and focus on the O1s signal; **a-b** sample with SDS, **c-d** sample 2, **e-f** sample 5.

Morphology of the particles

The morphology of the nanoparticles was analyzed by TEM analysis. In the case of Tego XP-1008, the particles are monodisperse, as seen in the TEM of sample 5 in Figure 29.

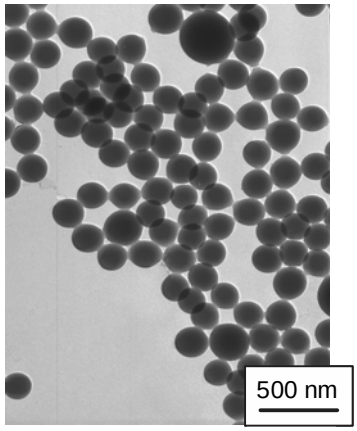

Figure 29. TEM micrograph of the polymer particles: sample 5.

Synthesis of nanocapsules

In a next step, the anionic polymerizable surfactant Tego XP-1008 was used for the preparation of hollow nanocapsules by the miniemulsion technique. As reported earlier, nanodroplets consisting of the hydrophobic oil and the monomer were created, if during the polymerization phase separation occurs since the polymer is immiscible with the hydrophobe, thus allowing the formation of the polymeric shell [**Tia2**_2001].

In the case of Tego XP-1008, hexadecane was used as hydrophobic oil. The polystyrene latex stabilized by 2.2 wt% (sample 15) of the surfmer results in a mixture of capsules and polymer particles (approximately 50/50% in number as detected by TEM, see Figure 30a). With increasing amount of surfactant, the average particle size and also the average molecular weight decrease, but there was still a mixture of nanocapsules and particles as it can be detected by TEM measurements (sample 16 and 17). The reference cited above [**Tia2**_2001] indicates clearly that the encapsulation is facilitated by the use of either a more hydrophilic monomer than styrene (e.g. MMA), or the addition of a hydrophilic comonomer. In reference [**Luo**_2004], capsules of polystyrene are produced also with the help of an additional hydrophilic monomer. Thus, we used divinylbenzene as the monomer, which is more hydrophilic than styrene. TEM micrographs in Figure 30 and the SEM micrographs in Figure 31 show clearly a hollow capsule structure. With increasing amount of surfactant to 5.2 wt%, the nanocapsule size can be decreased from 240 nm to 190 nm. The relatively high values of the surface tension reported in Table 8 indicate that the hexadecane is not present at the air surface and thus did not demix with the water phase. To our knowledge, it is the first time that a synthesis of hollow capsules in a presence of a polymerizable surfactant is reported. The SEM micrographs shown in Figure 31 confirm the success of the synthesis.

Table 8. Characteristics of the miniemulsion latexes for synthesis of the capsules

Sample	Surfactant (wt%) *	Initiator	Monomer/ hexadecane (g/g)	Diameter (nm) **	Surface tension ($mN \cdot m^{-1}$)	Solid content (%)	M_w ($g \cdot mol^{-1}$)
15	2.2	AIBN	Styrene: 3 HD: 3	174	60	10	70 460
16	3.9	AIBN	Styrene: 3 HD: 3	150	58	10	31 390
17	5.2	AIBN	Styrene: 3 HD: 3	146	57	9	29 570
18	2.3	AIBN	DVB: 3 HD: 3	241	60	10	X
19	4.0	AIBN	DVB: 3 HD: 3	195	60	10	X
20	5.2	AIBN	DVB: 3 HD: 3	187	58	10	X

* amount related to the dispersed phase

** diameter determined by DLS measurement

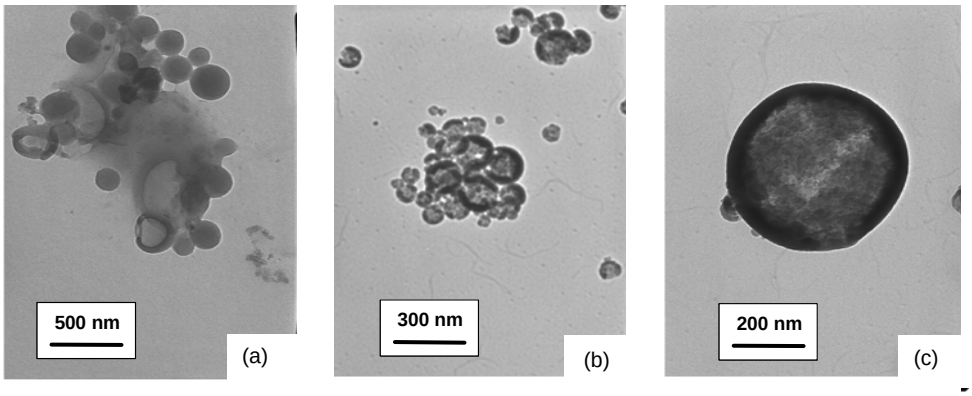

Figure 30a-c. TEM micrographs of the polystyrene and poly(divinylbenezene) capsules; **a** sample 15 (PS), **b-c** sample 18 (PDVB).

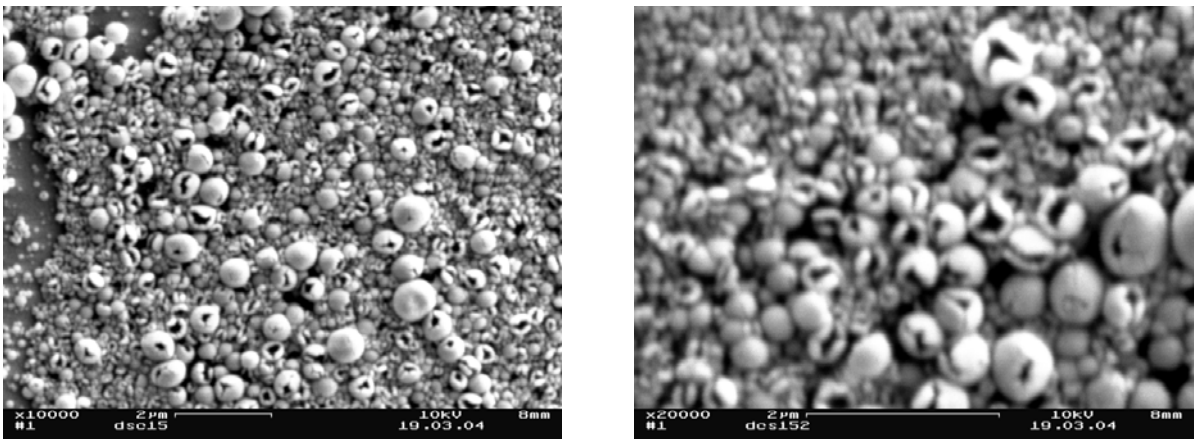

Figure 31. SEM micrographs of the poly(divinylbenezene) capsules from sample 18.

In conclusion, we synthesized latexes by miniemulsion polymerization in the presence of polymerizable surfactants. Polystyrene and poly(styrene-co-butyl acrylate) particles stabilized by these surfactants were found to be stable. The plot of the particle size of the latexes versus the concentration of surfactant had the same appearance than with the normal non-polymerizable surfactants. XPS measurements performed on dialysed samples show that the polymerizable surfactant was grafted onto the surface of the latexes during the polymerization. These results demonstrate well the efficiency of the polymerizable surfactants investigated. Remarkably, stable nanocapsules could be synthesized with the anionic surfactant Tego XP-1008 when using divinylbenzene as a comonomer.

4.1.2. Free-radical polymerization in inverse miniemulsion

4.1.2.1. Miniemulsion polymerization at high temperature

The stability of dispersed systems is a primordial topic in emulsion science. Concerning miniemulsions, studies refer usually to the influence of the concentration and nature of surfactant and osmotic pressure agent [**Sch**_2005], and of the concentration of salt in direct systems on the stability of the droplets. The temperature of the miniemulsion polymerization described in the literature exceptionally exceeds 100 °C; Cunningham et al. reported radical polymerization controlled by nitroxides in direct miniemulsion at 135 °C in a pressurized reactor [**Cun**_2002]. Industry and academy are interested in performing polymerization at high temperature since it heighten the polymerization rate, hence lowering the cycle time of the industrial process [**USP**_BASF]. Moreover, some polymerizations are only possible at high temperature. Thus, we investigated the behavior of the miniemulsion polymerization at high temperature (≥ 150 °C) under atmospheric pressure. Obviously, direct systems with water as continuous phase are not adapted to such conditions. We investigated the more promising inverse systems, which would allow high temperature reactions to occur in the mini-droplets and allow the use of water-sensitive chemicals.

Several surfactant systems with low HLB were tested in miniemulsion. For comparison, the HLB were evaluated according either to the Griffin or Davies calculations. The HLB of a non-ionic surfactant according to Griffin can be calculated as follow: $HLB_{(Griffin)} = 20*M_H/M$; where M is the molecular weight of the surfactant, and M_H the molecular weight of its hydrophilic part [**Gri**_1954]. The HLB according to Griffin are then between 0 (no hydrophilic part) and 20 (no hydrophobic part). The calculated Griffin´s HLB values for our surfactant are less than 10 and can be classified in the order of increased HLB: Lubrizol® U <

Brij® 72 < Span® 80 < P(B/E-*b*-EO). However, the immediate remark upon these calculations is that the HLB does not depend on the chemical structure of the surfactant but rather of the relative molecular weight of the hydrophilic part compared to the overall. Thus, the Griffin´s HLB may not be adapted to our system since we have different chemical structures for the hydrophilic part of our surfactants (pentamine for the Lubrizol® U, sorbitan ring for the Span® 80). We evaluated the HLB according to Davies, which are calculated as follow: $HLB_{(Davies)} = 7+mH_h+nH_l$ [**Dav**_1963]. *m* is the number of hydrophilic groups H_h and n the number of lipophilic groups H_l. The values H_h and H_l are tabulated and depend on the chemical structure of the hydrophilic or lipophilic groups. As shown in Table 9, the HLB values obtained are also low. The HLB of the P(B/E-*b*-EO) was found to be negative, i.e. super-hydrophobic, which is inconsistent with the proven amphiphilic nature of this molecule. The Davies´s HLB calculation is not suitable for polymeric surfactant since the contribution to the HLB of the B/E part is too big compared the properties of the P(B/E-*b*-EO) molecule.

Initial studies showed that a poly[(butylene-*co*-ethylene)-*b*-(ethylene oxide)] P(B/E-*b*-EO) consisting of a poly(butylene-*co*-ethylene) block (M_w = 3700 g·mol^{-1}) and a poly(ethylene oxide) block (M_w = 3600 g·mol^{-1}) was the thermally most stable stabilizer among a set of surfactant with low HLB (see Table 9).

Table 9. Decomposition temperature of some surfactant according to TGA measurements performed under nitrogen atmosphere. The HLB values were evaluated according to the Griffin and the Davies method [**Lag**_1997].

Name		Formula	HLB	Decomposition temperature °C
Acronym	Brij® 72	$C_{18}H_{37}(OCH_2CH_2)_nOH$, n~2	Griffin 5.87	271
Chemical name	polyethylene glycol octadecyl ether		Davies 1.01	
Acronym	Span® 80	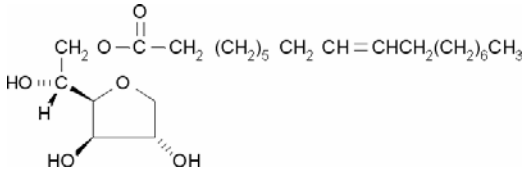	Griffin 6.19	285 (20 wt.%) 406 (80 wt.%)
Chemical name	sorbitan monooleate		Davies 8.025	
Acronym	Lubrizol® U	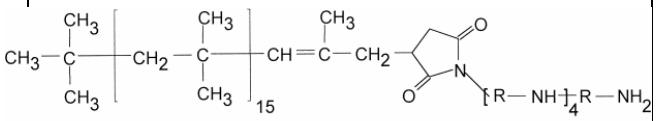 R = C_2H_4	Griffin 4.6	156 (6 wt.%) 270 (54 wt.%) 405 (40 wt.%)
Chemical name	polybutene-succinimide pentamine		3.325	
Acronym	P(B/E-*b*-EO)	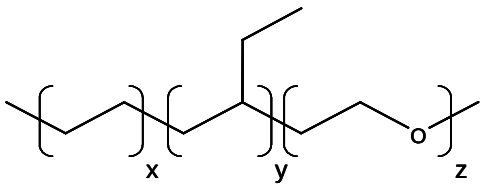 $M_{(x+y)}$ ~3700 g.mol^{-1}, M_z ~3600 g.mol^{-1}	Griffin 9.86	417
Chemical name	poly[(butylene-*co*-ethylene)-*b*-(ethylene oxide)]			

We investigated the temperature stability of some inverse miniemulsions with Isopar M as continuous phase. Miniemulsions were prepared at atmospheric pressure and at different temperatures: 150, 170, and 200 °C, depending on the dispersed phase used. We selected the following suitable dispersed phase/ continuous phase systems: DMSO/ Isopar M, 2-pyrrolidone/ Isopar M, ethylene glycol/ Isopar M and 1-vinyl-2-pyrrolidone/ Isopar M. The influence of a salt as lipophobe (K_2CO_3) and of an additional hydrophilic stabilizer (PVP ~ 40 000 g·mol^{-1}) was also investigated. We used the DMSO at 150 °C because of its "low" boiling point of 189 °C, and the 1-vinyl-2-pyrrolidone at 150 °C and at 170 °C. Let us notice that these temperatures are lower than the temperature of autopolymerization of the 1-vinyl-2-pyrrolidone (~200 °C). Using 2-pyrrolidone as dispersed phase allowed us to investigate the miniemulsions at 150 °C, 170 °C, and 200 °C. The results are summarized in Table 10.

The droplet size was always measured at room temperature on cooled samples at different time between 10 min and 1000 min by DLS. When the sample was found to be unstable after a certain time, it was not further measured and the heating was stopped. As shown in Table 10, there are two general behaviour of the dispersed phase toward the high temperature. The DMSO and the 2-pyrrolidone dispersed phase are further stabilized (see Figure 32) thanks to the polyvinylpyrrolidone stabilizer (with DMSO: DK27 at 150 °C; with 2-pyrrolidone: DK14 at 150 °C, DK11 at 170 °C, DK33 at 200 °C), which is put as additional surfactant to the P(B/E-*b*-EO). Without PVP as stabilizer, the droplet size increases with time from 484 to 1169 nm using DMSO as dispersed phase at 150 °C, or the miniemulsions are already unstable after 10 min at higher temperatures (DK13 at 150 °C, DK12 at 170 °C and DK39 at 200 °C). Adding some additional P(B/E-*b*-EO) surfactant to the formulation lead to the same observation, i.e. an unstable system (DK39). If a lipophobe such as K_2CO_3 is added to the minimulsion of 2-pyrrolidone in Isopar M without addition of PVP, the system is also unstable (DK31 at 150 °C, DK at 150 °C, and DK35 at 200 °C).

Consequently, with DMSO and 2-pyrrolidone as dispersed phase, the miniemulsions were only stable when PVP (~3.2 wt. % compared to the dispersed phase) was added to the system, and the droplets keep a constant size during time as shown in Figure 32. However, when PVP was used as the sole stabilizer (without P(B/E-*b*-EO) surfactant), no stable miniemulsion could be formed (DK38).

Table 10. Characteristics of the miniemulsions at high temperature.

Entry	Dispersed phase	Temperature °C	Stabilizer		Diameter (nm) *	
			Nature	Amount (mg)	t_{10}	t_{1000}
DK28	DMSO	150	P(B/E-*b*-EO)	75	484	1169
DK27	DMSO	150	P(B/E-*b*-EO) PVP	75 50	331	328
DK13	2-pyrrolidone	150	P(B/E-*b*-EO)	75	622	X
DK31	2-pyrrolidone	150	P(B/E-*b*-EO) K_2CO_3	75 25	739	X
DK14	2-pyrrolidone	150	P(B/E-*b*-EO) PVP	75 50	137	180
DK12	2-pyrrolidone	170	P(B/E-*b*-EO)	75	451	424
DK	2-pyrrolidone	170	P(B/E-*b*-EO) K_2CO_3	75 25	632	X
DK11	2-pyrrolidone	170	P(B/E-*b*-EO) PVP	75 50	177	182
DK36	2-pyrrolidone	200	P(B/E-*b*-EO)	75	1334	X
DK35	2-pyrrolidone	200	P(B/E-*b*-EO) K_2CO_3	75 25	650	X
DK39	2-pyrrolidone	200	P(B/E-*b*-EO)	125	657	X
DK38	2-pyrrolidone	200	PVP	125	unstable	X
DK33	2-pyrrolidone	200	P(B/E-*b*-EO) PVP	75 50	271	272
DK34	2-pyrrolidone	200	P(B/E-*b*-EO) PVP K_2CO_3	75 50 25	184	182
DK16	1-vinyl-2-pyrrolidone	150	P(B/E-*b*-EO)	75	217	513
DK15	1-vinyl-2-pyrrolidone	150	P(B/E-*b*-EO) PVP	75 50	193	410
DK29	1-vinyl-2-pyrrolidone	150	P(B/E-*b*-EO) K_2CO_3	75 25	153	176
DK26	1-vinyl-2-pyrrolidone	150	Span 80 K_2CO_3	75 25	unstable	X
DK25	1-vinyl-2-pyrrolidone	150	Span 80 PVP	75 50	unstable	X
DK24	1-vinyl-2-pyrrolidone	150	Brij 76 K_2CO_3	75 25	unstable	X
DK23	1-vinyl-2-pyrrolidone	150	Brij 76 PVP	75 50	unstable	X

Entry	Dispersed phase	Temperature °C	Stabilizer		Diameter (nm) *	
			Nature	Amount (mg)	t_{10}	t_{1000}
DK18	1-vinyl-2-pyrrolidone	170	P(B/E-*b*-EO)	75	327	694
DK19	1-vinyl-2-pyrrolidone	170	P(B/E-*b*-EO)	50	348	790
DK20	1-vinyl-2-pyrrolidone	170	P(B/E-*b*-EO)	25	642	1500
DK17	1-vinyl-2-pyrrolidone	170	P(B/E-*b*-EO) PVP	75 50	441	689
DK9	1-vinyl-2-pyrrolidone	170	P(B/E-*b*-EO) PVP	50 50	572	790
DK10	1-vinyl-2-pyrrolidone	170	P(B/E-*b*-EO) PVP	25 50	903	X
DK30	1-vinyl-2-pyrrolidone	170	P(B/E-*b*-EO) K_2CO_3	75 25	175	413
DK22	1-vinyl-2-pyrrolidone	170	Brij 72 K_2CO_3	75 25	unstable	X
DK21	1-vinyl-2-pyrrolidone	170	Brij 72 PVP	75 50	unstable	X

* hydrodynamic diameters determined by DLS after 10 minutes (t_{10}) and after 1000 minutes (t_{1000})

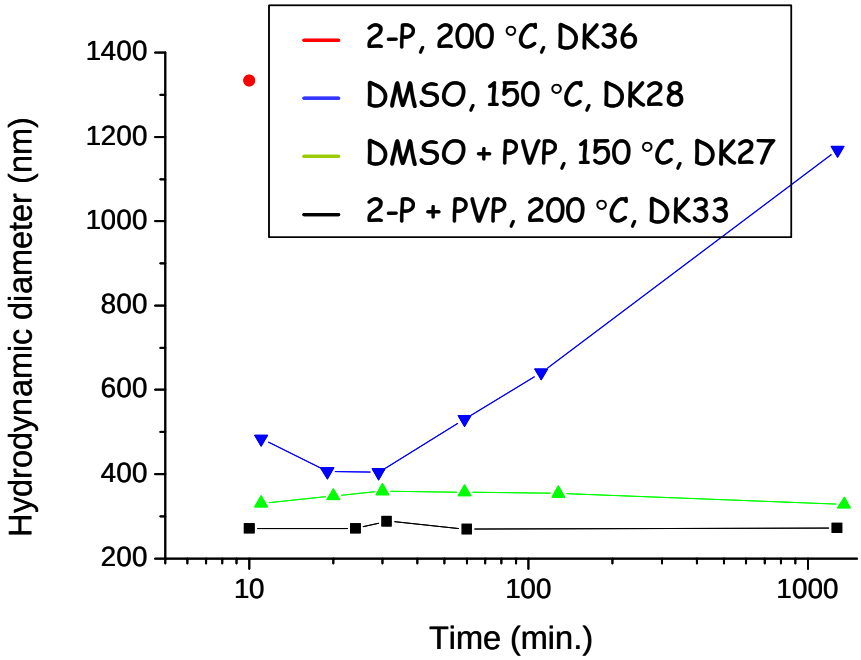

Figure 32. Influence of the presence of the additional PVP on the stability of the miniemulsions for two different dispersed phases: DMSO at 150 °C and 2-pyrrolidone at 200 °C.

In the case of 1-vinyl-2-pyrrolidone as dispersed phase, the effect of additional stabilization by the PVP is sensibly less marked since the additional PVP cannot prevent completely the increase in size of the droplets with time. In fact, the hydrodynamic diameters of the samples additionally stabilized by PVP at 150 °C (DK15), and at 170 °C (DK17), increase with time. Samples prepared with lower amounts of surfactant with (DK9, DK10) or without PVP (DK19, DK20) were also not stable. On the contrary to what was observed with 2-pyrrolidone as dispersed phase, the osmotic pressure agent K_2CO_3, which stabilizes the droplets of 1-vinyl-2-pyrrolidone was chosen because it is soluble in 2-pyrrolidone and 1-vinyl-2-pyrrolidone; a constant droplet size is kept at 150 °C for this system (DK29), while the droplet size at 170 °C increases (DK30), but in a lower manner than without K_2CO_3 (DK18, DK17). This experimental study has the additional interest to provide information about the stability of emulsions at high temperature. As shown in the Theoritical Part (2.1.4.2.), the miniemulsions are stabilized against both coalescence and Ostwald ripening. The stability at high temperature is very difficult to predict theoretically since many terms of the Ostwald ripening equation depends on this parameter. In fact, the rate of Ostwald ripening $d(D^3)/dt_a$ in a miniemulsion can be written as follows:

$$d(D^3)/dt_a = 64\sigma D_{opa} V_m C_{opa}(\infty)/(9RT\Phi_{opa})$$

where D is the average droplet diameter, t_a is the aging time, σ the dispersed/ continuous phase interfacial tension, V_m the molar volume of the dispersed phase, D_{opa} the molecular diffusivity of the osmotic pressure agent, $C_{opa}(\infty)$ the solubility of the bulk osmotic pressure agent in the continuous phase and Φ_{opa} the volume fraction of the osmotic pressure agent in the dispersed phase. The instability at high temperature with DMSO and 2-pyrrolidone as dispersed phase is probably due to the coalescence of the droplets and not the Ostwald ripening since the lipophobe salt plays no role in the stabilisation of the droplets in these conditions. In the case of the DMSO and the 2-pyrrolidone as dispersed phase, the PVP chains seem to partially "replace" the PEO chains of the P(B/E-*b*-EO), which become hydrophobic at high temperature. In the case of 1-vinyl-2-pyrrolidone, the Oswald ripening plays a role in the destabilization of the droplets at 150 °C since the osmotic pressure agent K_2CO_3 stabilizes efficiently the system. However, at higher temperature (170 °C), destabilization due to coalescence of the droplets cannot be avoided. Thus, the best stabilizer at high temperature for DMSO and 2-pyrrolidone is the PVP, whereas the K_2CO_3 stabilizes more efficiently miniemulsions with 1-vinyl-2-pyrroldione as dispersed phase at temperature ≤ 170 °C. For

higher temperature with 1-vinyl-2-pyrrolidone, Ostwald ripening could not be completely suppressed.

Polymerization of 1-vinyl-2-pyrrolidone

In order to illustrate the principle of reactions in miniemulsion at high temperature, we polymerized 1-vinyl-2-pyrrolidone at high temperature; 90 °C for entry DC660, 120 °C for entry DC679 as shown in Table 11. The particle size was similar for these two samples as shown in Table 11 and was 112 nm and 108 nm for entries DC660and DC679 respectively. For such application, the V-40 initiator whose structure is shown in Figure 33 was found more suitable than the AIBN initiator for this polymerization, since V-40 is more hydrophobic and better soluble in Isopar M than AIBN. Miniemulsions polymerizations of 1-vinyl-2-pyrrolidone performed at 160 °C lead to high conversion of the monomer (>99% determined by gravimetry) and to stable monodisperse particles as shown in Figure 34a-b.

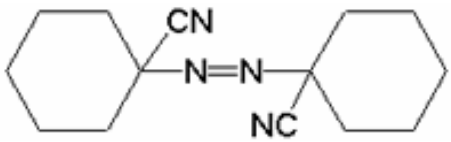

Figure 33. Structure of the V-40 initiator.

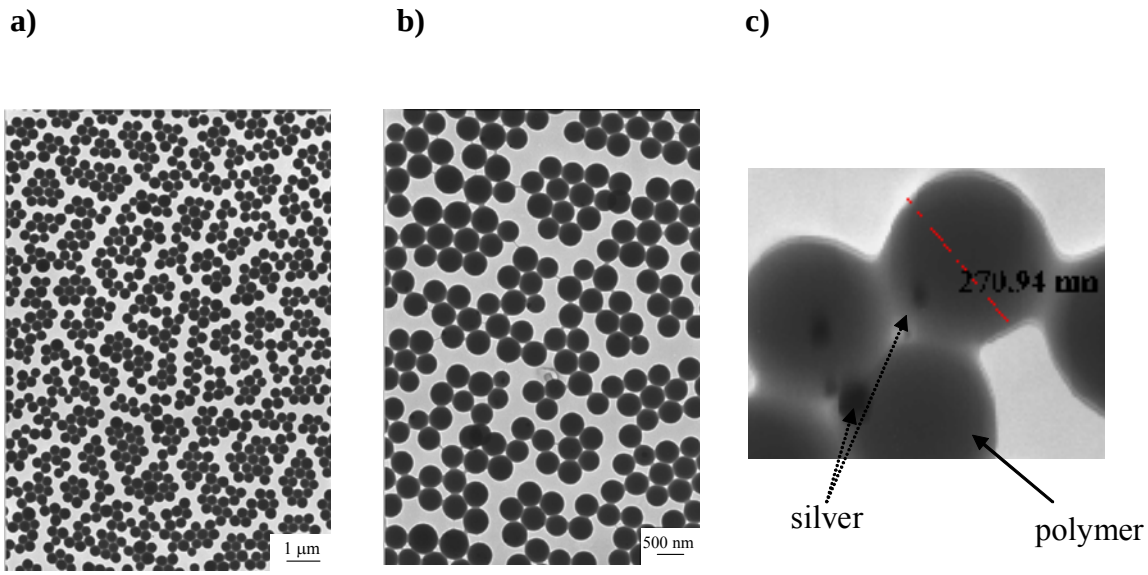

Figure 34a-c. a-b: TEM micrographs of a poly(vinylpyrrolidone) latex made at 160 °C (DC699); **c**: and of the silver nanoparticles/ polyvinylpyrrolidone hybrid latex (DC680).

Synthesis of silver/ polyvinylpyrrolidone hybrid latexes

The principle of reaction at high temperature in miniemulsion can be pushed one step further. We can use the droplets of 1-vinyl-2-pyrrolidone as nanoreactors and then polymerize them. Silver nitrate can be dissolved in the monomer. The introduction of ethylene glycol in the droplets of 1-vinyl-pyrrolidone allowed first the use of these droplets as nanoreactors to reduce silver nitrate into silver nanoparticles thanks to the so-called "polyol process". The "polyol process" is a solution phase process that allows the reduction of silver salt to silver nanoparticles [**Sun**_2002] or silver nanowires [**Sun2**_2002] by ethylene glycol at temperature close to 200 °C in the presence of PVP as sole stabilizer. In a second step, we polymerized the 1-vinyl-2-pyrrolidone droplets as shown in Table 11. It gives a hybrid latex where silver nanoparticles are embedded in polyvinylpyrrolidone matrix particles as shown in Figure 34.

The temperature has no strong influence on the droplet size for the same droplet composition as shown in Table 11 where DLS measurements were performed at room temperature on samples synthesized at different temperatures and after the reduction of silver nitrate. On the other hand, the droplet composition has a strong influence on the size. The droplets containing more ethylene glycol were bigger and this was observed independently from the temperature. At 120 °C, for the same amount of surfactant, PVP and silver nitrate, the droplet size increased from 120 nm for a sample containing 12 wt.% of ethylene glycol compared to the dispersed phase (DC704) to 314 nm for a sample with 71 wt.% of ethylene glycol (DC703). The amount of silver nitrate was also varied but did not lead to significant difference in term of silver nanoparticles diameter. As expected for a miniemulsion process, a decrease of the amount of surfactant from 75 mg to 50 mg leads to an increase of the particle size from 120 nm to 170 nm (samples DC704 and DC702 respectively). The increase of the amount of PVP (DC698) or the decrease of the amount of silver nitrate (DC680) in the droplets did not change significantly the droplet size.

Table 11. Characteristics of the miniemulsion polymerization of 1-vinyl-2-pyrrolidone with the eventual reduction of silver nitrate by ethylene glycol inside the miniemulsion droplets.

Entry	Temperature °C	Ethylene glycol (g)	1-vinyl-2-pyrrolidone (g)	PVP (mg)	$AgNO_3$ (mg)	P(B/E-*b*-EO) (mg)	Diameter (nm)*
DC660	90	0	1.5	20	0	75	112
DC702	120	0.2	1.3	50	70	50	170
DC704	120	0.2	1.3	50	70	75	119
DC703	120	1.15	0.35	50	70	75	314
DC679	120	0	1.5	50	0	75	108
DC680	160	0.1	1.4	50	30	75	139
DC697	160	0.2	1.3	50	70	75	153
DC698	160	0.2	1.3	100	70	75	171
DC700	160	1.15	0.35	50	0	75	204
DC701	160	1.5	0	50	70	75	318

Deposition of the hybrid silver/ polyvinylpyrrolidone latexes on a surface

The latexes were deposited and subsequently submitted to a plasma-etching process as described earlier in the part 4.1.1.2. The etching process successfully removed the polymer as shown in Figure 35. However, the order of the silver nanoparticles after etching is not as good as with the particles reported in 4.1.1.2. (see Figure 35).

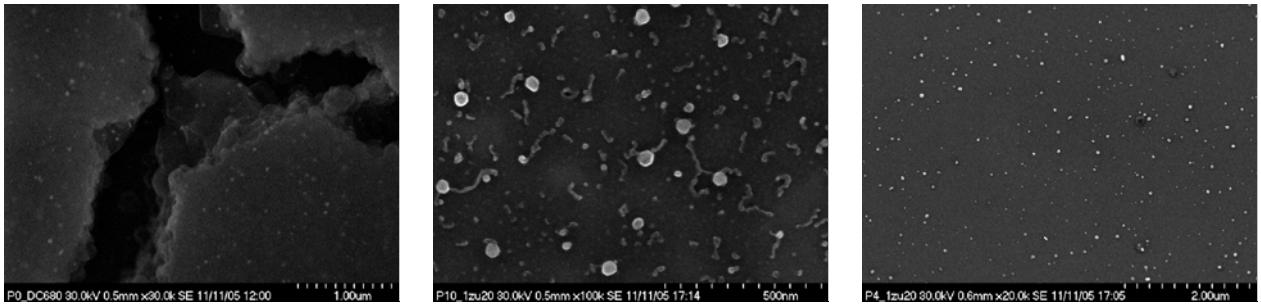

Figure 35. Silver nanoparticles/ poly(vinylpyrrolidone) hybrid particles (DC697) after plasma-etching.

In order to understand the reason of this behavior, we observed the hybrid latex deposited on TEM grids at different time. We found that the particles coalesced after three days at room temperature as shown in Figure 36. The particles made hence films, which cannot induce an ordering of the metal cluster during the plasma-etching. We believe that the particles coalesce because of residual high boiling point materials, namely the ethylene glycol and the Isopar M, which act as plastifiers for the polyvinylpyrrolidone polymer. Thus, the glass transition temperature decreases and the system can form films at room temperature.

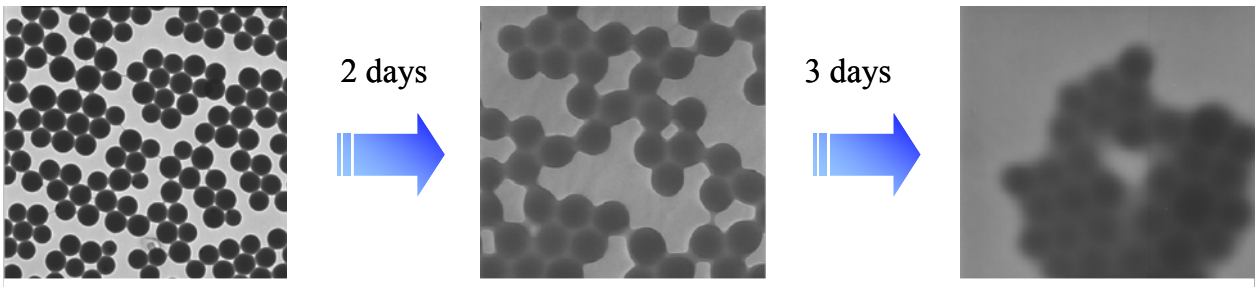

Figure 36. TEM micrographs of the poly(vinylpyrrolidone) latex at different time after preparation of the TEM grid.

4.1.2.2. Synthesis of nanocapsules via inverse free-radical miniemulsion polymerization

Tiarks and al. showed the versatility of the miniemulsion technique to obtain polymeric nanocapsules [**Tia2**_2001]. These polymer nanocapsules were synthesized via free-radical polymerization in a direct system. Some other authors used this technique and focused their studies on the mechanism of formation of capsules [**Luo**_2004], and on the encapsulation of biocompatible material [**Raj**_2003]. However, up to now, there is no description of the synthesis of nanocapsules in inverse miniemulsion. Yet an important part of the drugs are hydrophilic and thus it would be suitable to find a process, which allows the encapsulation of hydrophilic substances in polymeric drug-delivery carriers. We showed for the first time that it was possible to synthesize nanocapsules with an aqueous core via free-radical miniemulsion polymerization. The monomer N-N´-methylenediacrylamide and the hydrophilic KPS initiator were dissolved in water and then dispersed via ultrasonication in a solution of P(B/E-*b*-EO) surfactant in cyclohexane so as to build an inverse miniemulsion. The monomer was then polymerized by heating the miniemulsion. We produced nanocapsules of poly(N-N´-methylenediacrylamide) with a water core dispersed in cyclohexane. The characteristics of the latexes are shown in Table 12.

Table 12. Characteristics of the miniemulsion poylmerization of N-N´-dimethylacrylamide.

Entry	Monomer (g)	Water (g)	Continuous phase	P(B/E-*b*-EO) (mg)	Diameter (nm) *
I1	0.15	1.3	cyclohexane	50	242
I2	0.2	1.3	cyclohexane	50	253
I3	0.2	1.3	cyclohexane	75	202
I4	0.2	1.3	toluene	50	188

* determined by DLS

As expected, the size of the nanocapsules was found to be dependent on the amount of surfactant. Up to now, the wall thickness of the capsules could not be changed. In fact, the solubility of the N-N´-methylenediacrylamide in water is too low and hence the amount of monomer in dispersed phase cannot be significantly varied. The wall thickness determined by TEM micrographs of the entry I1 and I2 of the Table 11 showed the same wall thickness because the difference in the amount of monomer is too small to give a significant difference in the wall thickness. It is also possible to use toluene as continuous phase for the formation of the nanocapsules (entry I4). The formation of the nanocapsules shown in Figure 37 results from the precipitation of the polymer at the interface of the aqueous droplets. It is a similar mechanism as the one reported in [**Tia2**_2001]. In the method reported by Tiarks et al., the monomer and the hydrophobe are homogeneously distributed in the miniemulsion droplets. The polymer demixes during the polymerization because it is immiscible with the hydrophobe and form a shell at the interface of the miniemulsion droplets, which encapsulate the hydrophobe. We showed successfully that this method can be applied in an inverse miniemulsion.

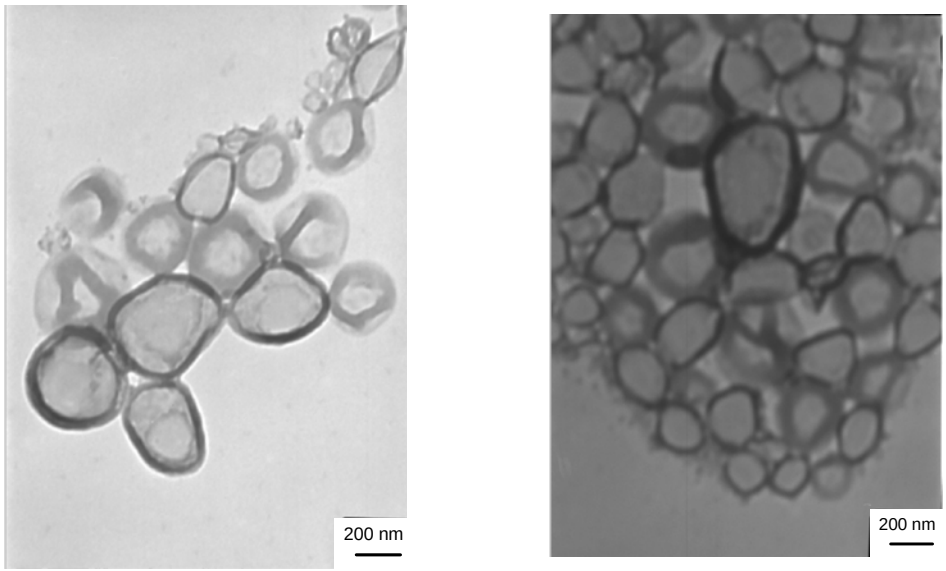

Figure 37. TEM micrographs of the poly(N-N´-methylenediacrylamide) nanocapsules prepared via free-radical polymerization in inverse miniemulsion.

4.2. Anionic polymerization of lactams in miniemulsion and synthesis of polyamide latexes

Polyamide-6 (PA6), also known as nylon-6, is a versatile material that combines excellent properties and competitive price, making it the most used type of polyamide worldwide. PA6 is either synthesized via anionic polymerization, which can be carried out at rather low temperature of 150 °C in the presence of an activator, or via a hydrolytic reaction at much higher temperature of 250 °C under pressure. During the anionic polymerization, an activator is usually added to the ε-caprolactam to speed up the activation step, and therefore the anionic polymerization is much faster than the hydrolytic reaction. The properties of PA6 made via anionic polymerization are affected by the irregularities in the polymer chain because of the side reactions, like Claisen-type condensations, that are occurring during the polymerization of ε-caprolactam. These side reactions are strongly favored by the weak heat exchange with the surrounding medium during a typical bulk polymerization. It is of great interest to synthesize this polymer as nanometer-sized stable particles in a heterophase polymerization in order to allow a more effective heat exchange during the synthesis and to have a material which can be easily processed as stable dispersion.

As shown by the polyaddition and polycondensation experiments in miniemulsion, the miniemulsion process provides the possibility to synthesize submicron particles of functional polymers even by nonradical polymerization. Some anionic polymerizations in heterogeneous media have shown their usefulness to prepare functional latex with an initiation via strong bases, too. We want to show that polymerizations initiated via strong bases can be done using the miniemulsion technique. Thus, we studied the anionic polymerization of ε-caprolactam (CL) in an organic solvent in order to obtain functional polyamide-6 nanoparticles in miniemulsion.

4.2.1. Anionic polymerization of ε-caprolactam

Miniemulsion of Molten and Dissolved ε-Caprolactam.

ε-Caprolactam is a hydrophilic monomer with a high solubility in water of 5200 $g \cdot L^{-1}$ at 25 °C and a melting point of 69 °C [**Lid**_1991]. Because of the high water solubility, direct miniemulsions are not possible, but inverse miniemulsions of ε-caprolactam in a hydrophobic medium should be obtained, either by melting the ε-caprolactam and dispersing it at higher temperature or by dissolving the ε-caprolactam and dispersing it at room temperature. It was

found that a stable (at least for a time scale of observation of several hours) miniemulsion of molten ε-caprolactam as droplets in the paraffinic oil Isopar M as continuous can be obtained at temperatures above 70 °C by using as low as 5 wt.% related to the monomer of the block copolymer P(B/E-*b*-EO). However, for the following polymerization, temperatures of 150 °C are required. At these high temperatures, the miniemulsion with molten ε-caprolactam droplets is extremely unstable, and during polymerization more than 90% of coagulum was obtained. Such instabilities can be assigned to a coalescence of the droplets due to the increased solubility of ε-caprolactam in the continuous phase at 150 °C. Using different osmotic pressure agents like low molecular weight PEO, 1-methyl-2-pyrrolidinone, acetamide, or dimethylacetamide in the polar phase did also not lead to a higher stability of the miniemulsions at the high polymerization temperature.

To overcome the stability problem, the droplets should also contain components which are much more polar and show a lower solubility in paraffinic oil at higher temperature than ε-caprolactam does. Therefore, the polar phase was constituted of ε-caprolactam dissolved in the polar solvent DMSO in a ratio 1:2. The salt sodium caprolactamate, which is produced by adding a small amount of NaH prior to emulsification, is used as initiator and osmotic pressure agent at the same time. Both the salt and the DMSO are more polar and show a lower solubility in the paraffinic oil at higher temperatures than the ε-caprolactam does, and thus it is expected to show a better stability against diffusion processes. A summary of the results is given in Table 13.

A stable miniemulsion was obtained at room temperature in Isopar M by using as low as 4 wt. % of the P(E/B-EO) block copolymer stabilizer compared to the dispersed phase. Then the activator *N*-acetylcaprolactam was added to the mixture and distributed by ultrasonication homogeneously in all the droplets. The miniemulsion was subsequently successfully polymerized at 150 °C obtaining a stable dispersion with particles of about 350 nm. The particles grow a little bit (e.g., from 198 to 226 nm for sample C2) during the heating at 150 °C because of the enhancement of the Ostwald ripening while increasing the temperature. As expected, by increasing the amount of the surfactant P(E/B-EO) in further experiments, a decrease of the particle size was observed (see Table 13, samples C1-4). At 10 wt.% of P(E/B-EO), particles of 150 nm were obtained. Please note that these hydrodynamic diameters are the diameter of the droplets DMSO + PA6 after polymerization dispersed in the continuous phase. The classical miniemulsions give a linear dependence of the logarithm of the hydrodynamic diameter on the amount of surfactant [**Lan**_2001]. Figure 38 shows that a

nonlinear dependence on the amount of surfactant is observed which might be due to the Ostwald ripening instabilities at high temperature.

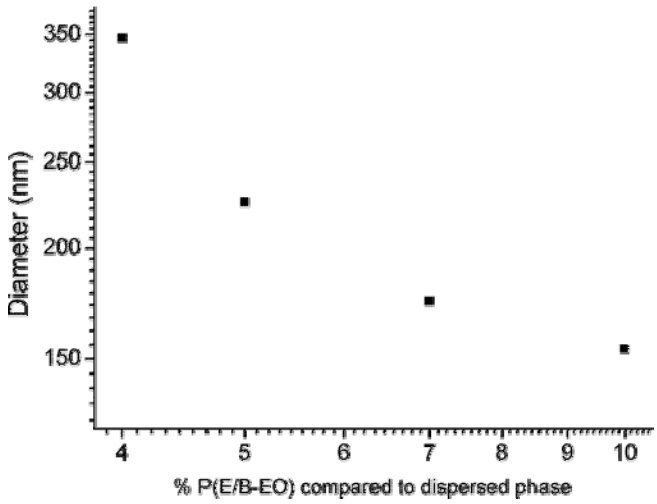

Figure 38. Influence of the amount of surfactant on the hydrodynamic diameter of the droplets.

Using the solvent dimethylacetamide (sample C5) instead of DMSO to dissolve the sodium ε-caprolactamate salt, at the same surfactant concentration of 5%, particles with a higher diameter were obtained than in the case of DMSO. As expected, decreasing the amount of initiator does not affect significantly the droplet size (sample C6). Increasing the ratio ε-caprolactam/DMSO (w/w) in the miniemulsion droplets from 1/2 to 3/5 with the same amount of surfactant relative to the dispersed phase of 5% leads to an increase of the hydrodynamic diameter in sample C7 from 226 to 312 nm. Sample C8 shows that increasing the ratio dispersed phase/continuous phase (w/w) give much bigger droplets (641 nm) for the same ratio of surfactant. The results show clearly that the droplet sizes are very sensitive to the amount of surfactant and to the ratio of the dispersed phase to continuous phase.

As a different continuous phase, decalin was used to allow creating stable particles with higher diameter of about 920 nm (sample C9). Polyisobutylene oil and silicon oil were found not to be suitable as continuous phase to provide stable miniemulsion of dispersed ε-caprolactam in DMSO.

Using acetamide as additional osmotic pressure agent in the sample C10 led to the same particle size, indicating that acetamide does not lead to a more efficient osmotic pressure inside the droplets. Acetamide was chosen because it is polar, has a high boiling point (222 °C at atmospheric pressure), and is inert toward all the reagents used in the process.

Table 13. Composition, yield and hydrodynamic diameters of the miniemulsions of ε-caprolactam.

Sample	Polar solvent	Ratio CL/polar solvent [w/w]	Dispersed phase [%]	P(E/B-EO) [wt.- %]*	Yield (%)	Diameter [nm] **
Variation of the amount of surfactant						
C1	DMSO	1 / 2	20	4	93	347
C2	DMSO	1 / 2	20	5	94	226
C3	DMSO	1 / 2	20	7	95	174
C4	DMSO	1 / 2	20	10	94	154
Variation of the polar solvent in the droplets						
C5	dimethylacetamide	1 / 2	20	5	93	349
Variation of the amount of initiator: 3.3 mg instead of 5 mg						
C6	DMSO	1 / 2	20	5	89	234
Variation of the ratio CL/DMSO						
C7	DMSO	3 / 5	20	5	91	312
Variation of the dispersed content						
C8	DMSO	1 / 2	30	4	90	641
Variation of the continuous phase						
C9	DMSO	1 / 2	20 in decalin	5	91	922
Using of an additional osmotic pressure agent (here: acetamide)						
C10	DMSO	1 / 2	20	5	94	235

* compared to the dispersed phase.

** diameter determined by dynamic light scattering.

Morphology of the Polymer Particles.

The morphology of the particles can be analyzed using TEM. After drying the dispersion and letting the DMSO evaporate, the TEM shows the PA6 particles. The precipitated particles are not spherical but ellipsoidal like and can have an average length (determined from TEM) of 27 ± 2.5 nm (σ = 9.26) and an average width of 14 ± 1.5 nm (σ = 5.58) (see TEM in Figure 39). The average aspect ratio was determined to be 1.93. Interestingly, it seems that the hydrodynamic radius does not have an influence on the geometrical radius of the PA6. This size corresponds nicely to the size which is determined by DLS after dialysis of the dispersion with hexane and Isopar M in order to get rid of the DMSO in the droplets. After dialysis, a particle diameter of 30 nm was detected which can be attributed to the pure polyamide particles.

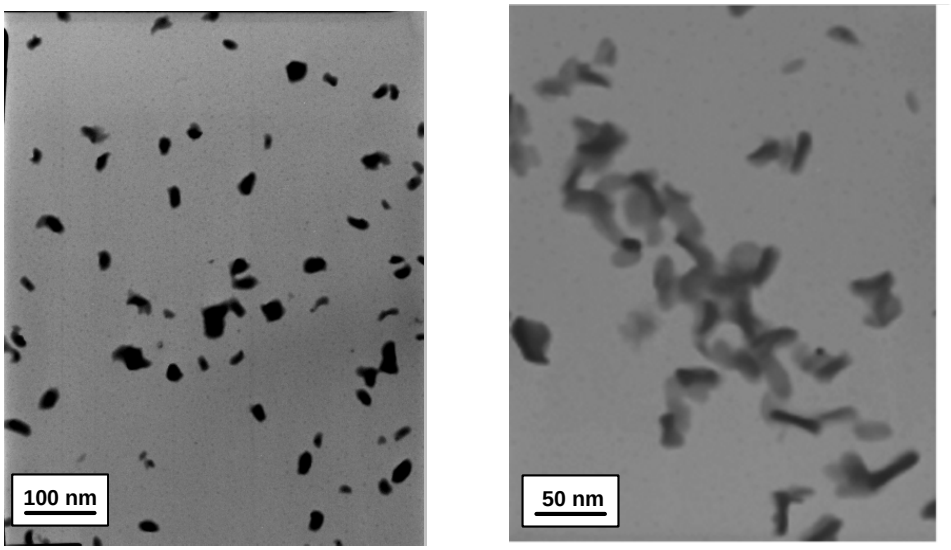

Figure 39. TEM micrographs showing the specific morphology of the PA6 nanoparticles synthesized in miniemulsion.

These special morphologies are due to the demixing between the solvent DMSO and the PA6 during polymerization. Because the PA6 is not soluble in DMSO, the system can be considered as a precipitation polymerization in the miniemulsion droplets. We summarized the principle of the synthesis in Figure 40.

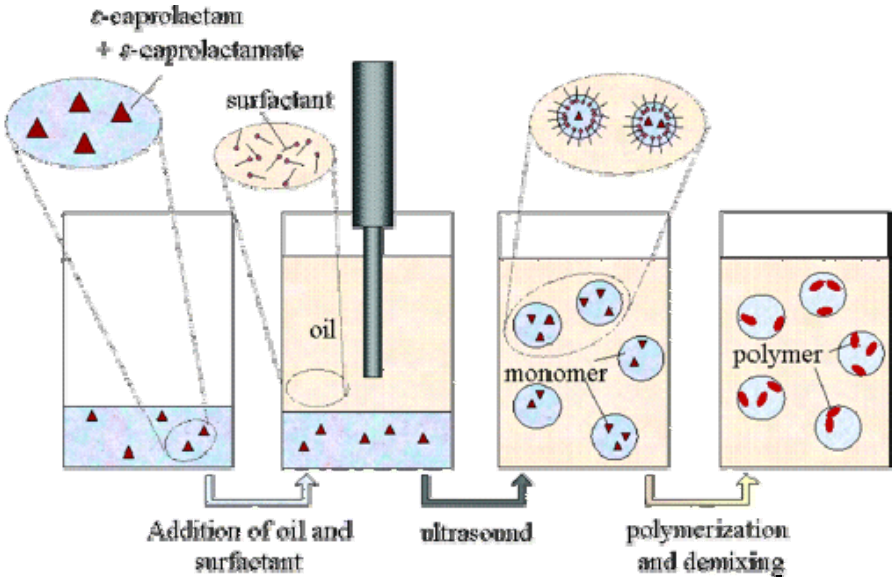

Figure 40. Synthesis of the polyamide-6 nanoparticles.

Molecular Weight of Polyamide-6 in Miniemulsion.

Since PA6 is only insoluble in the most common solvents, typical means like GPC cannot be used for the determination of the molecular weight, but the molecular weight has to be measured by viscosimetry, dissolving the polymer in sulfuric acid. Results are given in Table 14. The molecular weight was calculated using the following equation:

$[\eta] = 0.54 \cdot 10^{-3} \cdot M_v^{0.74}$

where $[\eta]$ is the intrinsic viscosity in $dL \cdot g^{-1}$.

In fact, we obtained relatively high molecular weight polyamide-6 of about 35 000 $g \cdot mol^{-1}$. We obtained an even higher molecular weight in decreasing the amount of initiator in the polar phase with the sample C6. Unfortunately, the yield of polymerization for sample C6 is only 89% compared to the 94% (see Table 13) observed for the other samples. The non-polymer part is known to be a mixture of non-reacted monomer, oligomers, and low molecular weight side products including the cycles [**Ric**_1999]. The molecular weight observed for sample C6 is less than the theoretical expected ones [**Ric**_1999], [**Ric**_2002], which might be due that some of the NaH became inactive or that the polymer precipitation limits the chain length.

Table 14. Influence of the composition of the miniemulsions on the polyamide 6 intrinsic viscosities and molecular weight.

Sample	[η] [dL·g^{-1}]	M_v [g·mol^{-1}]
C1	1.16	34 400
C2	1.19	35 600
C3	1.18	35 200
C4	1.18	35 200
C5	1.15	34 000
C6	1.30	40 100
C7	1.17	34 800
C8	1.15	34 000

As expected, there is no significant enhancement in the molecular weight in increasing or decreasing the amount of surfactant. The bigger molecular weight (sample C6) was obtained for "average values" of surfactant content. This is maybe due to the fact that for the lower content of surfactant the droplets are less stable and that the -OH-terminated PEO part of the surfactant could react with the initiator. That means if the content of surfactant increases, the side reaction occurs more probably.

In most of the studies done on ionic heterophase polymerization (emulsion, miniemulsion), an inisurf was the initiator, and thus the polymerization kinetics was governed by interfacial physiochemical parameters like the adsorption of the inisurf at the interface for instance. When using a Lewis acid surfactant catalyst for the polymerization of *p*-methoxystyrene, the initiation is located at the interface, and it was shown that it was quite difficult to obtain high molecular weight polymer. In such cases, oligomers with a molecular weight of only 1100-1400 g·mol^{-1} were prepared, which is due to the difficulty for the growing oligomer to diffuse inside the droplets and because of the presence of termination or even deactivation of the catalyst [**Tou**_2004]. In the case polymerizing PA6 in the miniemulsion system, the in situ prepared polar initiator sodium caprolactamate is homogeneously dispersed inside the droplets, and therefore a higher molecular weight is obtained.

The structure of our PA6 chains was checked by UV measurements given in Table 15. In fact, the peak of absorbance between 270 and 280 nm is usually considered as proportional as the amount of structural irregularities in the PA6 chains due to side reactions and cross-linking [**Seb**_1976]. The results show that PA6 obtained in miniemulsion has at least 2 times less irregularities as the sample we polymerized in bulk (see Figure 41).

Table 15. Maximum UV-absorbance observed for the PA6 prepared by miniemulsion and in bulk.

Sample	Absorbance max at 270-280 nm
C1	0.026
C2	0.024
C3	0.030
C4	0.027
C5	0.034
C6	0.035
C7	0.055
C8	0.049
Bulk	0.092

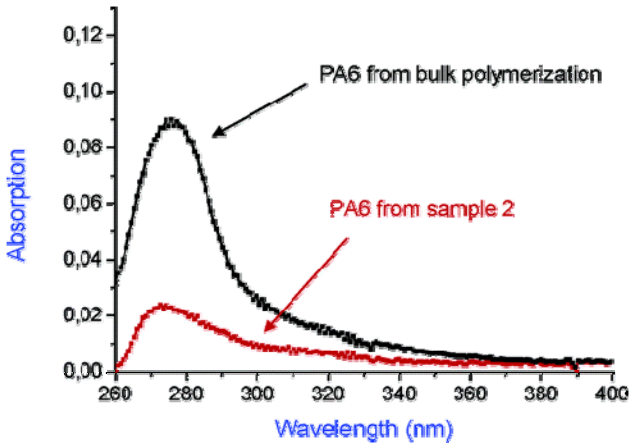

Figure 41. Comparison of UV-spectra of polyamide 6 samples prepared by polymerization of ε-caprolactam in miniemulsion and in bulk. The absorption in the region of the peaks represents the amount of cross-linking and hence structural defect of the material.

Use of different initiators

We investigated also several initiators for the anionic polymerization of ε-caprolactam. Tentative bulk polymerization of the monomer with the super base phosphazene-P_4-tBu failed to give a conversion superior to 10% at 150 °C. The temperature of the system is insufficient

to allow the polymerization to occur efficiently. This observation confirms the results of Memeger et al. who needed a temperature of 200-214 °C to polymerize the ε-caprolactam [**Mem**_1996]. We investigated also the miniemulsion polymerization of ε-caprolactam initiated by dispersions of sodium hydride and sodium. As described in the experimental part, the principle consisted in making a miniemulsion of the monomer, then make a dispersion of either sodium hydride or sodium in Isopar M, and finally mixing both dispersions and let it react at 150 °C. The temperature of 150 °C was fixed as an upper limit for our system owing to the boiling point of the DMSO, which is 189 °C. Unfortunately, this procedure gave unstable miniemulsions with an amount of coagulum superior to 95 wt.% because of the very large size of the sodium hydride and sodium particles (>1μm).

It was shown that nanoparticles of polyamide-6 could be synthesized using the inverse miniemulsion technique. Even though stable molten ε-caprolactam droplets could be created at low temperatures, these droplets show a limited stability at the reaction temperature of 150 °C. Therefore, the monomer ε-caprolactam, the initiator NaH, and the classical activator *N*-acetylcaprolactam were dissolved in DMSO in order to build the polar phase, which was stable after dispersing in the inexpensive isoparaffinic continuous phase also at 150 °C. The use of sodium or sodium hydride dispersions in Isopar M instead of dissolving the sodium hydride in the monomer leads to unstable miniemulsions. During the polymerization, a demixing of the DMSO and the polymer occurred, and the polymer precipitated inside the DMSO droplets, leading to anisotropic nonspherical nanoparticles as revealed by TEM. The polyamide-6 exhibited a relatively high molecular weight of 35 000-40 000 $g \cdot mol^{-1}$ as determined by viscosimetry measurements. The absence of structural defects, which could lead to less good mechanical properties of the polymer, could also be shown. These particles could be used as high-performance anisotropic reinforcement fillers for plastic blends.

4.2.2. Synthesis of polyamide 6 nanoparticles and nanocapsules via two miniemulsion/ solvent displacement techniques

We showed in the previous part that it is possible to obtain polyamide 6 nanocapsules dispersed in oil with the miniemulsion technique. We want to show that it is also possible to obtain polyamide 6 nanoparticles and nanocapsules dispersed in water with an unconventional miniemulsion technique. Because of the very high solubility of the monomers ε-caprolactam or ε-aminocaproic acid in water, we use directly the polymer in our system. A suitable dispersed phase would be only built with the polymer without the presence of a solvent. We

used then a combination of miniemulsion and solvent-displacement technique to synthesize polymer particles dispersed in water.

First process: synthesis of the particles

The process for the preparation of nylon 6 nanoparticles and nanocapsules is based on the different solubility of nylon 6 in formic acid and in water as for a standard solvent-displacement process. For the preparation of the nanoparticles, two different solutions are required: the first one consists of poly(vinyl alcohol) stabilizer dissolved in water or in a water/ methanol mixture, the second one of nylon 6 dissolved in formic acid. This second solution is added dropwise to the first solution while sonicating the system. Since the formic acid is soluble in the water based solution whereas the polyamide is not, the formic acid is diluted in the continuous phase and the polymer precipitates creating a translucent dispersion with probably small unstable precursor particles that coalesce subsequently to form a milky dispersion with the final particles as schematically shown in Figure 42. The final particles are stabilized against coalescence by collisions using an appropriate amount of the stabilizer PVA, which provides steric stabilization of the particles (Figure 42c). The sonication has the role to separated the polyamide chains efficiently from each other and the poly(vinyl alcohol) serves to stabilize the particles. The small operating window available for this system produces stable, low solid content latexes, ranging from 0.2 to 0.4%. We tentatively tried to increase the solid content by increasing the content of nylon 6 in the system but these experiments did not give sub-micron particles. The solid content could be increased to 1% by evaporation of the aqueous phase. However, a further evaporation leads to an instability of the system (precipitation of particles at the bottom and on the walls of the flask).

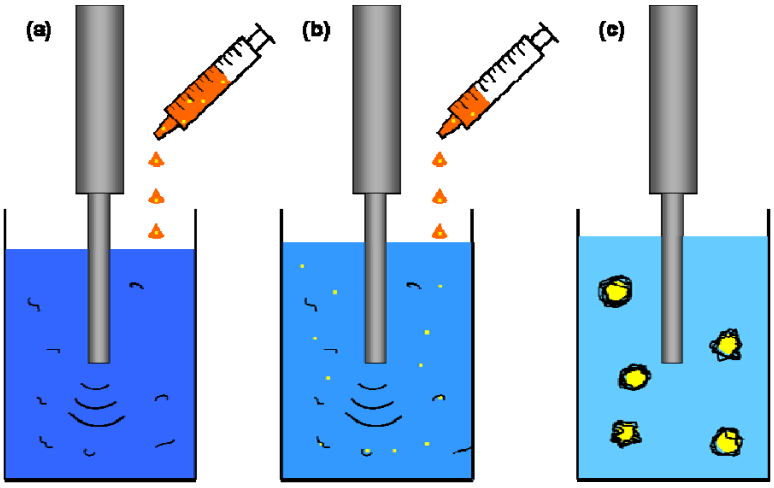

Figure 42a-c. Procedure for the miniemulsion/ solvent displacement technique. **a** addition of nylon 6 dissolved in formic acid to the aqueous continuous phase containing the PVA stabilizer. **b** formation of the precursor particles. **c** nylon 6 particles stabilized by the PVA in the final stage of the process.

Second process: synthesis of the nanocapsules

For the second method, a classical inverse miniemulsion is made first. The dispersed phase is made of the nylon 6 polymer dissolved in formic acid. The continuous phase is cyclohexane. Then the formic acid is reacted with added methanol under the conditions specified in the Experimental Section. The reaction gives water, which replaces the formic acid in the droplet. The reaction gives also the methyl formate, which evaporates. Replacing the dispersed phase from formic acid to water allows the precipitation of the nylon 6 at the interface of the droplets to form nanocapsules as shown in Figure 43. This method is also a kind of solvent-displacement technique. However, we gain significant advantages because we start our solvent-displacement from very stable miniemulsion droplets.

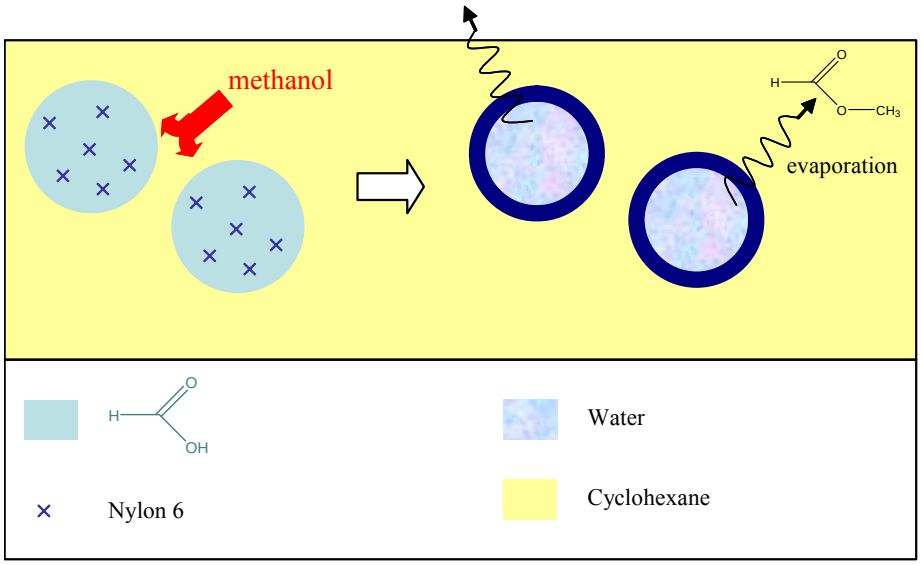

Figure 43. Procedure to make nylon 6 nanocapsules.

First Process: synthesis of the polyamide 6 particles

Influence of the amplitude and the time of sonication

As shown in Table 16, the process produces sub-micron particles only with the help of the ultrasonication, which makes the difference between our procedure and the classical solvent displacement technique. We can also see that the particle size does not depend on the amplitude provided that the amplitude is not too low. Thus, an amplitude of sonication of 15% is the inferior limit in this process. A longer time of ultrasonication leads also to bigger particles, because a longer time of ultrasonication increases the probability of coalescence of the particles and thus increases the average diameter of the particles.

Table 16. Influence of the sonication on the particle size for the PVA 72 000 g/mol with water and methanol (7.5/3 g/g) as continuous phases.

Entry	Type of sonication	Amplitude (%)	Time of sonication (s)	Diameter (nm) *
DC251	No sonication, 7 min addition under magnetic stirring			1900
DC252	No sonication, 30 s addition under magnetic stirring			1573
DC282	direct	70	7	353
DC280	direct	50	7	356
DC281	direct	25	7	381
DC283	direct	15	7	582

* determined by dynamic light scattering

Influence of the nature and quantity of the surfactant or stabilizer

Stable nylon 6 nanoparticles can be synthesized with poly(vinyl alcohol) as stabilizer. Table 17 shows that the particle size depends on the amount of the PVA. With increasing amount of PVA till 24 mg, a decrease of particle size is observed (see DC266, DC211, and DS210). A further increase of PVA leads to larger particles, which is probably due to an increase of the PVA shell thickness. These results differ from those obtained in typical miniemulsion processes, where the size of the droplet or particle decreases with the amount of surfactant [**Ant**_2002], even when PVA is used as the sole stabilizer [**Kim**_2003]. Table 17 shows also the influence of the PVA molecular weight and PVA hydrolysis degree on the particle size. It was found that the lowest particle size was obtained for a medium molecular weight stabilizer (~ 72 000 g/mol, see DC225).

Table 17. Influence of the different types and amounts of PVA on the particle size with water/ methanol mixture as continuous phase.

Entry	PVA molecular weight (g/mol)	Degree of hydrolysis (% mol)	PVA (mg)	Diameter (nm) *
DC266	22 000	98-99	10	839
DC221	22 000	98-99	15	407
DC210	22 000	98-99	24	359
DC267	22 000	98-99	30	730
DC550	40 500	98-99	24	363
DC549	40 500	87-88	24	598
DC225	72 000	98-99	24	292
DC548	155 000	98-99	24	400
DC547	155 000	87-88	24	629

* determined by dynamic light scattering

A higher degree of hydrolysis of the PVA leads to smaller particle size (DC548, DC547), which means that hydrogen bonding between nylon 6 and the stabilizer may be an important factor for the stability of the dispersion. Cesteros et al. studied the hydrogen bonding of poly(4-vinylpyridine)/ poly(vinyl acetate-co-vinyl alcohol) blends by IR-spectroscopy [**Ces**_1993]. It was possible to assign the difference of the IR spectra of the polymer and of the blend due to the hydrogen bonding between the two polymers, especially in the hydroxyl stretching region (3100-3650 cm^{-1}). We found a similar behavior for the IR spectrum as shown in Figure 44. The FT-IR samples were prepared by dissolving KBr in the latexes. The solvents were subsequently evaporated to yield a powder, which was used to make the pellets. The spectrum of the particles shows a shift in the maximum and a wider band in this region

than for the pure PVA because of the presence of additional interactions between the hydroxyl groups of the PVA and the carbonyl groups of the nylon 6.

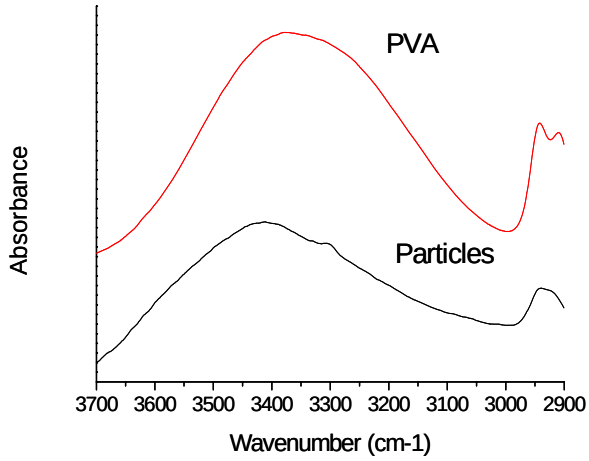

Figure 44. Scale-expanded infrared spectra in the range 2900-3700 cm^{-1} of the PVA 72 000 g/mol, degree of hydrolysis 98-99 (mol %) and the particles of DC225. The shift and the shape of the IR spectra of PVA depend on the hydrolysis degree (see [**Ces**_1993]). Thus, we put here the IR spectra of the particles (PA6+PVA) compared with the spectra of the same PVA: 72 000 g/mol, 98-99 % mol hydrolysis degree.

Apart from PVA, a large variety of other surfactants and stabilizers were used to try to stabilize the dispersions. Surfactants such as SDS, AOT (anionic surfactants), hexadecyltriethylammonium bromide (cationic), Lutensol AT-50 and Pluronic RPE 3130 (non-ionic) did not stabilize the dispersions upon the experimental conditions described above. Stabilizers such as poly(N-vinylpyrrolidone) M_w = 40 000 $g{\cdot}mol^{-1}$, dextran M_w = 70 000 $g{\cdot}mol^{-1}$, poly(acrylic acid) and poly(acrylic acid sodium salt), M_w = 20 000 $g{\cdot}mol^{-1}$ did not result in sub-micron particles.

Thus, the suitable stabilizer for the system is the non-ionic poly(vinyl alcohol) with a medium molecular weight.

Influence of the nature of the continuous phase

Stable sub-microns particles could be obtained without the use of methanol (only water) when using a poly(vinyl alcohol) with a molecular weight M_w of 22 000 $g{\cdot}mol^{-1}$ and a hydrolysis rate of 98-99% (see Table 18). Nevertheless, solutions of poly(vinyl alcohol) with higher molecular weight in water gave bigger particles or even unstable dispersions as shown in Table 18. In fact the difference of hydrodynamic diameter between DC541 and DC256 is 740 nm (see Table 18). As another second solvent, acetone was tried since it is miscible with

water and is easily removable due to its low boiling point. However, using acetone instead of methanol with the standard experimental conditions led to unstable particles (sample DC262).

Table 18. Influence of the nature of the solvents in the standards conditions.

Entry	Second part	(g)	Diameter (nm) *
DC262	PVA 22 000	0.024	unstable
	Water	7.5	
	Acetone	3	
DC255	PVA 22 000	0.024	276
	Water	10.5	
DC256	PVA 22 000	0.048	283
	Water	10.5	
DC542 20mg PA6	PVA 72 000	0.024	935
	Water	10.5	
DC541	PVA 72 000	0.048	1023
	Water	10.5	
DC543 disp. φ*2 (wt.)	PVA 72 000	0.048	1604
	Water	10.5	
DC257	PVA 155 000	0.024	unstable
	Water	10.5	
DC258	PVA 155 000	0.048	unstable
	Water	10.5	
DC213	PVA 22 000	0.024	unstable
	Methanol	10.5	

* determined by dynamic light scattering

Morphologies of the particles produced by the first process

TEM investigations on the particles synthesized by the miniemulsion/ solvent displacement technique in Figure 45 show quasi-spherical morphologies of the particles. In order to have three-dimensional topological information on the particles, we performed SEM measurements. As shown by HR-SEM in Figure 46, the particles present a rough surface. Interestingly, once washed the particles with methanol and water in order to remove the stabilizer, it was possible to look at the nylon 6 particle structure. This structure was found to be bumpy, being visibly the result of agglomerated primary spherical particles as shown in Figure 47. If we suppose that every nylon 6 chains of 19 000 $g \cdot mol^{-1}$ would form spheres because of the bad solvent conditions, the calculation of the diameter of the spheres formed

by one chain of nylon 6 gives around 3.8 nm [**Eli**_2001]. Thus, we believe that the precursor particles discussed previously are the nylon 6 chains contracted in spheres. These spheres agglomerate with one several polymer chains to form the bumpy particles shown in Figure 47. The calculated sphere diameter is slightly smaller than the diameter as shown in Figure 47 since the sphere is the most compact form that the chain would adopt.

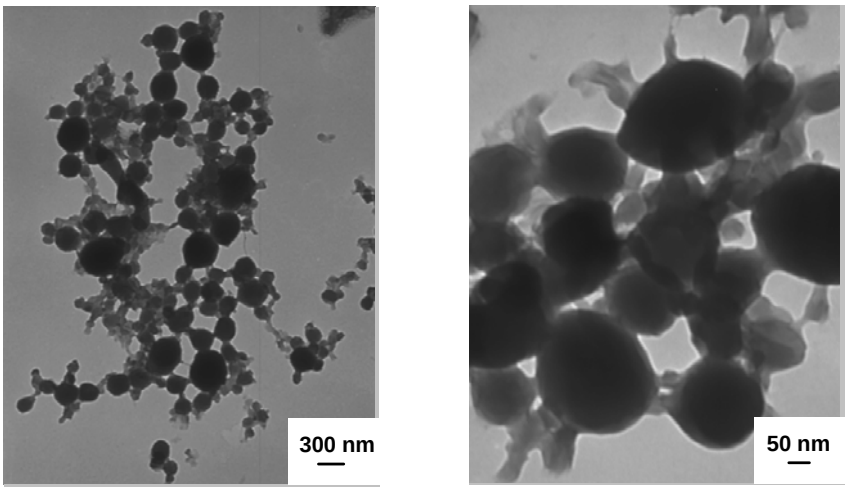

Figure 45. TEM micrographs of the particles from sample DC256.

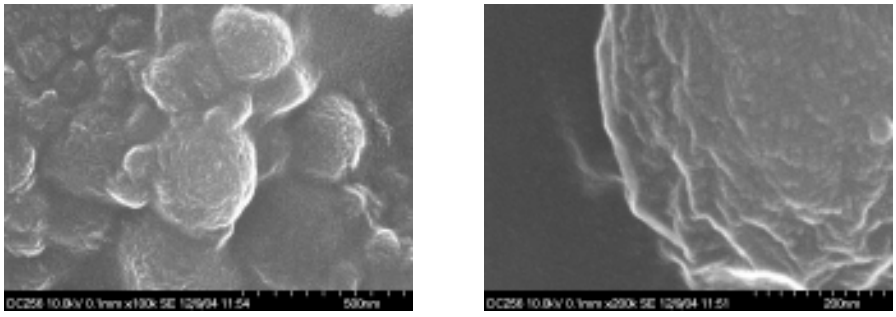

Figure 46. HR-SEM micrographs of the particles from sample DC256.

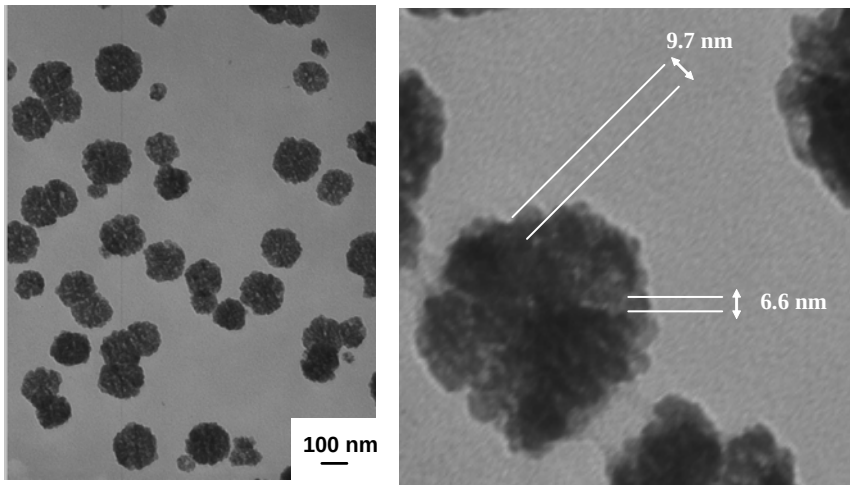

Figure 47. TEM micrographs of washed particles of sample DC256.

Influence of the temperature

Experiments were also performed at different temperatures. Dispersions made at 40 and 60 °C were found to be particularly unstable. This fact can be explained by two combined factors. First, the ester methyl formate is formed by condensation of the formic acid with the methanol under these experimental conditions (temperature + ultrasonication) as checked by NMR. The ester formation is believed to decrease the solubility of the PVA and thus the stability of the system. Secondly, it is known from the classical theory of nucleation that the frequency of the formation of nuclei follows an Arrhenius law, thus increasing when the temperature increases [**Hor**_2001]. The nuclei or precursor particles, as we called them in the previous discussion on the morphology of the particles, can therefore not be immediately stabilized and they coalesce to form bigger particles than at lower temperatures.

Modification of the polyamide 6 particles

We tried to alter the morphology of the particles by adding another reagent to the system to give additional chemical functionalities to the particles. We mixed aqueous solutions of KI/ I_2 or $Al(NO_3)_3$ to the miniemulsion prepared with the conditions of sample DC210. KI/ I_2 is known to interact with polyamide 6 [**Kaw**_2003], whereas $Al(OH)_3$ is described in the literature as an efficient physical cross-linker for the PVA polymer [**Amo**_2000]. The morphology of the particles is shown in Figure 48. These latexes were not further studied because they were unstable: they led to irreversible aggregation and precipitation.

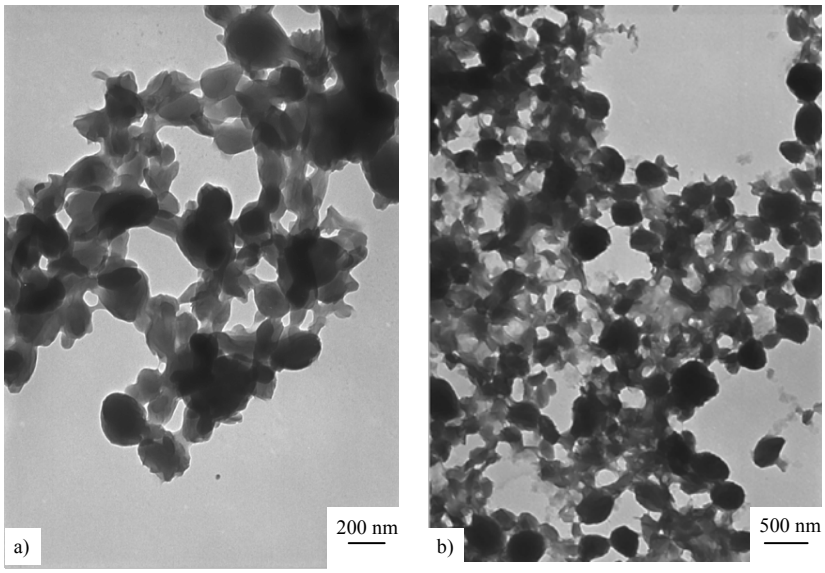

Figure 48. TEM micrographs of the modified latexes prepared via miniemulsion/ solvent displacement hybrid technique. **a**: modified with KI/I_2; **b**: modified with $Al(NO_3)_3$.

Morphology of the capsules produced by the second process

The second synthesis described in the experimental part leads to a nanocapsule morphology as shown in Figure 49. Before the reaction between methanol and formic acid, the polyamide 6 is dissolved in the formic acid dispersed phase. A certain amount of P(B/E-*b*-EO) surfactant is dissolved in cyclohexane to build the continuous phase. The third part, i.e. the part added after the miniemulsification of the two different phases described above, is the methanol as shown in Table 19.

Table 19. Characteristics of the miniemulsion for the synthesis of nylon 6 capsules.

Dispersed phase		Continuous phase		Third part	
Chemical	Amount (g)	Chemical	Amount (g)	Chemical	Amount (g)
Formic acid	0.75	Cyclohexane	7.5	Methanol	0.75
Nylon 6	0.03	P(B/E-*b*-EO)	0.05		

During the reaction between methanol and formic acid, the polymer precipitates at the interface because the water by-product of the reaction is not a solvent for the polyamide 6. After the melting of the polyamide 6, the TEM micrographs show that the polymer forms very small spheres (Figure 49). In this particular system, the interface plays a much bigger role than in the traditional macroscopic domains. We believe that the polymer choose the

entropically favourable situation, e.g. the intramolecular rather than the intermolecular hydrogen bonding.

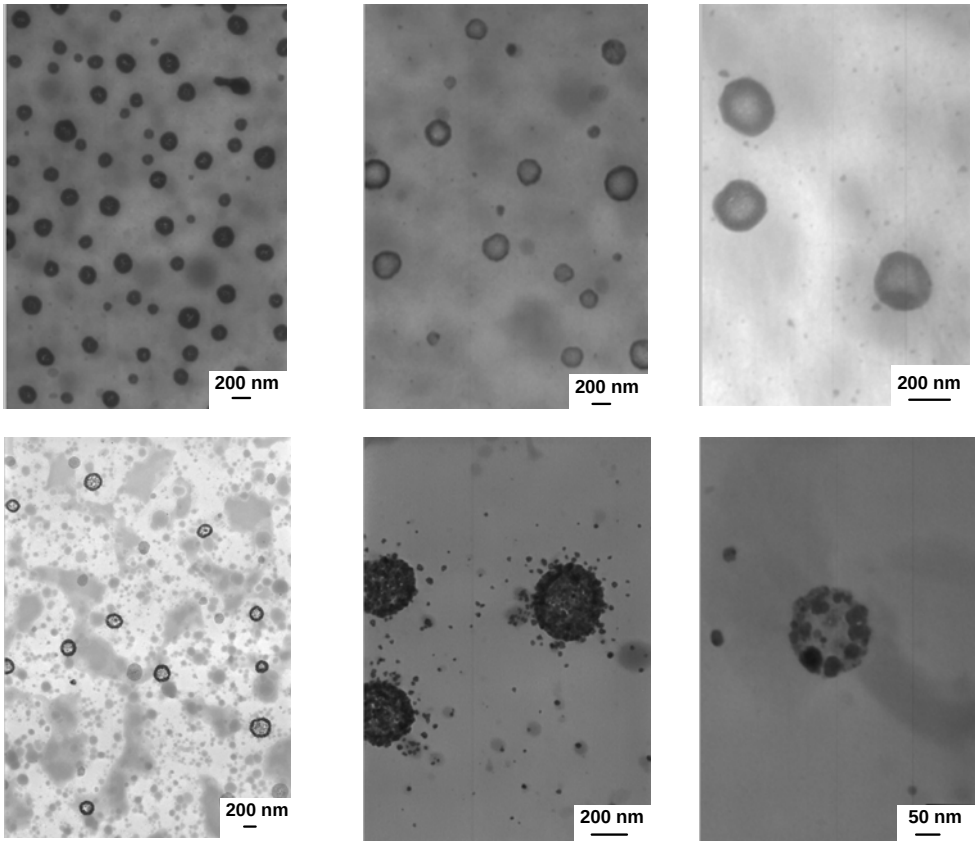

Figure 49. TEM micrographs of the nylon 6 nanocapsules. Above: nanocapsules; bottom: nanocapsules after washing of the TEM grids with toluene and melting of the polymer.

4.3. Polycondensation in miniemulsion systems

4.3.1. Polyamide latexes in miniemulsion polycondensation

4.3.1.1. Tentative synthesis of polyamide latexes in direct miniemulsion at low temperature

Similar synthesis in direct systems reported in the literature are usually done in suspension polymerization. The molecular weight obtained via this method is always low due to the reaction of the poly(acyl halide) with water. In our case, the ultrasonication facilitates the contact between the water and diacyl chloride, which react violently and destabilize the system. The observation of the destabilization of a miniemulsion due to a reactive compound was also done by Takasu et al. [**Tak**_2005] using tolylene-2,4-diisocyanate and

hexamethylene diisocyanate in an aqueous continuous phase. Thus, the best system would employ an inert continuous phase. These experiments showed that the inverse miniemulsion process would be more suitable to perform polyamide synthesis since we did not build stable direct miniemulsion of oil in pure DMSO or DMF.

4.3.1.2.Tentative synthesis of polyamide latexes at low temperature in an inverse system

Experiments were unsuccessful concerning the synthesis of polyamide capsules in miniemulsion. Several chemicals and methods were tried, including the addition of the pure second monomer to the miniemulsion and the addition of a solution of second monomer to the miniemulsion as shown in Table 20. We believe that the miniemulsions are unstable upon addition of the diacyl chloride. These unstabilities are due to the production of HCl and thus acid salt of the organic base used to quench the HCl. We used the pyridine and poly(2-vinylpyridine) to quench the HCl, which lead to pyridinium chloride and poly(2-vinylpyridinium chloride) respectively. These salts, unable to dissolve in the organic phases (either polar or apolar), are believed to create “nucleus of unstabilities”, which would favour the progressive increase of size of the aggregates with time, then giving micrometer to millimetre-size aggregates. These experiments showed that the use of acyl chlorides in miniemulsion polycondensaion is not suitable to obtain stable latexes. We tried then to find an alternative synthesis to perform miniemulsion polycondensation, i.e. the Yamazaki synthesis of polyamides.

Table 20. Characteristics of the miniemulsions.

Entry	Dispersed phase		Continuous phase		Added part	
	Chemical	Amount (g)	Chemical	Amount (g)	Chemical	Amount (g)
DCPA665	molten HMDA at 45 °C	1.5	Isopar M P(B/E-*b*-EO)	7.5 0.075	sebacoyl chloride	3.1
DCPA666	HMDA acetonitrile	0.5 1	Isopar M P(B/E-*b*-EO)	7.5 0.075	sebacoyl chloride	1.0
DCPA667	HMDA DMA	0..5 1	Isopar M P(B/E-*b*-EO)	7.5 0.075	sebacoyl chloride	1.0
DCPA668	HMDA NMP	0.5 1	Isopar M P(B/E-*b*-EO)	7.5 0.075	sebacoyl chloride	1.0
DCPA672	HMDA water NaOH	0.3 1.25 0.03	Isopar M P(B/E-*b*-EO)	7.5 0.075	sebacoyl chloride	0.6
DCPA697	HMDA water NaOH	0.3 1.25 0.03	Isopar M P(B/E-*b*-EO)	7.5 0.075	adipoyl chloride	0.5
DCPA699	HMDA DMA	0.5 1	Isopar M P(B/E-*b*-EO)	7.5 0.075	adipoyl chloride	0.8
DCPA6103	terephtaloyl chloride 1,4-phenylenediamine DMA	0.15 0.15 1.2	Isopar M P(B/E-*b*-EO)	7.5 0.075	none	
DCPA6107	HMDA DMF	0.3 1	cyclohexane P(B/E-*b*-EO)	7.5 0.075	cyclohexane P(B/E-*b*-EO) sebacoyl chloride	5 0.05 0.75
DCPA6108	HMDA DMF	0.3 1	cyclohexane P(B/E-*b*-EO)	7.5 0.075	cyclohexane P(B/E-*b*-EO) adipoyl chloride	5 0.05 0.5
DCPA6114	HMDA DMSO	1 0.3	cyclohexane P(B/E-*b*-EO)	7.5 0.075	cyclohexane P(B/E-*b*-EO) adipoyl chloride	5 0.05 0.24
DCPA6115	HMDA DMSO	1 0.3	cyclohexane P(B/E-*b*-EO) pyridine	7.5 0.075 0.41	cyclohexane P(B/E-*b*-EO) adipoyl chloride	5 0.05 0.47

4.3.1.3. Tentative synthesis of polyamide latexes at higher temperature

Synthesis reported in the experimental part were done with the Yamazaki method of synthesis of polyamides [**Han**_1989]. This method allows to decrease the temperature normally necessary to react a diamino-compound with a dicarboxylic acid compound by the use of triphenyl phosphite and pyridine. The synthesis is carried out normally in a polar solvent and in the presence of either LiCl or $CaCl_2$ to retard the precipitation of the polyamide in the solvent. We tried to perform the Yamazaki synthesis of polyamide in inverse miniemulsion droplets. Unfortunately, the latexes were not stable. We believe this was due to the large presence of pyridine and triphenyl phosphite, which is put in equimolar ratio compared to the monomer for this synthesis.

4.3.2. Polyurea and polyurethane latexes in miniemulsion polycondensation

The goal of this part is to synthesize either polyurea or polyurethane particles in inverse miniemulsion via interfacial polycondensation. The targeted morphologies are particles and capsules.

The synthesis of hollow polymeric particles capsules with sizes ranging from 50 nm to 50 μm has an intense interest in materials science. They offer unique properties as nano- or microreactors and are suitable materials for drug delivery systems. There are generally two approaches to make hollow polymeric particles, which can be differentiated by the presence or absence of a sacrifical core. In the first method, a core particle is used as template and therefore coated with a polymeric shell. The coating of the sacrificial core is obtained by adsorption of a preformed polymer or by polymerization on the surface of the core; subsequently the core is removed by chemical or physical means as dissolution or calcination. The technique of formation of a polymeric shell by adsorption on a sacrifical core comprises the layer-by-layer technique, putting alternatively polyelectrolytes or nanoparticles of opposite charges on a mineral or organic sacrificial core. This method was used for capsule diameters ranging from 70 nm to 10 μm. The thickness of the capsule wall is simply controlled by the number of cycles of the layer-by-layer deposition [**Car**_1998], [**Car**_1999], [**Car**_2001], [**Car2**_2001], [**Par**_2001]. Hollow spheres of 200 to 400 nm were also obtained by dissolution or enzymatic degradation of the core on non-covalently connected core-shell micelles [**Dua**_2001]. Fleming et al. synthesized hollow microcapsules via assembly of polystyrene nanoparticles (100-200 nm) on silica microparticles (3-10 μm), followed by heating the polymer above the *T*g to give a homogeneous shell and finally chemical etching of the silica with HF [**Flem**_2001]. The assembly proceeded via chemical (amine-aldehyde) or biochemical (avidin-biotin) interactions between the nanoparticles and the microparticles. The polymer shell can also be created by polymerization around the sacrificial core. Thus, polymeric shells were polymerized in a dispersion process [**Bou**_1998], [**Bou**_1999], [**Zha**_2002], [**Zha**_2003], [**XuX**_2004]. Living polymerizations (ATRP and anionic polymerization) confined at the surface of a silica core with potential subsequent etchning of this core can lead to hollow polymeric capsules, too [**Perr**_2001], [**Von**_2001], [**Mor**_2002], [**Kam**_2003], [**Man**_2000], [**Zho**_2002]. Marinakos et al. obtained hollow nanocapsules via the polymerization of pyrrole and N-methylpyrrole on gold nanoparticles followed by etching of the gold particles (50-300 nm) [**Mar**_1999]. The thickness of the nanocapsules was

controlled by the polymerization time. Finally, an original lost-wax technique was reported to synthesize nanoparticles and nanocapsules in an inverse opal [**Jia**_2001].

Obviously, the techniques that do not use a sacrificial core are more suitable since they need less steps for the synthesis. In this case, the shell formation is driven by self-assembly or by surface tension forces. Thus, capsules can be made by the "ouzo effect" [**Gan**, 2005], the self-assembly of block copolymers [**Won**_2002], the photo-polymerization of a monomer in phospholipid liposomes [**Les**_2005], the crosslinking of polymerizable liposomes [**Liu**_2002], or the neutralization of a polymeric charged core [**Pav**_2001]. Hollow particles were successfully obtained by phase separation during a suspension (~ 5 μm) [**Oku**_1998] or an emulsion polymerization [**McD**_2000] process (0.2-1 μm). A particular seeded emulsion polymerization with the dynamic swelling technique gave hollow capsules because of the *s*elf-*a*ssembly of *p*hase *se*parated *p*olymer (SaPSeP) at the interface with the aqueous medium (~ 2 μm) [**Min2**_2005]. The same method allows the preparation of cured epoxy micron-sized hollow particles [**Min**_2005]. The well-known interfacial polymerization technique can be applied also to dispersed systems. Thus, the microemulsion process was used for the microencapsulation of osmium tetroxide [**Ley**_2003], palladium (II) acetate and Pd(0) (20-250 μm) in a polyurea matrix [**Pea**_2005]. The polyurea was synthesized by polycondensation at the interface of the oil droplets. However, the synthesis did not lead to hollow capsules, but rather to solid core particles.

Recently, the miniemulsion technique was found to be a suitable technique for the synthesis of well-defined nanocapsules because of the high stability of the droplets. Such stability ensures a copy 1:1 from the droplets to the final object (nanoparticle or nanocapsule). It was also found possible to create nanocapsules with an aqueous core with the direct use of a polymer instead of polymerizing monomers. Thus, our group reported on the synthesis of poly(methyl methacrylate) capsules by controlled nanoprecipitation of the polymer on stable droplets on an inverse miniemulsion [**Pai**_2006]. Several groups have reported that hydrophobic compounds could be efficiently encapsulated in thin shells made by free-radical polymerization [**Tia3**_2001], [**Raj**_2003], [**Luo**_2004]. Torini et al. have described the encapsulation of hydrophobic compounds by interfacial polycondensation in miniemulsion [**Tor**_2005]. The process took place in a direct system (o/w) where the stable diisocyanate IPDI was reacted with the 1,6-hexanediol monomer at the interface of the droplets. The capsule morphology was not evidently shown. Scott et al. described an original synthesis of nanocapsules in direct miniemulsion via interfacial free-radical polymerization [**Sco**_2005]. A surface active initiator was used to start an alternating copolymerization between one

monomer present in the dispersed oil phase and a monomer present in the aqueous continuous phase. Breitenkamp and Emrick developed a method for the synthesis of larger capsules (~ 40 μm) made by cross-metathesis at the oil in water droplets interface [**Bre**_2003]. Additionally, a completely different approach was recently reported by Im et al. [**ImJ**_2005]. First, polystyrene nanospheres were swollen with toluene to increase their volumes followed by freezing with liquid nitrogen. The freezing involves shrinkage of the particles and hence the creation of a void inside the particles due to liquid to solid phase transition of toluene. The toluene is then evaporated below 0 °C, leaving a hole at the particle surface because of the flux of toluene. The final materials are hollow polystyrene nanocapsules. Upt to know, the techniques discussed above do not allow the encapsulation of hydrophilic compounds in a hollow capsule structure. Thus, no report exists about the synthesis of capsules by interfacial polycondensation in an inverse miniemulsion system (w/o). We present the synthesis of hollow nanocapsules made of polyurea, polythiourea or polyurethane. These nanoreactors are used for the reduction of silver nitrate to silver nanoparticles as model reactions. This is to our knowledge the first time that inorganic nanoparticles are encapsulated in a hollow structure without the use of a sacrificial core.

Table 21 shows a typical recipe for such synthesis. Figure 50 describes the principle of the experimental procedure for the synthesis of the nanocapsules with the eventual use of these nanocapsules as nanoreactors for the reduction of silver nitrate. The first monomer is dissolved in a hydrophilic solvent and the mixture is miniemulsified by ultrasonication in a solution of surfactant in a hydrophobic solvent. The first is then located in the droplets. A solution of the second monomer in the hydrophobic solvent is then added to the miniemulsion. The polymer is created by the polycondensation of the hydrophilic and the hydrophobic monomers. This should lead to capsules formation, however in some case it does not. It is possible to dissolve silver nitrate in the hydrophilic solvent prior to the miniemulsification. Miniemuslion droplets containing silver nitrate and the first monomer are then synthesized. The second monomer is subsequently added to the miniemulsion leading to the formation of a polymer followed by the introduction of a reducing agent, which reduces the silver nitrate to silver nanoparticles in the miniemulsion droplets.

Table 21. Typical composition of the miniemulsions for the synthesis of nanoparticles and nanocapsules.

Composition		Polyurea nanocapsules	Polyurethane nanocapsules	Polythiourea nanocpasules
Dispersed phase (g)	Polar solvent	1.3	1.3	1.3
	Monomer 1 or polymer: hydrophilic	0.1	0.1	0.1
	Lipophobe NaCl Lipophobe $AgNO_3$	0.03 0.02 to 0.12	0.03	0.03
Continuous phase (g)	Apolar solvent	7.5	7.5	7.5
	Surfactant P(B/E-*b*-EO)	0.075	0.075	0.075
Third part (g)	Apolar solvent	5	5	5
	Surfactant P(B/E-*b*-EO)	0.035	0.035	0.035
	Monomer 2: hydrophobic	0.25	0.28	0.30

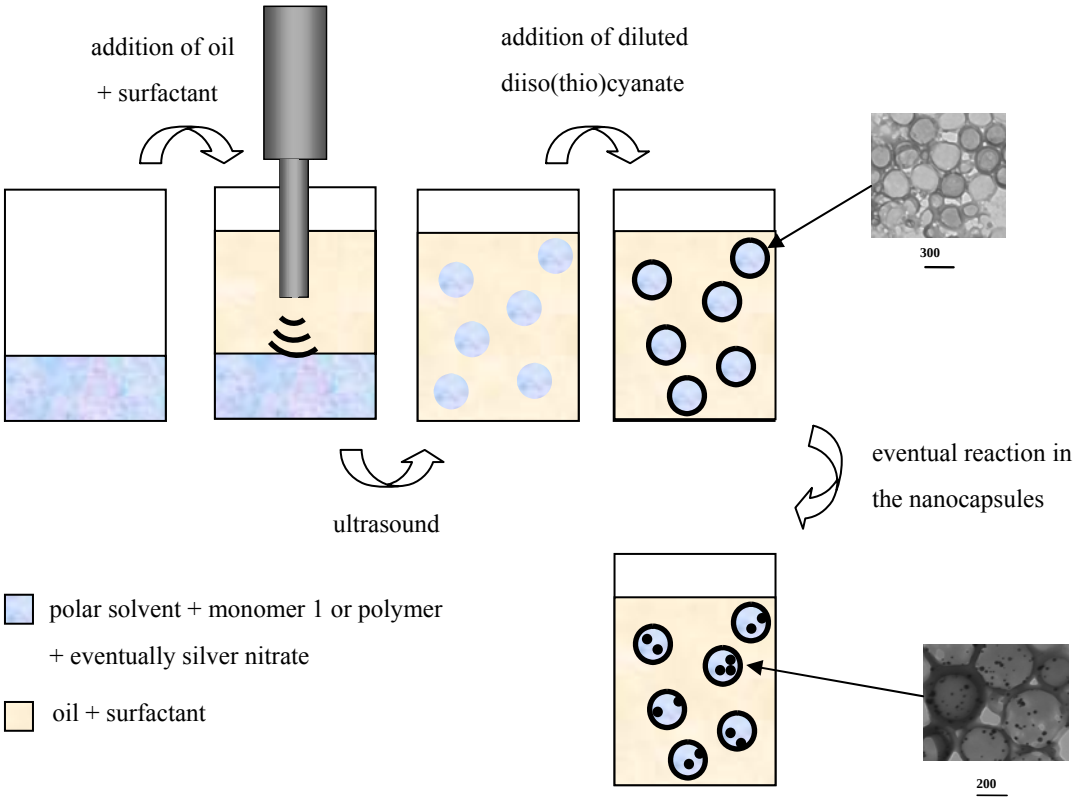

Figure 50. Synthesis of polymeric capsules with their eventual use as nanoreactors for the reduction of silver nitrate.

As shown in Table 22, it was possible to synthesize either polyurea nanoparticles or nanocapsules in inverse miniemulsion, depending on the reagents used, but at fixed wt.% ratios of monomers compared to the dispersed phase. The P(B/E-*b*-EO) surfactant was found to stabilize efficiently the capsules against coalescence, while a little amount of NaCl was used as lipophobe since it is known to stabilize inverse miniemulsions against Ostwald ripening when water is the dispersed phase [**Mon**_2003]. As shown in Table 22, we performed experiments with DMSO (entries P1-P4), 1-vinyl-2-pyrrolidone (entries P5-P6), N-vinylformamide (entries P7-P8), 2-pyrrolidone (entries P9-P10), formamide (entries P11-P24) and water (entries P25-32) as liquid cores. We could synthesize either particles or capsules depending on the nature of these liquid cores.

Table 22. Characteristics of the miniemulsions that give either nanoparticles or nanocapsules; the ratios in weight monomer/ polar solvent/ surfactant/ continuous phase are always the same.

Entry	Dispersed phase		Continuous phase		Object *	Polymer	Diameter (nm) **
	Solvent	Monomer 1	Solvent	Monomer 2			
P1	DMSO	HMDA	cyclohexane	HMDI	P	polyurea	190
P2	DMSO	DET	cyclohexane	HMDI	P	polyurea	213
P3	DMSO	DET	cyclohexane	IPDI	P	polyurea	242
P4	DMSO	DET	cyclohexane	TDI	P	polyurea	100
P5	1-V-2-P	DET	cyclohexane	HMDI	P, U	polyurea	130
P6	1-V-2-P	DET	cyclohexane	TDI	P, U	polyurea	109
P7	N-VFA	DET	cyclohexane	HMDI	P	polyurea	178
P8	N-VFA	DET	cyclohexane	TDI	P	polyurea	154
P9	2-pyrrolidone	DET	cyclohexane	HMDI	P, U	polyurea	181
P10	2-pyrrolidone	DET	cyclohexane	TDI	P, U	polyurea	165
P11	formamide	DET	cyclohexane	HMDI	P	polyurea	191
P12	formamide	DET	cyclohexane	IPDI	P	polyurea	272
P13	formamide	DET	cyclohexane	TDI	C	polyurea	250
P14	formamide	DET	toluene	TDI	C + P	polyurea	265
P15	formamide	DET	hexane	TDI	C	polyurea	292

Entry	Dispersed phase		Continuous phase		Object *	Polymer	Diameter (nm) **
	Solvent	Monomer 1	Solvent	Monomer 2			
P16	formamide	DET	cyclohexane	bisphenol A diglycidyl ether	P	epoxy	250
P17	formamide	DET	cyclohexane	TDIT	C	polythiourea	377
P18	formamide	HMDA	cyclohexane	TDI	C	polyurea	175
P19	formamide	cysteamine: 10wt.% DET: 90wt.%	cyclohexane	TDIT	C	polythiourea polyurea	424
P20	formamide	glycerol	cyclohexane	TDI	C	PU	203
P21	formamide	1,6-hexanediol	cyclohexane	TDI	U	PU	
P22	formamide	DBA	cyclohexane	TDI	C	polyurea	
P23	formamide	PEI	cyclohexane	TDI	C	crosslinked PEI	
P24	formamide	starch	cyclohexane	TDI	C	crosslinked starch	
P25	water	DET	cyclohexane	HMDI	C	polyurea	329
P26	water	DET	cyclohexane	TDI	C	polyurea	216
P27	water	DAB	cyclohexane	TDI	C	polyurea	354
P28	water	HMDA	cyclohexane	TDI	C	polyurea	381
P29	water	1,6-hexanediol	cyclohexane	TDI	U	PU	
P30	water	L-arginine	cyclohexane	TDI	C	polyurea	
P31	water	starch	cyclohexane	TDI	C	crosslinked starch	
P32	water	dextran	cyclohexane	TDI	C	crosslinked dextran	

* P = particles, C = capsules, U = unstable

** determined by DLS

Synthesis of the nanoparticles

Miniemulsion polycondensation was carried out by the reaction between a monomer dissolved in a polar solvent that build the droplets and a second monomer, which come from the continuous phase, i.e. from outside the droplets. The results summarized in Table 22 show that when DMSO (P1-P4), 1-vinyl-2-pyrrolidone (P5-P6), N-vinylformamide (P7-P8) or 2-pyrrolidone (P9-P10) were the polar solvent in the dispersed phase, polyurea nanoparticles and no nanocapsules were formed independently from the monomers that were used (see morphologies in Figure 51). With DMSO as the polar solvent, the combinations of monomers HMDA/ HMDI (P1), DET/ HMDI (P2), DET/ IPDI (P3), and DET/ TDI (P4) were used. With 1-vinyl-2-pyrrolidone as the polar solvent, the combinations of monomers DET/ HMDI (P5) and DET/ TDI (P6) were carried out. The combinations of monomers DET/ HMDI (P7) and DET/ TDI (P8) were tried with N-VFA and as the polar solvent. And finally, the combinations DET/ HMDI (P9) and DET/ TDI (P10) were also performed with 2-pyrrolidone as the polar solvent.

In the case of the 1-vinyl-2-pyrrolidone polar solvent, it is possible to polymerize it via free-radical polymerization. Thus, we performed a miniemulsion polycondensation as described above with 1-vinyl-2-pyrrolidone as the dispersed phase and then polymerized the 1-vinyl-2-pyrrolidone. Remarkably, the nanoparticles were crumpled when only 1-vinyl-2-pyrrolidone was used as both polar solvent and monomer for free-radical polymerization (without formamide or water) as shown in Figure 52. In our case, the reaction is performed in an inverse system and hence the use of TDI yielded stable particles. Takasu and Kawaguchi also reported the formation of spherical polyurea shell/ polystyrene core particles but in a direct miniemulsion [**Tak**_2005]. In their case, the TDI monomer was found not to be suitable in such case to obtain stable latexes because of its high reactivity. The reaction is then lowered compared to the reaction observed with the less reactive IPDI monomer.

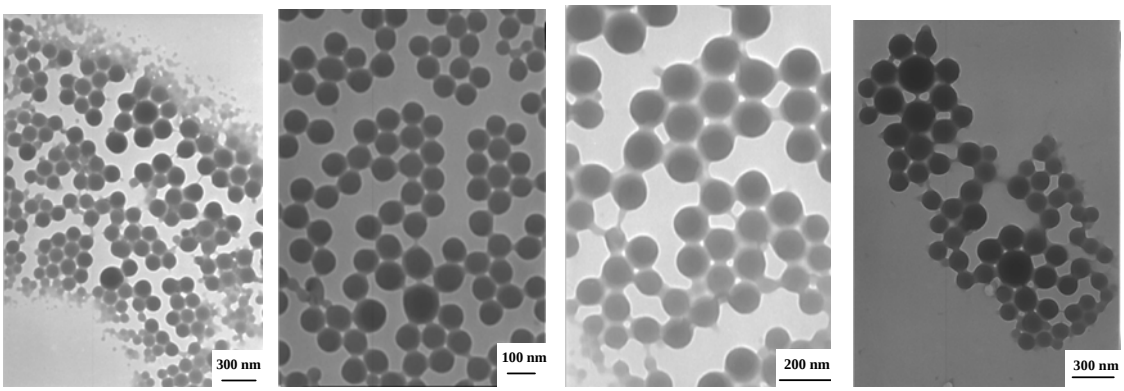

Figure 51. TEM micrographs of polyurea particles. Samples P3 (DET and IPDI as monomers), P5 (DET and HMDI), P7 (DET and HMDI) and P9 (DET and HMDI).

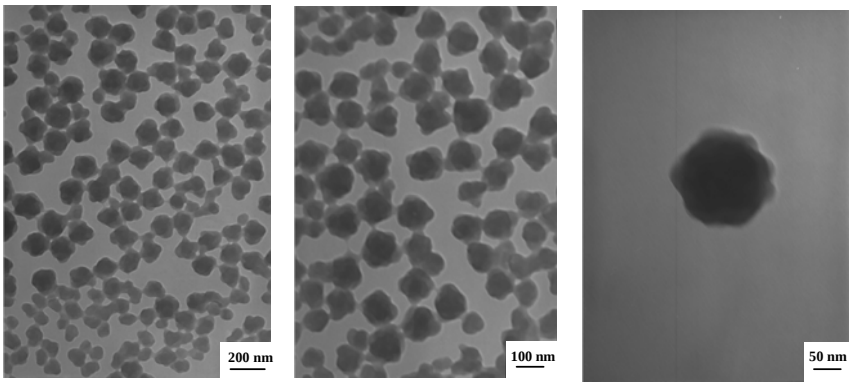

Figure 52. TEM micrographs of the sample P6 composed of poly(vinylpyrrolidone)/ polyurea (DET and TDI) hybrid nanoparticles.

Synthesis of nanocapsules

It is suitable to provide heterophase synthesis that allows the formation of nano-materials other than plain particles. In fact, the nanocapsule morphology is particularly interesting thanks to the capacity of the shell to encapsulate a large amount of material in the core. We changed the influence of the composition of the dispersed phase on the latex morphology. Water and formamide were found to be more suitable for the formation of nanocapsules than the other polar solvents described above; i.e. DMSO, 1-vinyl-2-pyrrolidone, N-VFA, and 2-pyrrolidone. The successful synthesis of nanocapsules was also closely related to the kind of monomers for water and formamide as liquid core. Thus, the reaction between tolylene-2,4-diisocyanate and either diethylenetriamine, 1,6-diaminohexane or 1,4-diaminobutane yields to a nanocapsule morphology when water is the liquid core as shown in Table 22 (entry P26-P28). With water, the reaction between diethylenetriamine and hexamethylenediisocyanate

gave also nanocapsules (entry P25). When formamide is the liquid core, the reaction between tolylene-2,4-diisocyanate and diethylenetriamine or hexamethylenediamine formed nanocapsules (entry P13 and P18 respectively). The reaction between diethylentriamine and the diisothiocyanate was found suitable to form a nanocapsule morphology (entry P17) whereas the reaction of diethylenetriamine with hexamethylenediisocyanate (entry P11) or IPDI (entry P12) or bisphenol diglycidyl ether (60 °C to form epoxy, entry P16) yielded nanoparticles. With formamide as liquid core, the use of hexane instead of cyclohexane for the continuous phase gives also nanocapsules (entry P15), whereas toluene as continuous phase gives a mixture of nanoparticles and nanocapsules (~70 % of nanoparticles and ~30 % of nanocapsules according to the TEM measurements, entry P14). All these results can be interpreted in term of phase separation and interfacial tension. A suitable system for the formation of nanocapsules is obtained when the hydrophilic monomer and the hydrophobic monomer tends to form a polymer, which will phase-separate at the interface of the droplets. This means that despite the principle of the synthesis of the nanoparticles and the nanocapsules is the same, i.e. one monomer in the droplets and one monomer outside the droplets, different morphologies of the latex are obtained depending on the composition of the dispersed phase.

Polyurea nanocapsules with functional carboxylic acid groups could be synthesized with 3,4-diaminobenzoic acid (entry P22) with formamide as liquid core, or L-arginine (entry P30) with water as liquid core, as hydrophilic monomers. They could hence eventually be used as pH-responsive nanocontainers [**Tai**_2005]. The principle of the synthesis described above was extended to the crosslinking of functional polymers. Interfacial crosslinking of polyethyleneimine, starch and dextran gave also nanocapsules morphologies.

The Table 23 shows that the size of the polyurea capsules with formamide or water as liquid cores is influenced by the amount of surfactant as expected for the miniemulsion technique (entry P33-P36), i.e. the particle size decreases when the concentration of surfactant increases [**Lan**_2001]. By using 8.6 wt.% surfactant compared to the dispersed phase (entry P35), we could even obtain a nanocapsule size down to 160 nm. A nanocapsule size of 258 nm could be reached with 4.4 wt.% surfactant compared to the dispersed phase (entry P34). This is approximatively the minimum size attainable since the use of more surfactant did not significantly change the nanocapsule diameter. Our synthesis involves the addition of the second monomer to miniemulsion droplets containing the first monomer. The addition time of the second monomer may have an influence on the colloidal properties of the latex. Thus, we analyzed the influence of the addition time of the second monomer to the miniemulsion on the

capsule size. Nanocapsules with different time of addition of the solution of tolylene-2,4-diisocynate were prepared (entries P13, P37-P38 with formamide as liquid core and P26, P39, P40 with water as liquid core). As shown in Table 23, addition time of the solution of diisocyanate monomer to the miniemulsion plays an important role for the size of the nanocapsules. With increasing addition time from 300 to 1200 s, the nanocapsules size also increases from 250 to 331 nm with formamide as the liquid core, and from 216 to 260 nm with water as the liquid core. A control experiment was made without the addition of the diisocyanate monomer and present droplets with a hydrodynamic diameter of 235 nm, close to the value of the experiment with fast addition (sample P13: 250 nm). Therefore, a fast addition "freezes" the state of the droplets by forming a solid polymer shell, whereas a longer addition allows the system to expand by swelling to the continuous phase. In fact, calorimetric measurements shown in Figure 53 reveal that the polymerization is very fast. The samples with a short addition time of 300 s (P13 with a formamide core, P26 with an aqueous core) have a reaction time of about 500 s and display a single heat peak. The samples with a longer addition time of 600 s (P37 with a formamide core, P39 with an aqueous core) display several heat peaks, which correspond to the different injections of the second monomer. They have a reaction time of about 600 s. Finally, the reaction profile of the polythiourea formation is a single peak with a reaction time of about 700 s. This means that the reaction is very fast and that the time of reaction is almost the time of addition of the second monomer.

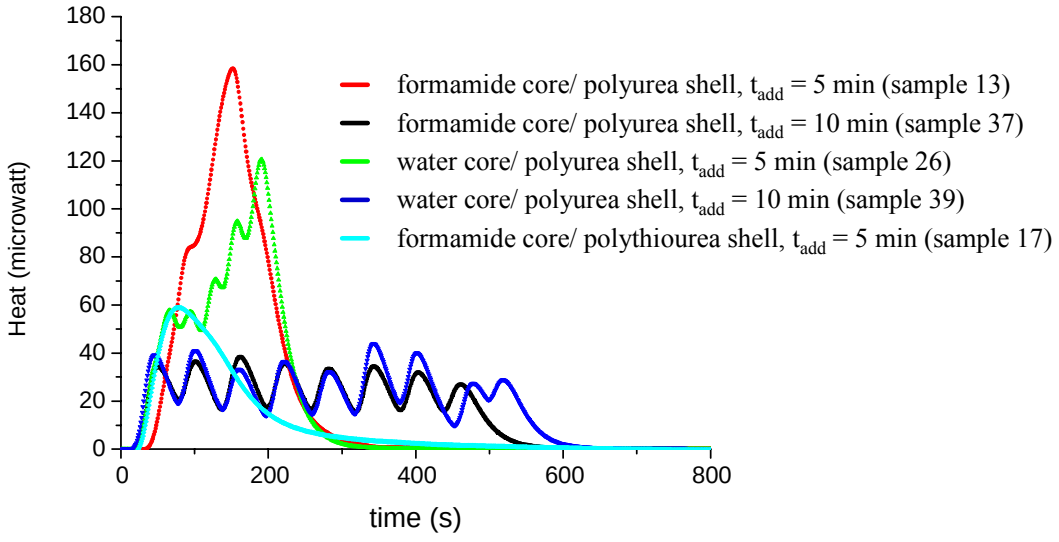

Figure 53. Calorimetry curves of the reaction performed with different time of addition of the second monomer (t_{add}). The different peaks are the consequence of the non-continuous (discrete) nature of the addition.

Table 23. Dependence of the size of the particles on the dispersed phase, on the time of addition of the diisocyanate solution and on the concentration of surfactant.

Entry	Dispersed phase	Time of addition of the solution of hydrophobic monomer (s)	Surfactant (wt.%)	Diameter in cyclohexane (nm)*	Diameter in water (nm)*
variation of the amount of surfactant					
P33	Formamide	300	2.3	1212	unstable
P34	Formamide	300	4.4	258	766
P13	Formamide	300	6.5	250	584
P35	Formamide	300	8.6	160	228
P36	Formamide	300	13	153	378
variation of the time of addition					
P37	Formamide	600	6.5	275	591
P38	Formamide	1200	6.5	331	385
P26	Water	300	6.5	216	414
P39	Water	600	6.5	235	227
P40	Water	960	6.5	260	293

* determined by DLS

We showed that it is possible to synthesize nanocapsules via interfacial polycondensation in inverse miniemulsion. We could vary the size of the capsules simply by changing the amount of surfactant in the formulation. It would be also interesting to vary the wall thickness of the nanocapsules, which would probably be a key parameter in the control of the release behavior of these nanocontainers. Because the monomers are the building material of the capsule wall, we studied the influence of the amount of monomer on the wall thickness of the capsules. It is expected that the larger the amount of monomers is, the thicker the wall of the capsules would be. The results shown in the Table 24 indicate that the hydrophilic monomer amount has an

influence on the wall thickness of the nanocapsules. Conversely, the variation of the amount of hydrophilic or hydrophobic monomers has no significant influence on the diameter of the nanocapsules. Table 24 shows that the concentration of the diethylenetriamine monomer in the droplets is the critical factor for the control over the wall thickness. In fact, for different amount of diethylentriamine, the wall thickness is significantly varied from 15 nm for entry P45 to 39 nm for entry P41. The wall thickness can be then controlled simply by varying the amount of monomer in the formulation as shown in Figure 54. It is observed that the wall thickness is much larger if the mass of monomers is increased in the miniemuslion formulation and that the nanocpasules still keep a spherical shape independently on the amount of monomers employed. The amount of diisocyanate does not play a significant role for the wall thickness: entries P13, P42, P43, and entries P44 and P45 have the same wall thickness. In fact, the loss of volume due to the use of less diisocyanate is compensated by the fact that the less cross-linked polyurea has more freedom to extend.

Table 24. Characteristics of the polyurea latexes with formamide as liquid core synthesized with different amounts of monomers.

Entry	DET (g)	TDI (g)	Diameter (nm) *	Diameter in water (nm) *	Diameter (nm) **	Wall thickness (nm) **
P41	0.2	0.5	272	625	221	39
P13	0.1	0.26	250	584	209	23
P42	0.1	0.13	218	833	192	24
P43	0.1	0.05	213	807	203	20
P44	0.055	0.13	244	381	189	15
P45	0.05	0.06	202	546	196	13

* determined by DLS

** determined by TEM

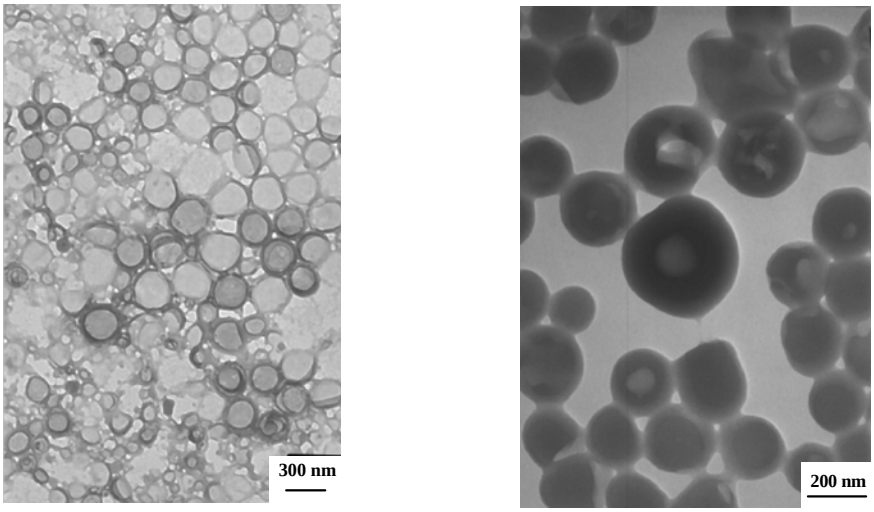

Figure 54. TEM micrographs of polyurea nanocapsules prepared with different amount of monomers; links: entry P13, right: entry P41 prepared with a double amount of monomers compared to entry P13.

Morphology of the capsules

As shown in the Figure 55, the synthesized nanocapsules have a hollow structure detected by TEM with a thin polymeric wall. The nanocapsules with formamide as liquid core are spherical whereas some of the nanocapsules with water as the liquid core have a prolate spheroid shape (olive-shaped). As shown in Figure 56, the sample P26 with an aqueous core is composed of big non-spherical particles and small spherical nanoparticles. The particles produced in heterophase polymerization processes are most often spherical since the system tends to minimize the interfacial energy between the two phases. One exception was reported in the case of miniemulsion polymerization of ε-caprolactam (see this thesis chapter 4.2.1.). Ellipsoidal particles of polyamide-6 were formed because of the phase separation that occurred in the miniemulsion droplets between the polyamide and the DMSO. Xu and al. reported that thin polymeric capsules can be irreversibly deformed during the process of evaporation of the liquid core even for highly cross-linked capsules because they are more flexible than thick capsules [**XuX**_2004]. In our case, the nanocapsules formed with water are more deformable than those with formamide as dispersed phase. Indeed some of the isocyanate groups reacted with the water as revealed by the presence of urea groups in IR spectra, hence lowering the stiffness of the polymer.

We investigated further the structure of the polyurea nanocapsules with water as liquid core with AFM measurements because in the undried state they should not be deformed by any external forces. The measurements were taken while the cyclohexane continuous phase, or after evaporation at room temperature, or after letting the deposited latex in an excicator for 12 h, or finally submitting the deposited latex to vacuum for 10 min. The images shown in Figure 57 indicate that only some of the large capsules are deformed while the nanocapsules stayed intact. This observation confirms the TEM data, i.e. the presence of some large deformed capsules in coexistence with the spherical nanocapsules. Therefore it can be concluded that the large capsules are originally in dispersion spherical and become folded when they are submitted to a certain force. In fact, according to Yang et al., the deformation of the nanocapsule-like objects could be explained by the fact that the force of the AFM cantilever causes the change of the morphology [**Yan**_2005]. Besides, SLS combined with DLS measurements show that the capsules with water does not have the typical scattering behavior of an ellipsoid but rather the one of a sphere (see Figure 58). SLS measurments can provide information about the size, the molecular weight, but also the shape of an object by analyzing the scattering behavior of this object at different angles and concentrations. However, the capsules with water as liquid core did not show the deviation at higher scattering angles expected for an ellipsoidal structure. This observation indicates that the nanocapsules have a spherical shape in the undried state.

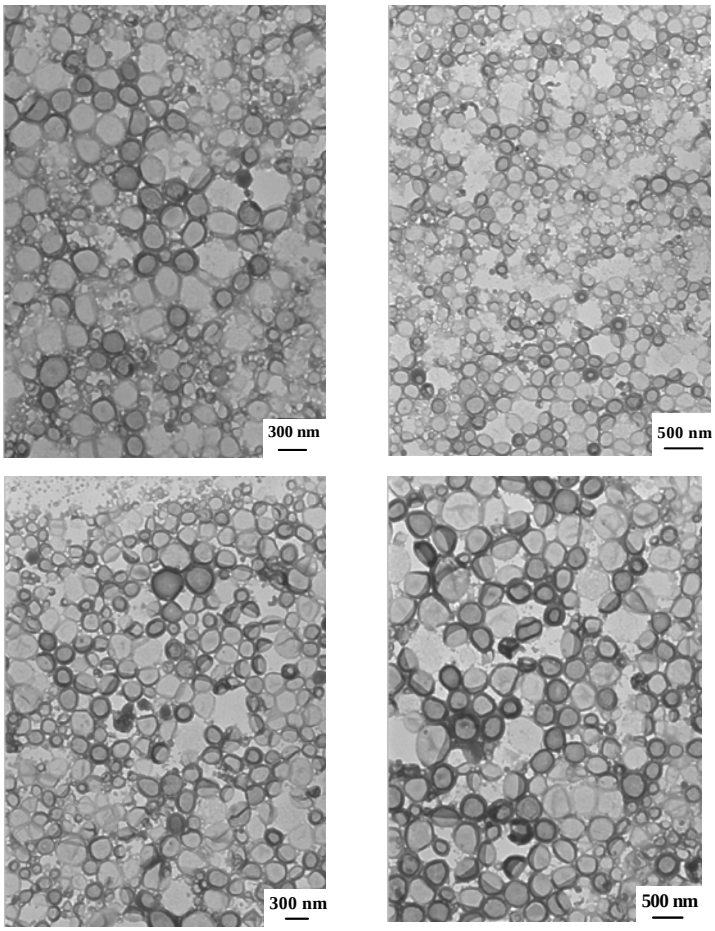

Figure 55. TEM micrographs of the samples P13 (above) and P37 (bottom) prepared with formamide as the liquid core. The capsules have a spherical shape.

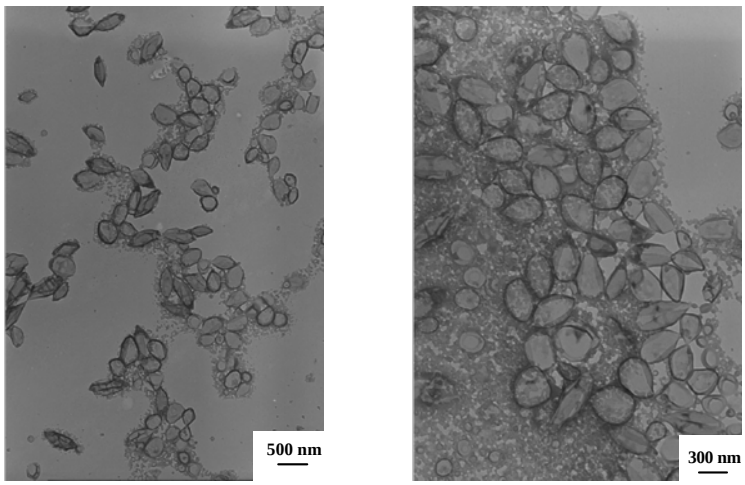

Figure 56. TEM micrographs of the sample P26 prepared with an aqueous core. The capsules have a prolate spheroid shape.

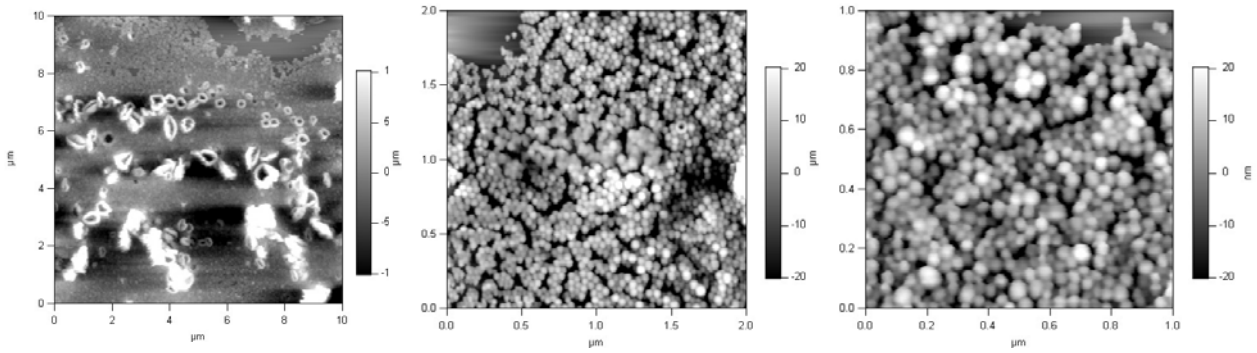

Figure 57. AFM micrographs of the sample P26.

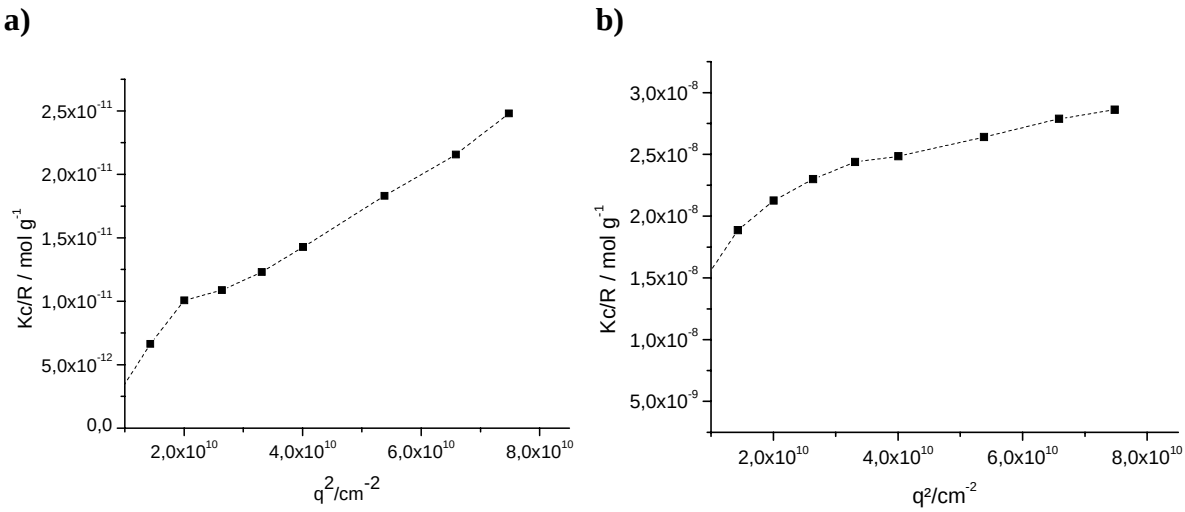

Figure 58. SLS measurements of the latexes; **a**: sample P13 with a formamide core, **b**: sample P26 with an aqueous core.

The capsules made of crosslinked starch displayed also some other interesting morphologies as shown in Figure 59. When water was the liquid core, the capsules have spherical morphologies (sample P31). When formamide is the liquid core (sample P24), the capsules collapsed in the TEM due to the strong vaccuum. The starch mechanical properties seem to be different in the presence of water or formamide, which would explain the observed differences in morphologies.

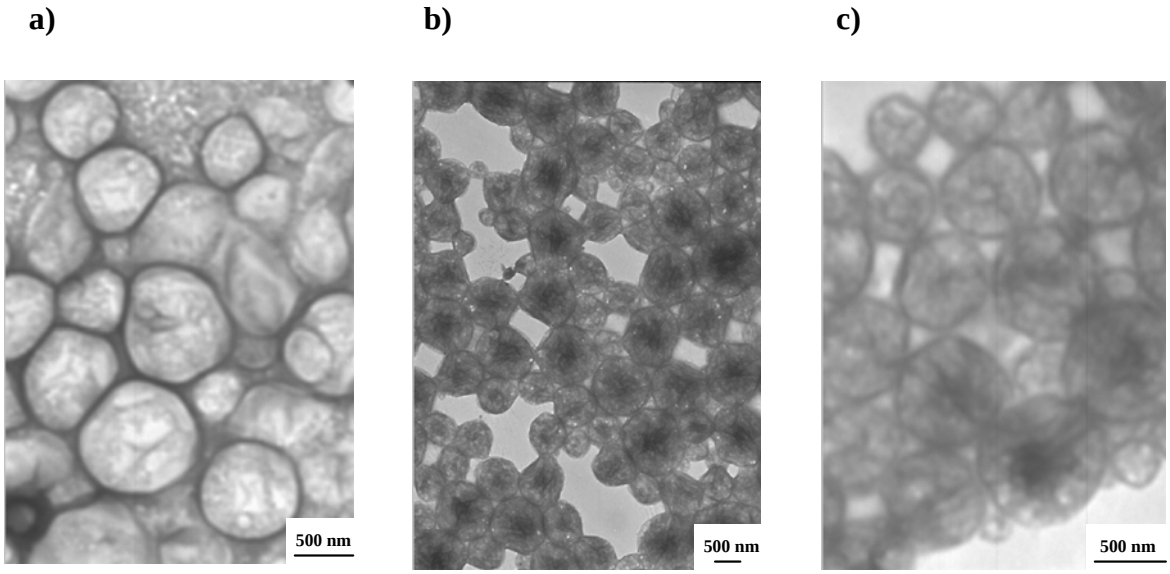

Figure 58a-c. TEM micrographs of the nanocapsules. **a**: sample P31, water as liquid core; **b-c**: sample P24 (formamide as liquid core).

Dispersion in water

Up to now the capsules are dispersed in an organic solvent. A transfer to an aqueous dispersion would be suitable for eventual biomedical application. The dispersion of nanocapsules in cyclohexane was taken and mixed with an aqueous solution of SDS. The mixture was coarsely mixed in a sonication bath and then ultrasonicated during short time. The cyclohexane was then evaporated. This procedure was chosen in order to achieve a minimum size of the droplet of cyclohexane in the system. In fact, with such conditions, we can decently assume that the system is composed of droplets of cyclohexane with a minimum of nanocapsules down to one nanocapsule and empty cyclohexane droplets. If the size of the cyclohexane droplets would be bigger, the re-dispersion being provided by a standard stirring system, they would contain several nanocapsules. During the subsequent evaporation process of the cyclohexane, the droplets of cyclohexane shrink and would lead to coalescence of the nanocapsules. The procedure described in the experimental part is also preferable to the traditional freeze-drying technique since the nanocapsules tend to stick together upon drying of the continuous phase. The dispersion in water is accompanied by an increase of the hydrodynamic diameter, depending on the quality (nature) of the dispersed phase (Table 25). The use of formamide as dispersed phase instead of water prevents subsequent hydrolysis of still non-reacted isocyanate groups. Hence, the capsules containing formamide are submitted

to hydrolysis to amino-groups during the dispersion in water. These groups are highly hydrophilic and drive the capsules toward an expansion in water.

Polythiourea and polyurethane capsules

Polythiourea capsules containing formamide in the core were successfully obtained with the process discussed before for polyurea capsules. For the synthesis of polythiourea capsules, the tolylene-2,4-diisocyanate used for the formation of polyurea capsules was replaced by an equivalent molar amount of tolylene-2,4-diisothiocyanate. Similarly, polyurethane capsules were synthesized at 60 °C by using an equivalent molar amount glycerol instead of the diethylenetriamine monomer in the dispersed phase. After the removal of the surfactant and the continuous phase, the polymers were identified by IR to be a polythiourea and polyurethane free from urea groups. Remarkably, the polyurethane capsules formed monolayers while packing upon deposition of the miniemulsion on TEM grids as shown visibly in Figure 60. To check if the speed of cooling of the latexes have an influence on their stability, DLS measurements were made on polyurethane latexes after slow (in the oil-bath that was switched off) and fast cooling (in ice). As expected for a stable latex, both latexes have the same hydrodynamic diameter.

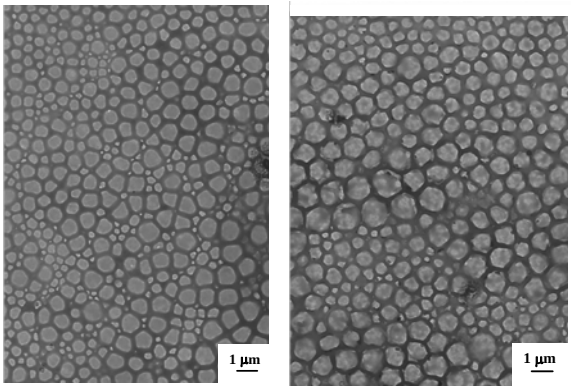

Figure 60. TEM micrographs of the polyurethane capsules from sample P20.

The polyurea nanocapsules as nanoreactors

Because of their hollow structure, the nanocapsules can be used as nanocontainers for reactions in hydrophilic media. We choose the reduction of silver nitrate in silver nanoparticles as model system to show the polyurea capsules can be used as nanoreactors.

The preparation of the silver nanoparticles loaded capsules involves the dissolution of the silver nitrate salt in the dispersed phase followed by the polymerization of the shell. The metal salt is subsequently reduced by the addition of hydrazine to the miniemulsion under short ultrasonication, which diffuses through the thin capsule wall. Ultrasonication is used to facilitate the migration of the hydrazine through the cyclohexane to the capsules since the hydrazine is not soluble in cyclohexane continuous phase. To check the reactivity of hydrazine toward our dispersed phase, non-encapsulated droplets containing silver nitrate were reduced in a control experiment. Figure 61 shows the silver nanoparticles obtained via this process. We investigated then the formation of polyurea capsules followed by the reduction of the encapsulated silver nitrate by hydrazine. It was possible to prepare capsules loaded with different amounts of silver inside as shown in Table 25, simply by varying the concentration the silver salt in the dispersed phase from 1.2 wt.% (20 mg) to 6.8 wt.% (120 mg) compared to the dispersed phase. We chose to reduce the silver salt by the hydrazine to accelerate the process of reduction. The formamide is known to be a reducing agent for the silver nitrate in certain systems [**Sar**_2005], but we found that the hydrazine was more suitable in our particular case.

Table 25. Characteristics of the latexes prepared with different amounts of silver nitrate.

Entry	$AgNO_3$ (mg)	Monomers		Capsules diameter (nm) *	Capsules diameter (nm) **	Ag NP diameter (nm) **	Ag NP per capsules
		TDI (g)	DET (g)				
P38	20	0.25	0.1	221	208 ± 38	24 ± 2	1.08
P39	30	0.25	0.1	350	252 ± 47	29 ± 2	1.06
P40	30	0.25	0.1	378	277 ± 52	33 ± 2	1.33
P41	30	0.37	0.15	249	171 ± 32	27 ± 2	1.07
P42	30	0.37	0.15	268	185 ± 35	22 ± 1	1.39
P43	60	0.25	0.1	391	239 ± 45	14 ± 1	6.06
P44	60	0.25	0.1	272	266 ± 50	14 ± 1	3.4
P45	60	0.38	0.16	290	274 ± 51	26 ± 1	1.44
P46	60	0.39	0.16	293	271 ± 51	26 ± 2	3.78
P47	120	0.25	0.1	260	328 ± 61	16 ± 2	20.59

* determined by DLS

** determined by TEM

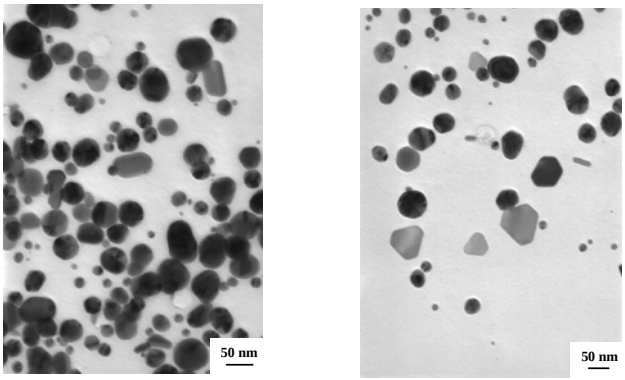

Figure 61. TEM micrographs of the control experiment: no second monomer was added to the miniemulsion.

When the silver nitrate inside the polymer capsules was reduced, the spherical shape of the nanocapsules is not changed compared to the one of the polyurea capsule as shown in Figure 62 by SEM measurements.

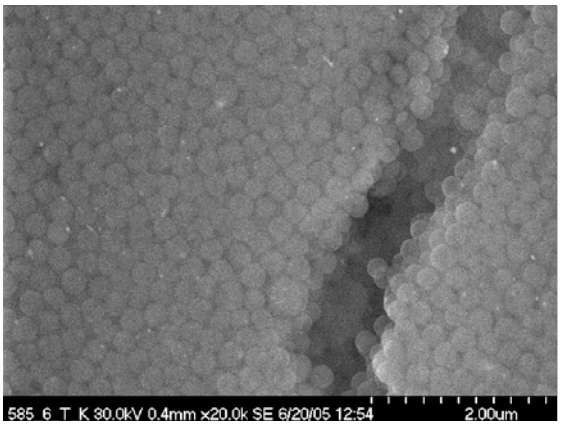

Figure 62. SEM micrographs of the capsules containing silver nanoparticles (sample P39).

The nanocapsules containing high amount of silver nanoparticles were found to have a bigger size; 328 nm for sample P47 containing 120 mg silver nitrate compared to the dispersed phase, and 208 nm for sample P38 containing 20 mg silver nitrate. In fact, it is expected that the PEO part of the block copolymer surfactant probably complex the silver ion. Such an interaction lowers the efficiency of the surfactant. For the low amounts of silver nitrate (< 30 mg) in the nanocapsules, the silver nanoparticles average size increases from 24 to 29 nm when the size of the polymeric nanocontainers increases from 208 to 252 nm. For high amount of silver nitrate (≥ 60 mg), the number of silver nanoparticles increases from 6 to 21 while the size of the nanocontainers increases from 239 to 328 nm (see Figure 63). In a general trend, the size of the capsule increases with the amount of silver nitrate. Note that no valid information about the size of the silver nanoparticles could have been given by the DLS measurements. In principle, the silver nanoparticles may have a different coefficient of diffusion than the droplet surrounding it and a DLS program able to detect multimodal distribution of size could evidence this fact. But wide discrepancies in size observed between the DLS and the TEM measurements led to conclude that the DLS was not a suitable technique to measure the size of the silver nanoparticles in our particular case. This phenomenon could be explained by the fact that the synthesis of the silver nanoparticles was made without capping or stabilizing agent. The silver nanoparticles are probably stabilized by the polymeric wall of the capsules and hence reduce the mobility of the silver in the nanoreactors.

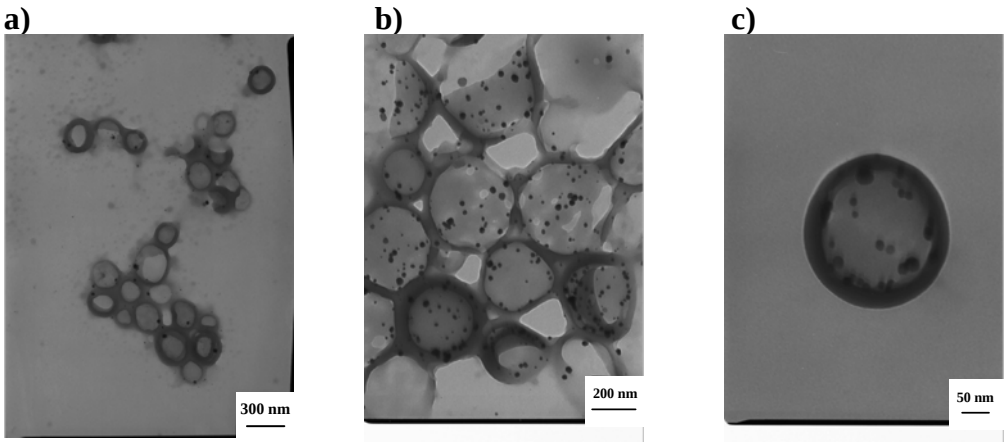

Figure 63a-c. TEM micrographs of polyurea capsules loaded with different amount of silver nanoparticles; **a**: sample P39, **b-c**: sample P47. We can observe that sample P47 contain much more silver nanoparticles than sample P39 (see Table 25).

The extinction UV-Vis spectra shown on Figure 64 give also interesting information about the size, the shape and the direct environment of the silver nanoparticles, which can be correlated to the TEM measurements as shown in Figure 63. In fact, very small silver nanoparticles (~ 2 nm) have a spectrum of metallic crystal since the Plasmon band is strongly damped due to the low electron density in the conduction band. Conersely, bigger nanoparticles show a muc more intense plasmon band. As shown in Table 26, the usual maximum absorbance λ_{max} around 420 nm observed for spherical silver nanoparticles [**Moc**_2002], is red-shifted when hydrazine is used as reducing agent. Note that the polymeric capsules without silver nanoparticles inside did not contribute to the optical spectra in the 400 to 800 nm region. When the amount of silver nitrate increases, the plasmon band absorbance increases and λ_{max} is red-shifted; from λ_{max} = 431 nm for entry P39 ([$AgNO_3$] = 0.14 g·mol^{-1}) to λ_{max} = 444 nm for entry P43 ([$AgNO_3$] = 0.56 g·mol^{-1}) with a formamide core; from λ_{max} = 433 nm for entry P50 ([$AgNO_3$] = 0.13 g·mol^{-1}) to λ_{max} = 442 nm for entry P51 ([$AgNO_3$] = 0.25 g·mol^{-1}) with an aqueous core. On the contrary to the work of Sarkar et al. [**Sar**_2005], we made bigger silver nanoparticles, hence yielding to a red-shifting of the plasmon band, when the concentration of silver nitrate increases as shown in Table 25. The size of the nanoparticles depends mainly on the nucleation and growth processes, either the growth by autocatalysis or the growth by ripening. We believe that the "film" or surrounding layer around the silver during the synthesis is very flexible since we did not add any compounds such as protective colloids to stabilize them. In this case, the growth is controlled by the ripening according to Tojo et al. [**Toj**_1997]. Thus, an increase of the silver nitrate concentration leads both to more nanoparticles and bigger ones, when the fast reduction process by hydrazine is used.

Table 26. Effect on the silver nitrate concentration and the reducing agent on the maximum of the plasmon band.

Entry	Liquid core	$AgNO_3$ ($mol \cdot l^{-1}$) *	Reducing agent	λ_{max} (nm)
P39	formamide	0.14	hydrazine	431
P48	formamide	0.14	formamide	419
P43	formamide	0.56	hydrazine	444
P49	formamide	0.56	formamide	400
P50	water	0.13	hydrazine	433
P51	water	0.25	hydrazine	442

* concentration in the dispersed phase

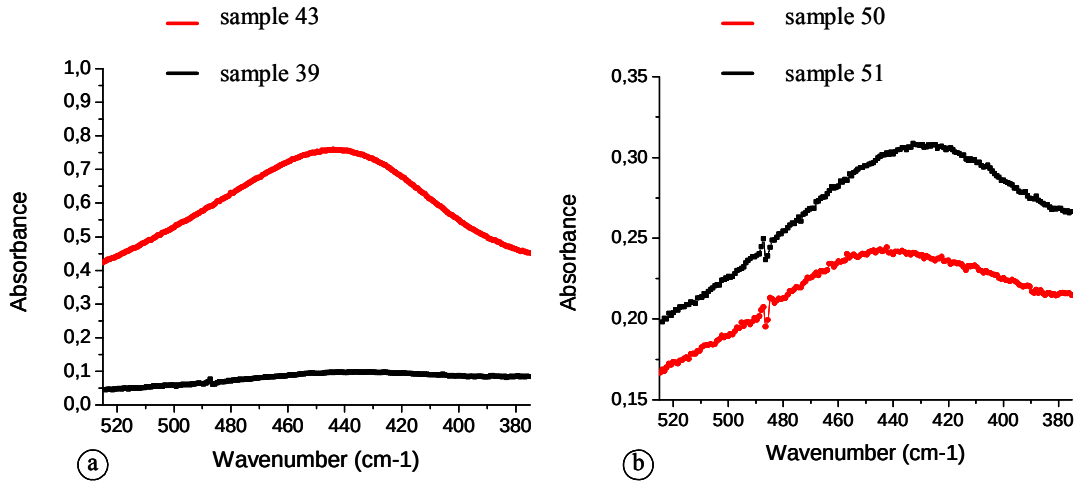

Figure 64. UV-spectra of the silver/ polyurea miniemulsions; **a**: with formammide core, **b**: with water core.

Particles and capsules can be synthesized via the condensation between a monomer present in the dispersed phase and a monomer present in the continuous phase. As discussed above in the article, it is possible to increase the wall thickness of the nanocapsules by increasing the amount of monomers employed. We wanted to test another approach to increase the shell thickness of the capsules and to form capsules with two different polymeric shells. Thus we increased the wall thickness of the previously synthesized polyurea nanocapsules by coating

the nanocapsules via free-radical polymerization of a third monomer around the shell. N-vinylcaprolactam was poylmerized around polyurea nanocapsules containing silver nanoparticles prepared with the standard recipe as shown in Figure 65. We chose this monomer because the monomer is hydrophobic but gives an amphiphilic polymer, which stays at the interface of the nanocapsules. Thus, we obtained a rather complex material in a one-pot synthesis with three different steps: interfacial polycondensation to make the polyurea shell, reduction of the encapsulated silver salt to make the silver nanoparticles and finally free-radical polymerization to make a second shell (see Table 27).

Table 27. Characteristics of the latex P52 before and after coating with poly(vinylcaprolactam).

Characteristics	Before coating	After coating
Nanocapsule diameter *	280	330
Silver nanoparticles diameter *	18	

* determined by TEM

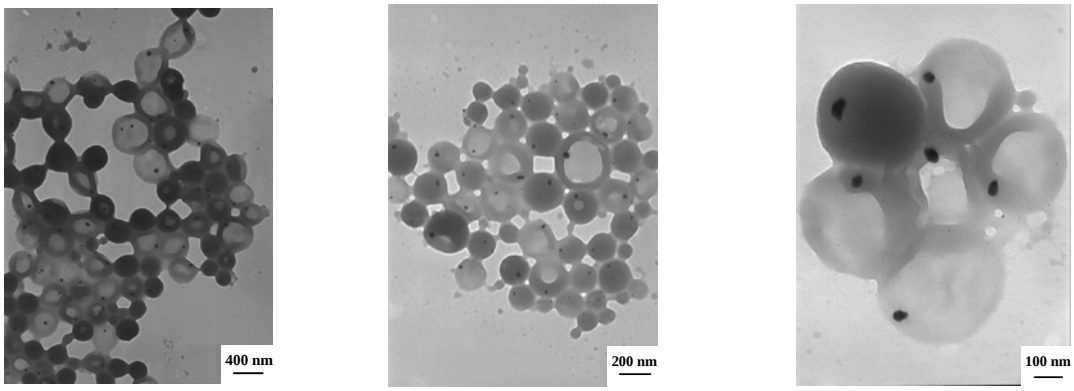

Figure 65. TEM micrographs of the polyurea nanocapsules coated with poly(vinylcaprolactam) (sample P52)**.**

We successfully synthesized polymeric nanoparticles and nanocapsules via miniemulsion polycondensation. A hydrophilic monomer or functional polymer present dissolved in a polar solvent building the dispersed phase was condensed with a hydrophobic monomer present in the continuous phase to give polyurea, polythiourea, polyurethane and crosslinked

biopolymers. Nanoparticles were synthesized if DMSO, 1-vinyl-2-pyrrolidone, N-VFA or 2-pyrrolidone were used as polar solvents, whereas nanocapsules were obtained if water and formamide the polar solvents. We found that the wall thickness of polyurea capsules was controlled by the amount of hydrophilic monomer introduced in the formulation. It was possible to use these capsules as nanoreactors for the reduction of silver nitrate into silver nanoparticles inside the core of the capsules. Remarkably, the capsules were found to be re-dispersable in water. It was also possible to increase the shell thickness of the polyurea capsules by the addition of the N-vinylcaprolactam monomer and its subsequent polymerization around the polyurea shell.

5. Conclusion and perspectives

Despair is the conclusion of fools.

Benjamin Disraeli (1804-1881)
English politician.

We described in this document new advances in miniemulsion polymerizations. This work was devoted to two important aspects: the investigation of new processes and the synthesis of high added value materials. These new processes either lower the cost of production, or allow new materials to be synthesized, or are more environmentally responsible. The second aspect of the work is dedicated to the material itself. To make value with a material is possible if it possesses one or several physical or chemical interesting characteristics (magnetic properties, thermo-responsive, light-emitter…) or special abilities (able to encapsulate hydrophilic compounds). In term of a polymer latex colloid, this is given by the kind of polymer used and by the morphology of the colloid.

Thus we investigated described different polymerizations in miniemulsion in order to obtain different latex functionalities. First, we performed free-radical polymerizations of styrene and divinylbenzene. These polymerizations were done in the presence either of octane or toluene in the dispersed phase. It was shown that the ratio between the monomer and the hydrophobic solvent regulates the morphology of the particles. Capsules could be obtained with the presence of octane in the dispersed phase with very low ratio monomer/ dispersed phase compared to the results of similar synthesis published before. We showed that it was also possible to tune the roughness of the particle surface by the addition of a crosslinker to the monomer.

Hybrid polymer/ metal latexes were synthesized in direct miniemulsion. Hydrophobic platinum complexes were encapsulated in polystyrene particles matrix. These particles were deposited in an ordered monolayer on silicon substrates due to their monodispersity. These latexes were further used by the Solid State Physics department of Ulm to obtain ordered metal clusters on silicon surface via plasma-etching of the particles. It would be possible to synthesize Fe/Pt or Fe/Co nanoparticles on a surface, which have interesting magnetic properties, using a similar technique. The desired latex could be synthesized in a very easy way, i.e. by a miniemulsion polymerization of styrene in the presence of a hydrophobic cobalt complex followed by the absorption of vinylferrocene into the latex. Note that it may be possible to perform controlled radical polymerization of the styrene with a cobalt complex by QTRP (Quinone Transfer Radical Polymerization) [**Cai**_2005].

A set of borohydride salts were used as unconventional initiators to polymerize styrene in direct miniemulsion. Satisfactory yields and high molecular weight of the polymer could be obtained with the use of iodomethane as transfer agent.

We copolymerized styrene and divinylbenzene with a surfactant bearing vinylic functions in direct miniemulsion. Stables polystyrene and poly(styrene-*co*-butyl acrylate) particles, but also poly(divinylbenzen) capsules could be obtained with the surfmer as sole surfactant. The polymerizable surfactant or surfmer was efficiently grafted to the surface of the particles as shown by XPS spectroscopy.

The stability of the miniemulsions against temperature was shown at very high temperature for heterophase systems. Experiments performed at temperature superior to 150 °C showed that miniemulsions are usually getting unstable with time due to coalescence facilitated at high temperature. When the additional stabilizer PVP was used in the miniemulsions containing DMSO or 2-pyrrolidone as the dispersed phase, the miniemulsion were stable at high temperature even for period of more than 10 hours. For temperatures ≤ 170 °C, the osmotic pressure agent K_2CO_3 was a better stabilizer than PVP for the miniemulsions containing 1-vinyl-2-pyrroldione as the dispersed phase. Miniemulsions with 1-vinyl-2-pyrrolidone as the dispersed phase performed at temperature > 170 °C were unstable. Two applications of the high temperature miniemulsion were successfully carried out to demonstrate the versatility of the technique; the polymerization of 1-vinyl-2-pyrrolidone by free-radical polymerization and the reduction of silver nitrate by ethylene glycol in miniemulsion droplets. A combination of both reactions gave hybrid metal/ polymer latexes. These results broaden the use of the miniemulsion technique to higher temperatures, thus allowing new nanomaterials to be synthesized in the miniemulsion droplets.

We showed for the first time that polymeric nanocapsules with a hydrophilic core can be created via an inverse miniemulsion polymerization. The monomer N-N´-dimethylacrylamide is dissolved in the aqueous dispersed phase. During the polymerization, the poly(N-N´-dimethylacrylamide) demixes owing to its immiscibility with the water and form a polymeric shell around the water droplets.

Secondly, we synthesized polyamide latexes via different techniques. Anionic polymerization was performed in inverse miniemulsion to give polyamide-6 latexes. Miniemulsions of ε-caprolactam in DMSO were more stable than miniemulsions with the sole ε-caprolactam as dispersed phase. Polyamide-6 nanoparticles were created by the precipitation of the polyamide inside the miniemulsion droplets. The polyamide had a relatively high molecular weight, which was around 36 000 $g \cdot mol^{-1}$) and had less structural irregularities than the polymer prepared in bulk. We strogly believe that our strategy, which employs polar solvents such as DMSO for the polymerization, can be also applied to prepare polymer particle of

other polar monomers that are normally slightly soluble in the apolar phase. This would allow one to polymerize water-sensitive polar monomer or any kind of polar monomers with a water-sensitive initiating system.

Polyamide-6 dispersions in water were prepared under sonication upon addition of polyamide-6 dissolved in a water miscible solvent, to an aqueous solution containing a stabilizer. This novel process combines some features of the solvent displacement process and the miniemulsion technique. Only a small operating window was found to be suitable in order to get stable sub-microns particles. This operating window includes the nature of the concentration of the stabilizer, the concentration of the polymer in the water miscible solvent, the nature of the miscible solvent, the nature of the aqueous solution, the amplitude of sonication and the temperature. Investigations made on the particles show a polyamide-6-core/ polyvinyl alcohol-shell morphology, where the polyamide-6 part is totally wrapped by the stabilizer. Beyond the synthesis of polyamide-6 dispersions, this process may be a suitable method to synthesize dispersions from polymers with strong intermolecular forces. Thus, the method could be applied to obtain aqueous dispersions of other polyamides. Finally, other groups reported the synthesis of metal nanoparticles in an aqueous phase via a sonochemical approach. We believe that our process could be profitable to make metal-polymer hybrid latexes if the sonication would be both used for dispersing the nylon 6 and synthesizing the metal nanoparticles.

Polyamide-6 nanocapsules were prepared by another miniemulsion/ solvent displacement technique. A solution of polymer polyamide-6 in formic acid was used to build the dispersed phase of an inverse miniemulsion system. The miniemulsion was heated and methanol was added to the miniemulsion. The product of the reaction, i.e. the methyl formate ester, was evaporated during the process whereas the polyamide-6 demixed because it is not soluble in the water by-product of the reaction and formed a polymeric shell.

Finally we investigated the synthesis of polymer latexes by polycondensation in miniemulsion. Hollow polymeric capsules containing a hydrophilic liquid core were obtained in a simple one-pot miniemulsion process without the use of a sacrificial core. The polyurea, polythiourea or polyurethane shells are made by polycondensation at the interface of the droplets. The functionality of the shell is governed by the nature of the monomers and the ratio between the two monomers introduced in the miniemulsion. The size of the capsule is dependent on the concentration of the surfactant, but also on the time of addition of the second monomer. The thickness of the wall of the capsules is controlled by the amount of

monomers employed. The shape of the capsules was always found to be round except when diethylenetriamine in water was used as the dispersed phase. Capsules loaded with silver nanoparticles were synthesized upon reduction of silver nitrate encapsulated in polyurea shell. Remarkably, the capsules were found to be re-dispersable in water. The polyurea is also a biocompatible material, which make these capsules suitable for biomedical application. For instance, polyurea microcapsules synthesized with diethylentriamine and tolylene-2,4-diisocyanate were found to have excellent oxygen-binding abilities in their use as artificial red blood cells [**ElG**-2004]. Further interesting work would include studies on the membrane permeability and the efficiency of these capsules as drug-delivery systems.

Thus, we showed in this document that unconventional polymerizations or unconventional processes can be easily performed in miniemulsion. They lead to functional nanomaterials with different morphologies. Because of the versatility of the miniemulsion technique, we believe that similar unconventional synthesis will be more often reported in the forthcoming literature, and that their status will change to very conventional synthesis. The first document on the miniemulsion technique was reported in 1973, i.e. 33 years ago [**Uge**_1973]. Amusingly, the number 33 represents universal nurturing in numerology. For long time, the miniemulsion was always the little sister in the family of the dispersion processes. But muc more than the other dispersion processes, the miniemulsion technique is adapted to the growing field of nanotechnologies.

6. Experimental part

Ya gots to work with what you gots to work with.

Stevie Wonder (1950- /)
American singer.

6.1. Miniemulsion free-radical polymerization

6.1.1. Free-radical polymerization in direct miniemulsion

6.1.1.1. Free-radical polymerization in direct miniemulsion in the presence of a solvent in the disperse phase

Materials

The monomers styrene (Merck) and divinylbenzene (Aldrich) were distilled under reduced pressure prior to use. Sodium dodecyl sulfate (Alfa Aesar), hexadecane (Merck), AIBN (Fluka) and toluene (Merck) were used as received.

Synthesis of the latexes

A known amount of the monomer styrene or divinylbenzene, a known amount of solvent toluene or octane, and 60 mg of n-hexadecane were mixed with 25 mg of AIBN and added to a solution of 25 mg of SDS in 7.5 g of water. After the mixture was stirred for 1 h, the mixture was miniemulsified by ultrasonication for 180 s with a Branson sonifier W450 Digital at 70% amplitude. To avoid polymerization due to heating, the mixture was cooled in an ice-bath during sonication. The miniemulsion was subsequently transferred to an oil-bath at 75 °C. Samples containing styrene and divinybenzene without solvents were prepared via the following way: a known amount of styrene and of divinylbenzene and 250 mg of *n*-hexadecane were mixed with 100 mg of AIBN and added to a solution of 72 mg of SDS in 24 g of water. After the mixture was stirred for 1 h, the mixture was miniemulsified by ultrasonication for 120 s with a Branson sonifier W450 Digital at 90% amplitude. To avoid polymerization due to heating, the mixture was cooled in an ice-bath during the sonication. The miniemulsion was subsequently transferred to an oil-bath at 75 °C.

6.1.1.2. Free-radical polymerization in the presence of metal complexes in direct miniemulsion

Materials

The monomer styrene (99%, Merck) was distilled under reduced pressure prior to use. Acrylic acid (99%, Aldrich) was passed through a column of aluminium oxide (97%, Acros). Sodium dodecyl sulfate (Alfa Aesar), *n*-hexadecane (Merck), and AIBN (Fluka) were used as received. Nickel (II) naphtenate (60% in toluene), and nickel (II) cyclohexanebutyrate were purchased from STREM. Platinum (II) acetylacetonate 99.99% was purchased from Aldrich.

Preparation of the miniemulsions

The total given amount of monomer(s), *n*-hexadecane (osmotic pressure agent), and the metal complex were mixed with a known amount of AIBN and added to a solution of a known amount of the SDS surfactant in 7.5 g of water. The mixture was covered with an aluminium foil and pre-emulsified by magnetic stirring for 1 h, and then miniemulsified by ultrasonication for 180 s with a Branson sonifier W450 Digital at 70% amplitude (1/2" tip). To avoid polymerization, the mixture was cooled with an ice-bath during sonication. The miniemulsion was subsequently transferred to an oil-bath at 75 °C. The polymerization was performed for 20 h at stirring rate of 500 rpm.

6.1.1.3. Free-radical polymerization initiated by borohydrides in direct miniemulsion

Materials

The monomers styrene, vinyl acetate, and methyl methacrylate MMA (all from Merck, 99%) were distilled under reduced pressure prior to use. Sodium dodecyl sulfate SDS (Alfa Aesar, 99%), *n*-hexadecane (Merck, 99%), lithium borohydride (Aldrich, 90%), sodium borohydride (Merck, 96%), potassium borohydride (Aldrich), 4-iodophenol (Aldrich, 99%), iodomethane (Merck, 99%), iodoform (Fluka, 99%), perfluorohexyl iodide (Aldrich, 99%), 4-iodoaniline (Aldrich, 98%), indium (III) chloride (Aldrich, 99.999%), lithium chloride (Aldrich, 99.99%), triethylene glycol dimethyl ether (Aldrich, 99%), diisopropylamine (Aldrich, 99%) and diethylene glycol dimethyl ether (Aldrich, 99%) were used as received. The solvents dioxane and N-methylpyrrolidone (both Merck) were of analytical grade. Demineralised water was used throughout the work.

Preparation of the miniemulsions

The total amount of 6 g of monomer, $5.5 \cdot 10^{-4}$ mol of chain transfer agent, and 250 mg of *n*-hexadecane were mixed and added to a solution of 72 mg of SDS, and a known amount of indium (III) chloride when noted, in 24 g of water. The mixture was pre-emulsified by magnetic stirring for 1 h in the dark, and then miniemulsified by ultrasonication for 120 s with a Branson sonifier W450 Digital at 90% amplitude (1" tip). To avoid polymerization, the mixture was cooled with an ice-bath during sonication. Then a solution or solid of a known amount of 0.0265 g of $NaBH_4$, or 0.015 g of $LiBH_4$, or 0.038 g of KBH_4 (i.e. $7 \cdot 10^{-4}$ mol of borohydride salt) in 2 g of a solvent, i.e. diisopropylamine, dioxane, triethylene glycol monomethyl ether, diglyme, dioxane or water was added to the miniemulsion. The overall

mixture was degassed for 10 min in argon and subsequently transferred to an oil-bath at 55 °C for 3 h.

6.1.1.4. Free-radical copolymerization with a surfactant in direct miniemulsion

Materials

The monomers styrene, butyl acrylate BA (both form Merck, 99%) and divinylbenzene (Aldrich) were distilled under reduced pressure prior to use. Sodium dodecyl sulfate (Alfa Aesar), *n*-hexadecane (Merck), AIBN and KPS (both purchased from Fluka, 98%) were used as received. The anionic surfactant Tego XP-1008 (M_n ~ 1150 g·mol^{-1}), a phosphate terminated polyethylene oxide-co-polypropylene oxide with vinyl groups was kindly provided by Degussa Goldschmidt GmbH. Demineralised water was used throughout the work.

Preparation of the miniemulsions

The total amount of 6 g of the monomer(s), 250 mg of *n*-hexadecane for the synthesis of particles or 3 g of monomer and 3 g of hexadecane for the synthesis of nanocapsules were mixed with 200 mg of AIBN and added to a solution of known amounts of the polymerizable surfactant XP-1008 in 24 g of water. The mixture was pre-emulsified by magnetic stirring for 1 h, and then miniemulsified by ultrasonication for 120 s with a Branson sonifier W450 Digital at 90% amplitude (1/2" tip). To avoid the polymerization, the mixture was cooled with an ice-bath during sonication. The miniemulsion was subsequently degassed with argon for 10 min and transferred to an oil-bath at 75 °C. If the water-soluble initiator KPS was used for the synthesis, the initiator was added after miniemulsification. The polymerization was performed for 20 h at stirring rate 500 rpm. For comparison between XPS measurements, a reference latex was synthesized with SDS instead of the surfmer using the same experimental conditions as described above.

6.1.2. Free-radical polymerization in inverse miniemulsion

6.1.2.1. Miniemulsion polymerization at high temperature

Materials

1-vinyl-2-pyrrolidone (from Aldrich, 99%) was passed trough a column and Isopar M (Exxon) was dried and then distilled under reduced pressure. Ethylene glycol (wasserfrei, Aldrich), silver nitrate (Merck, p.a.), 2-pyrrolidone (Aldrich, 99%), DMSO (p.a., Merck), potassium carbonate (Aldrich, 99%), polyvinylpyrrolidone M_w ~ 40 000 g·mol^{-1} (Aldrich),

Lubrizol U (Lubrizol), Brij 72 (Aldrich), Span 80 (Aldrich), and the initiator V-40 (Wako) were used as received. The block copolymer emulsifier poly[(butylene-*co*-ethylene)-*b*-(ethylene oxide)], P(B/E-*b*-EO), consisting of a poly(butylene-*co*-ethylene) block (M_w = 3700 g·mol^{-1}) and a poly(ethylene oxide) block (M_w = 3600 g·mol^{-1}) was synthesized starting from Kraton liquid (Shell), which was dissolved in toluene, by adding ethylene oxide under the typical conditions of anionic polymerization.

Preparation of the miniemulsions

1.5 g of liquid polar disperse phase (1-vinyl-2-pyrroldione, ethylene glycol, 2-pyrrolidone, DMSO) was mixed either with 50 mg of PVP, 25 mg of K_2CO_3, or both, or with a know amount of silver nitrate. The polar phase was mixed with a solution of a known amount of P(B/E-*b*-EO) surfactant in 7.5 g of Isopar M. The mixture was pre-emulsified by magnetic stirring for 1 h in the dark, and then miniemulsified by ultrasonication for 180 s with a Branson sonifier W450 Digital at 70% amplitude. The mixture was cooled with an ice-bath during sonication. 30 mg of the initiator V-40 dissolved in 1 g of xylene was added to the miniemulsion. Then, the miniemulsion was bubbled with argon for 10 min and transferred in a round-bottom flask equipped with a reflux condenser to an oil-bath at a given temperature. The miniemulsions containing silver nitrate turned brown after approximatively 10 min because of the reduction of silver nitrate to silver nanoparticles.

6.1.2.2. Synthesis of capsules with hydrophilic liquid core via radical miniemulsion polymerization

Materials

N,N′-Methylenebis(acrylamide) (Sigma, 99%), fluorescein (Fluka) and potassium peroxodisulfate KPS (Fluka, 98%) were used as received. Demineralised water was used throughout the work.

Synthesis of the capsules

0.1g of N,N′-Methylenebis(acrylamide) and 12.5 mg of KPS were dissolved in 1.3 g water and subsequently added to a solution of 50 mg P(B/E-*co*-EO) surfactant dissolved in 7.5 g of cyclohexane or toluene. The mixture was pre-emulsified by magnetic stirring for 1 h, and then miniemulsified by ultrasonication for 180 s with a Branson sonifier W450 Digital at 70% amplitude. The mixture was cooled with an ice-bath during sonication. The overall mixture

was subsequently bubbled with argon for 10 minutes and transferred in a round-bottom flask at 65 °C.

6.2. Anionic polymerization of lactams in miniemulsion and synthesis of polyamide latexes

6.2.1. Anionic polymerization of ε-caprolactam

Chemicals

The monomer ε-caprolactam was purchased from Aldrich (99+%) and then recrystallized twice in cyclohexane and vacuum-dried over P_2O_5. The activator *N*-acetylcaprolactam (ABCR, 99%) was used as received. The initiator of the polymerization NaH was purchased from Merck-Schuchardt (60% in suspension), washed with dried perfluoroether, and dried. Dimethyl sulfoxide (DMSO) from Merck was dried under CaH_2 for 15 h and then distilled under reduced pressure. Dimethylacetamide was shaken with BaO for 1 week, refluxed with BaO for 1 h, and then fractionally distilled under reduced pressure. Then the dimethylacetamide was dried under CaH_2 for 15 h and then distilled again under reduced pressure. The block copolymer emulsifier poly[(butylene-*co*-ethylene)-*b*-(ethylene oxide)], P(B/E-*b*-EO), consisting of a poly(butylene-*co*-ethylene) block (M_w = 3700·g mol^{-1}) and a poly(ethylene oxide) block (M_w = 3600·g mol^{-1}) was synthesized starting from Kraton liquid (Shell), which was dissolved in toluene, by adding ethylene oxide under the typical conditions of anionic polymerization. P(B/E-*b*-EO) was vacuum-dried prior to use. P(B/E-*b*-EO) was chosen as the surfactant because of its strong ability to stabilize inverse emulsions and its inertness related to the NaH and the sodium caprolactamate. The hydrophobic apolar isoparaffinic hydrocarbon Isopar M was a gift by Exxon Chemical. Isopar M and decalin were refluxed with CaH_2 for 15 h and then distilled from the CaH_2 under vacuum. Formic acid from Merck-Schuchardt (99%) was refluxed with boric anhydride for 3 d, distilled under vacuum, and then used for UV analysis. CaH_2, BaO (both from Aldrich), and phosphazene base P_4-t-Bu (Fluka, solution 1.0 M in hexane) were used as received. Finally know amounts of sodium (Merck) were cut in pieces and conserved in a know amount of dried Isopar M.

Synthesis of PA6 particles.

A typical miniemulsion polymerization procedure occurred in the following way: 0.5 g of the monomer, 1 g of DMSO, and 5 mg of NaH (polar phase) were mixed at room temperature to create the sodium caprolactamate in DMSO. For some experiments as shown in Table 1, 100 mg of acetamide was added to the polar phase to use it as an additional osmotic pressure agent. The mixture was then added to a solution of a controlled amount of surfactant in 7.5 g of the continuous phase (usually Isopar M as apolar phase). After stirring 1 h for preemulsification, the miniemulsion was prepared by ultrasonicating the mixture for 225 s, with 10 s pulse on and 5 s pulse off cycles, at 65% amplitude (Branson sonifier W450 Digital, tip size 6.5 mm) under argon at 0 °C with ice cooling in order to prevent polymerization. Then 0.05 mL of *N*-acetylcaprolactam was added to the mixture, and ultrasonication was performed for 20 s at the same amplitude as before. The miniemulsion was subsequently transferred in an oil bath at 150 °C to allow the polymerization to occur. Completion of reaction was observed after 25 min as checked by ^{1}H NMR measurements of the monomer. The PA6 solid used for the polymer characterization was obtained by drying the miniemulsion for 96 h at 40 °C under vacuum. The monomer and oligomer were then extracted from the crude polymer with water. Finally, we washed the solid with hexane, dried the solid again, and weighed the resulting polymer to calculate the yield of polymerization. FT-IR (KBr): 3300 (vs, NH), 2933 (s, CH_2), 2860 (m, CH_2), 1642 (vs, amide I), 1541 (s, amide II), 1371 (w, CH_2), 1261 (w, CH_2), 1200 (w, CH_2), 1120 (w, CC); DSC: T_m = 211 °C.

Variation of the initiator and experimental set-up

The previous synthesis was also done with the following variation. We initiated the polymerization with additional dispersion of NaH or dispersion of sodium in Isopar M with the experimental set-up shown in Figure 66. To perform these experiments, we used a special set-up shown in Figure. The dispersion of NaH was composed of 5 mg of NaH in 2 g of dried Isopar M. The dispersion of sodium was composed of Na in 2 g of dried Isopar M and was kept liquid at 100 °C before the ultrasonication. As an alternative to the NaH initiator, phosphazene P_4-t-Bu was tried as initiator in the anionic bulk polymerization of ε-caprolactam in the presence of the activator N-acetylcaprolactam at 150 °C. The measured conversion was always less than 10% and thus the system was not further studied.

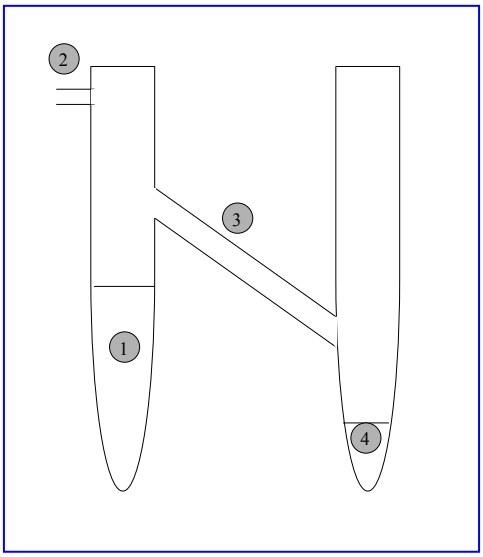

Figure 66. Experimental set-up for the miniemulsion polymerization of ε-caprolactam initiated by sodium or sodium hydride dispersed in Isopar M. The mixture of ε-caprolactam in Isopar M is first miniemulsified in the reservoir **1** under argon thanks to the inlet in position **2**. The initiator in Isopar M is dispersed with ultrasonication under argon in the reservoir **4**. The dispersion in **4** is then transferred via **3** to go to the reservoir **1** and the mixture is miniemulsfied again.

6.2.2. Synthesis of polyamide 6 nanoparticles and nanocapsules via two miniemulsion/ solvent displacement hybrid techniques

Chemicals

Nylon 6 was purchased from Aldrich (M_v ~ 19 000 g·mol^{-1}). Formic acid 99%, sulfuric acid 95-97% and methanol 99% were purchased form Merck-Schuchardt. Poly(vinyl alcohol) (PVA; M_w ~ 22 000 g·mol^{-1}; hydrolysis rate = 98 - 99%) and poly(vinyl alcohol) (PVA; M_w ~ 72 000 g·mol^{-1}; hydrolysis rate = 98 - 89%) were purchased from Fluka. The block copolymer emulsifier poly[(butylene-*co*-ethylene)-*b*-(ethylene oxide)] P(B/E-*b*-EO) consisting of a poly(butylene-*co*-ethylene) block (M_w = 3700 g·mol^{-1}) and a poly(ethylene oxide) block (M_w = 3600 g·mol^{-1}) was synthesized starting from Kraton liquid (Shell), which was dissolved in toluene, by adding ethylene oxide under the typical conditions of anionic polymerization. Cyclohexane was refluxed with CaH_2 for 15 h and then distilled from the CaH_2. $Al(NO_3)_3$

(98%, Fluka), NaOH (99%+, Sigma-Aldrich), H_2SO_4 (98%, Merck), KI (99%, Sigma), I_2 (99%+, Sigma-Aldrich) were used as received.

Synthesis of nylon 6 nanoparticles

First method; a solution containing 24 mg of surfactant or stabilizer (PVA if not marked otherwise), 7.5 g of water and 3 g of methanol was ultrasonicated for 30 s at 70% amplitude (Branson sonifier W450 Digital, tip size 6.5 mm) under ice cooling. Then a solution of 15 mg of nylon 6 in 0.75 g of formic acid was added within 6 min (~6 $ml \cdot h^{-1}$) while keeping the sonication at the same amplitude under ice cooling. Finally, sonication was continued for 30 s.

Modification of the nanoparticles

4 mg of KI and 7 mg of I_2 or 5 mg of $Al(NO_3)_3$, dissolved in 1.5 g of water was added to a sample synthesized with the conditions of sample DC210.

Synthesis of nylon 6 nanocapsules

The total amount of 0.75 g of formic acid, 0.03 g of nylon 6 were added to a solution of 0.05 g of P(B/E-*b*-EO) surfactant in 7.5 g of cyclohexane. The mixture was pre-emulsified by magnetical stirring for 1 h, and then miniemulsified by ultrasonication for 180 s with a Branson sonifier W450 Digital at 70% amplitude. To avoid the heating, the mixture was cooled with an ice-bath during the sonication. The miniemulsion was subsequently transferred to an oil-bath at 40 °C. 0.75 g of methanol was then subsequently added for 180 s.

6.3. Polycondensation in miniemulsion

6.3.1. Polyamide latexes in miniemulsion polycondensation

Chemicals

Hexamethylene diamine (98%, Aldrich), putrescin (99%, Aldrich), diethylenetriamine (98%, Aldrich), adipic acid (99%, Aldrich), adipoyl chloride (98%. Aldrich), triphenyl phosphite (97%, Aldrich), sebacoyl chloride (99%, Fluka), DMSO (p.a., Merck), 2-pyrrolidone (99%,Aldrich), LiCl (99%, Aldrich), 1,2-dichlorobenzene (99%, Aldrich), Isopar M (Exxon), pyridine (p.a., Merck) were used as received. 2- vinylpyridine was distilled under pressure.

Synthesis of poly(2-vinylpyridine) latex in miniemulsion

6 g of 2-vinypyridine and 250 mg of hexadecane were eventually mixed with 300 mg of AIBN and then mixed a solution of 72 mg of SDS in 24 g of water. The resulting mixture was stirred vigorously for 60 min and subsequently miniemulsified by ultrasonication for 120 s with a Branson sonifier W450 Digital at 90% amplitude. To avoid the heating, the mixture was cooled with an ice-bath during the sonication. The miniemulsion was then transferred to an oil-bath at 75 °C. 300 mg of KPS dissolved in 6 g of water was eventually added to the miniemulsion to start the reaction. The miniemulsions performed with KPS as an initiator were found to be unstable (only coagulum) because of the amphiphilic nature of the 2-vinylpyridine monomer whereas the polymerizations initiated by AIBN gave 6 wt.% coagulum. The poly(2-vinylpyridine) synthesized with AIBN initiation was analyzed by GPC in THF with PS-standards and the molecular weights were found to be: M_n = 18 500 g·mol^{-1}, M_w = 48 000 g·mol^{-1}, PDI = 2.6.

6.3.1.1. Tentative synthesis of stable polyamide latexes by direct miniemulsion polycondensation at low temperature

0.77 g of terephtaloyl chloride dissolved in 4 g of dibutylphtalate was mixed with a solution of 0.045 g of SDS or hexadecyltriethlammonium chloride or 0.05 g of Lutensol AT-50 in 15 g of water. The mixture was stirred for 2 min and then miniemulsified by ultrasonication for 120 s with a Branson sonifier W450 Digital at 90% amplitude. To avoid the heating, the mixture was cooled with an ice-bath during the sonication. A third part consisting of 0.3 g of diethylenetriamine and 0.32 g of NaOH dissolved in 2 g of water was subsequently added to the miniemulsion for 300 s under argon. The miniemulsions prepared via this method were always found to be unstable.

6.3.1.2. Tentative synthesis of stable polyamide latexes by inverse miniemulsion polycondensation at low temperature

A known amount of molten or dissolved monomer was stirred with a solution of 0.075 g of P(B/E-*b*-EO) in 7.5 g of Isopar M for 1 h. The mixture was then miniemulsified by ultrasonication for 180 s with a Branson sonifier W450 Digital at 70% amplitude. To avoid the heating, the mixture was cooled with an ice-bath during the sonication, except when molten monomer was used. A third part consisting of a known amount of the second monomer was added to the miniemulsion.

6.3.1.3. Tentative synthesis of stable polyamide latexes by miniemulsion polycondensation at higher temperature

A known amount 1,6-hexadecane, diethylenetriamine or 1,4-diaminobutane were mixed with triphenyl phosphite, adipic acid and 1.3 g of DMSO. The monomers were in equimolar amount and the total amount was varied from 0.1 g to 0.2 g. was stirred with a solution of 0.075 g of P(B/E-*b*-EO) in 7.5 g of Isopar M for 1h. The mixture was then miniemulsified by ultrasonication for 180 s with a Branson sonifier W450 Digital at 70% amplitude. To avoid the heating, the mixture was cooled with an ice-bath during the sonication, except when molten monomer was used. The mixture was then allowed to react in an oil-bath at 150°C for 3 h.

6.3.2. Polyurea and polyurethane latexes in miniemulsion polycondensation

Chemicals

The hydrophilic monomers 1,4-diaminobutane (DAB), 1,6-diamonohexane (HMDA) and diethylenetriamine (DET), glycerol, 1,6-hexandiol (all 99%), and 3,4-diaminobenzoic acid (DBA, 97%) were purchased from Aldrich. L-Arginine (Ph Eur, USP) was purchased from Merck-Schuchardt. The hydrophilic polymers dextran from Leuconostoc spp. M_r 70 000 g·mol^{-1} and soluble starch from potatoes M_r = 162.14 g·mol^{-1} were purchased from Fluka. Water-free poly(ethylene imine) high molecular weight (PEI) was purchased from Aldrich. The tolylene-2,4-diisocyanate (TDI, 98%) and hexamethylene diisocyanate (HMDI, 98%) were purchased from Fluka while the isophorone diisocyanate (IPDI, 98%) and tolylene-2,4-diisothiocyanate (TDIT, 97%) were purchased from Aldrich. The salts sodium chloride, sodium hydroxide and silver nitrate were p.a. chemicals from Merck. Formamide (99.5%) from Aldrich and demineralised water were used throughout the work. The reducing agent hydrazinium hydroxide (99%) was purchased from Merck. All reagents were used as received. N-vinylformamide (N-VFA, 98%) and 1-vinyl-2-pyrolidone (1-V2P, 99%+), both from Aldrich, were distilled under reduced pressure. Dimethyl sulfoxide (DMSO) from Merck and 2-pyrrolidone from Aldrich (99%+) were dried under CaH_2 for 15 h and then distilled under reduced pressure. The block copolymer emulsifier poly[(butylene-*co*-ethylene)-*b*-(ethylene oxide)] P(B/E-*b*-EO) consisting of a poly(butylene-*co*-ethylene) block (M_w = 3700 g·mol^{-1}) and a poly(ethylene oxide) block (M_w = 3600 g·mol^{-1}) was synthesized starting from Kraton liquid (Shell), which was dissolved in toluene, by adding ethylene oxide under the typical conditions of anionic polymerization. Cyclohexane was refluxed with CaH_2 for 15 h

and then distilled from the CaH_2. Potassium persulfate (99%) was purchased from Fluka and hydrazine (98%) was purchased from Aldrich.

Synthesis of the hollow nanocapsules

A typical procedure occurred in the following way: 0.1 g of the amino-monomer or hydroxyl containing monomer or hydrophilic polymer, 1.3 g of the polar solvent in the droplet that forms the liquid core, and 30 mg of NaCl were mixed at room temperature. This mixture was then added to a solution of a controlled amount of the P(B/E-*b*-EO) surfactant in 7.5 g of the continuous phase (usually cyclohexane was used as non-polar phase except mentioned otherwise). After stirring 1 h for pre-emulsification, the miniemulsion was prepared by ultrasonicating the mixture for 180 s at 70% amplitude (Branson sonifier W450 Digital, tip size 6.5 mm) with ice cooling in order to prevent polymerization. Then a defined amount of diisocyanate or diisothiocynate diluted in cyclohexane with P(B/E-*b*-EO) was added to the miniemulsion usually during 300 s, except when mentioned otherwise. The mixture was allowed to react for 2 h at 25 °C for the polyurea nanocapsules, and at 60 °C for the polyurethane, the cross-linking of starch or dextran, and the formation of the polythiourea nanocapsules. For the polymerization of 1-vinyl-2-pyrrolidone inside the nanoreactors, a controlled amount of this monomer and the initiator KPS was added to the dispersed phase. For the reduction of silver nitrate in the nanocapsules, a controlled amount of silver nitrate was added to the dispersed phase and acted as the lipophobe instead of the sodium chloride. Then for the samples containing silver nitrate, two different methods were chosen for the reduction of the salt. With the first method, 0.2 ml of hydrazine was added to the miniemulsion. With the second method, a macroemulsion containing 0.2 ml of hydrazine, 2 ml of cyclohexane and 0.1 g of P(B/E-*b*-EO) was added to the miniemuslion. For both methods, the miniemulsion was ultrasonicated during the addition for 60 s with pulses of 5 s and pauses of 3 s at 70% amplitude (Branson sonifier W450 Digital, tip size 6.5 mm) at 0 °C with ice cooling and was kept overnight at 25 °C. Typical formulations of the latexes are shown in Table 1 and the overall synthesis of the capsules loaded with silver nanoparticles is summarized in Figure 1. The dispersion of the nanocapsules in water was done via the following way: 0.15 g of the synthesized latex was mixed with a solution of 5 mg of SDS in 6 g of water. The resulting mixture was ultrasonicated for 1 min at 70% amplitude (Branson sonifier W450 Digital, tip size 6.5 mm) with ice cooling. Then 10 wt.-% of the dispersion was evaporated and subsequently put in an ultrasonic bath for 5 min. This procedure was found to

be more suitable than the traditional freeze-drying technique in order to re-disperse the nanocapsules.

7. Appendix

The folly of mistaking a paradox for a discovery, a metaphor for a proof, a torrent of verbiage for a spring of capital truths, and oneself for an oracle, is inborn in us.

Paul Valery (1871-1945)
French author and philosopher.

7.1. Methods

AFM

For the part 4.3.2., Atomic Force Microscopy was performed during evaporation of the cyclohexane continuous phase with a soft cantilever with a contact mode (MFP-3D microscope, Asylum Research), after evaporation of the cyclohexane, after drying the latex deposited on the substrate in a exciccator for 12 h, and after submitting the latex deposited on the substrate to strong vacuum for 10 min (all tapping mode). The sample was prepared either by dropping or by spin-coating a 10 wt.% diluted latex on mica substrates.

Calorimetry

Calorimetry was performed for the part 4.3.2. with a Micro Reaction Calorimeter μ-RC™ from THT. Samples of 0.5 ml of the miniemulsion were prepared and 280 μl of the diiso(thio)cyanate in cyclohexane and surfactant was subsequently added to study the kinetics of the reaction at 20 °C for the polyurea shell and 60 °C for the polythiourea and the polyurethane shells. Reference experiments without diiso(thio)cyanate were investigated to determine the contribution of the energy of mixing of the liquid added to the miniemulsion.

Dialysis

Latexes stabilized by the Tego XP-1008 were dialyzed against demineralised several times in a Sigma centrifuge at 3900 rpm for 25 min until the conductivity of water remains constant at a value below 3 μS/cm. Four dialyse cycles were found to be enough to fulfil the previous requirement. The membranes were purchased from Millipore (Amicon Ultra-4 30000 M_w).

Differential Scanning Calorimeter (DSC)

DSC measurements were made with samples of about 10 mg on a Perkin Elmer DSC 7 system. Cooling and heating rates were 10 °C/min.

Dynamic Light Scattering (DLS)

The particle sizes were measured by photocorrelation spectroscopy using a Nicomp particle sizer (model 370, PSS Santa Barbara, CA) at a fixed scattering angle of 90 °. The data were processed using the cumulants method.

Gel Permeation Chromatography (GPC)

Gel permeation chromatography (GPC) experiments were performed with chloroform on Waters–Styragel columns (pores sizes: 105, 104, 103, and 106 A) using a Waters 410 differential refractometer and a Viscotek H502B detector. The molecular weights were calculated on the basis of narrow molecular weight distribution polystyrene standards using PSS (Mainz) software.

High Resolution Scanning Electron Microscopy (HR-SEM)

High resolution scanning electron microscopy was performed on a Hitachi S-5200.

Infra-Red Spectroscopy (IR)

The FT-IR measurements were performed to check for the vanishing of the lactam bond and the creation of polyamide bonds with KBr pellets in a FTIR 113v Bruker spectrophotometer equipped with a DTGS detector using 100 signal-averaged scans at a resolution of 2 cm^{-1}. The solid used for the IR measurements was obtained by drying the miniemulsion for 96 h at 40 °C under vacuum, then washing the solid with water, hexane and dry the solid again.

The FT-IR samples of aqueous dispersions of polyamide-6 were prepared by dissolving KBr in the latexes. The solvents were subsequently evaporated to yield a powder, which was used to make the pellets.

Matrix Assisted Laser Desorption Ionization Time-Of-Flight Spectrometry (MALDI-TOF)

MALDI-TOF spectra were recorded with Bruker-Franzen REFLEX III, N2 laser (337 nm) with a DHB (2,5-dihydroxybenzoic acid) matrix.

Nuclear Magnetic Resonance (NMR)

Proton nuclear magnetic resonance (^{1}H-NMR) spectra were recorded on a Bruker Avance 400 spectrometer at 400 MHz in deuterated chloroform solvent using TMS as internal standard.

Plasma-etching

The plasma-etching reported in this thesis was performed by the department of Solid State Physics of the University of Ulm. It was performed on a OXFORD PLASMALAB 80PLUS (Oxford Instruments). The chamber temperature was set to 20 °C, the pressure 80 mTorr and the O_2 flow flowed at 30 sccm. The RF power was 1W and the ICP forward power was 100

W (anisotropic plasma in the chamber). The silicon substrates (CRYS TEC) are 3 inch diameter, 375 μm, orientation (100) and have a specific resistance bigger than 1 Ohm·cm.

Scanning Electron Microscopy (SEM)

Scanning electron microscopy (SEM) micrographs were obtained with a DSM 962 SEM (Zeiss, Germany). A thin layer of Au/Pd alloy (about 5 nm) was sputtered onto the samples prior to imaging.

Static Light Scattering

Static laser light scattering experiments were performed with ALV-Instruments ALV/CGS-8F laser goniometer system and ALV-5000 multi digital correlator to determine the R_g/ R_h ratio of the nanocapsules. The light source was JDS Uniphase helium/neon 22 mW laser operating at lambda = 633 nm. The correlation functions obtained were analyzed using the CONTIN program and the scattering angle was varied from 20 to 150°.

Tensiometry

Surface tension measurements of the latexes were carried out at 25 °C using a DCAT11 tensiometer from Dataphysics, employing the Du Nouy ring method. The ring radius of the Pt-Ir ring is 9.4425 mm and the wire radius is 0.185 mm. Each measurement was repeated 10 times and the average value was taken as result.

Thermogravimetry

Gravimetric measurements were performed with a Kern RH 120-3 gravimeter to measure the solid content of the latexes.

Transmission Electron Microscopy (TEM)

Electron microscopy was performed with a Phillips 400T TEM spectrophotometer operating at 80 kV. The miniemulsions were diluted in cyclohexane and then applied to a 400 mesh carbon-coated copper grid and left to dry. No further contrasting was applied.

Ultrasonication

Miniemulsification or homogeneization were performed with a Branson sonifier W450 Digital. The tip size used depends on the sonified volume. For volume exceeding 10 ml, the tip size was 10 mm and 6.5 mm for smaller volumes. Ultrasonication was generally

performed at 0 °C with ice cooling in order to prevent polymerization. Eventually, a thermostated oil bath was used for sonication at higher temperature.

Ultraviolet-Visible Spectroscopy (UV-Vis)

UV analyses were carried out with a Perkin Elmer UV/Vis spectrometer Lambda 16. PA6 solutions in anhydrous formic acid of 0.5% (w/w) were analyzed, searching for optimum density maxima at 270-280 nm. The measurements were done between 250 and 400 nm.

For the capsules synthesized in inverse miniemulsion, UV-Vis analyses were carried out with a Perkin-Elmer UV/Vis spectrometer Lambda 16. The latexes were 50 times diluted (w/w) in dried cyclohexane.

Viscosimetry

Viscometry measurements were performed using an AVS 350 Schott Geräte rheometer to evaluate the mass weighted molecular mass on polymer solution 0.05 $g \cdot dL^{-1}$ in H_2SO_4 (95-97% from Merck) at 20 °C.

X-ray Diffraction (XRD)

Wide-angle diffraction patterns of the polymers were obtained at room temperature, using nickel-filtered Cu Kα radiation. Slightly pressed flat samples were mounted perpendicularly to the primary X-ray beam. A flat-film camera with a sample-film distance of 90 mm was used to record the reflections. Optical density data were collected from the photographically obtained patterns using a linear scanning microdensitometer LS20.

X-ray Photoelectron Spectroscopy (XPS)

X-ray photoelectron spectroscopy (XPS) analysis was performed using an X-Probe 206 spectrometer (Surface Science Instruments, USA). The binding energies were referenced to hydrocarbon at 285.0 eV. The emission angle of electrons was set at 55 ° with respect to the sample, which results in an information depth of about 10 nm.

7.2. Abbreviations

AAm	Acrylamide
AFM	Atomic Force Microscopy
AIBN	*α,α′*-Azoisobutyronitrile
ATRP	Atom Transfer Radical Polymerization
BA	Butyl acrylate
CCC	Critical coagulation concentration
CL	ε-caprolactam
CTMA-Cl	Cetyltrimethylammonium chloride
DAB	1,4-diaminobutane
DET	diethylenetriamine
DLS	Dynamic light scattering
DMA	Dimethyl acetamide
DMF	Dimethyl formamide
DMSO	Dimethyl sulfoxide
DVB	divinylbenze
FT-IR Spectroscopy	Fourier Transform Infra Red Spectroscopy
GPC	Gel Permeation Chromatography
HD	Hexadecane
HMDA	Hexamethylenediamine
HMDI	Hexamethylenediisocynate
IR Spectroscopy	Infra-Red Spectroscopy
IPDI	Isophorone diisocyanate
KPS	Potassium peroxydisulfate
MMA	Methyl methacryate
NMP	Nitroxides Mediated Poylmerization
NMR	Nuclear Magnetic Resonance
OPA	Osmotic Pressure Agent
2-P	2-pyrrolidone
PA6	Polyamide-6
P(B/E-*b*-EO)	Poly[(butylene-*co*-ethylene)-*b*-(ethylene oxide)]
PEGA	Poly(ethylene glycol) azo-initiator

PEI	Polyethyleneimine
PEO	Poly(ethylene oxide)
PMMA	Poly(methyl methacrylate)
PPO	Poly(propylene oxide)
PU	Polyurethane
P2VP	Poly(2-vinylpyridine)
PVA	Poly(vinyl alcohol)
PVP	Polyvinylpyrrolidone
RAFT	Radical Addition Fragmentation Transfer
RIE	Reactive Ion Etching
S	Styrene
SANS	Small Angle Neutron Scattering
SDS	Sodium dodecyl sulfate
SEM	Scanning Electron Microscopy
SLS	Static Light Scattering
TDI	Tolylene-2,4-diisocyanate
TDIT	Tolylene-2,4-diisothiocyanate
TEM	Transmission Electron Microscopy
UV	Ultraviolet
XPS	X-ray photoelectron spectroscopy
XRD	X-ray Diffraction

7.3. Symbols

C_{OPA}	Solubility of the bulk osmotic pressure agent in the continuous phase
d	Hydrodynamic diameter
D	Diffusion coefficient
D_{OPA}	Molecular diffusivity of the osmotic pressure agent
k	Boltzmann´s constant
M_n	Number averaged molecular weight
M_v	Viscosimetric molecular weight
Mw	Weight averaged molecular weight
R	Hydrodynamic radius
t_a	Aging time
T	Temperature
T_g	Glass transition temperature
V_m	Molar volume
$wt.\%$	Weight percentage
Φ_{OPA}	Volume fraction of the osmotic pressure agent in the disperse phase
η	Dynamic viscosity
$[\eta]$	Intrinsic viscosity
σ	Standard deviation

Acknowledgements

L’idée de *la gratitude*

Quelqu’un m’a dit que la gratitude n’était qu’une idée
qui nous arrive après que nous avons reçu quelque chose—
soit un cadeau, soit un pardon, soit de la manne tombée
du ciel—une idée, une chose abstraite. Et je suppose
qu’il avait raison, mais j’ai peur qu’on aille déduire
de tout cela que la gratitude, étant abstraite, n’existe pas.
Parce qu’on ne peut pas la voir, qu’on ne peut pas la sentir—
effectivement, c’est un fantôme qui fréquente l’au-delà
où rôdent tous nos rêves d’être plus gentils, plus sensibles,
plus reconnaissants. ... Mais cette terre, où nous nous trouvons,
d'après Thoreau, menant des vies de plus en plus terribles
dans leur *désespoir silencieux*, peut être une chanson
faite d'ondes, de vents et d'oiseaux--de petites choses
qui nous remplissent de gratitude, d'où vient la vie en rose.

Lynne Knight
American poetess.

The little poem above shows that the reasons of gratitude should not be enumerated to express fully the harmony between the transmitter and the receptor. Gratitude is a comfortable feeling, an unexpected and spontaneous bliss: “la vie en rose”, the life in rose of the poem. Of course the writer is a woman and you may not like the rose colour. However, we can decently assume that the author would not be upset if you choose your favourite colour, in my case: yellow. You do not need necessarily to climb the Everest or to dive in deep water to live extreme instants. A PhD is filled with moments of enthusiasm and moments of depression. And if my life in Ulm was pretty yellow, it is because of the support of people around me.

I would like to thank first Katharina who allows me to start a PhD under her guidance. Despite the numerous responsibilities, your advices were wise and accurate and you always radiated motivation and enthusiasm around you. I am sure you will reach the firmament in polymer and colloid science. It was my good fortune to cohabit with nice people in the office 456: Nicole, Verena, Andy the “benefitor”, Andreas S. and Pyrrha, my computer, which never failed under my directorship. Andy and Andreas: if you do not know how to use the redeemer, do not use it. Verena: don´t do this, this hurts! Nicole: I still believe that Regensburg is one of the most beautiful city we visited in Germany. These visits could not be performed without the Deutsche Bahn, which offers excellent prices for local travels with Baden-Württemberg and Bayern tickets (highly recommended for those who want to visit South-Germany with friends). Marcel was an excellent and nice recruit for my lab (4202: das schönste Labor der Welt) in spite of the fact that he is repeating “don´t do this!” all the time (a syndrome of the PhD student?). I thank the members of the neighbouring lab 4204: Sonja and Eyk, my spiritual heir. Despite the geographical position of the glove box laboratory, its inhabitants are not forgotten. I wish all the best for Axel and to Günther, whatever you choose to do in the future. The guardian of the office of the room 425, Ulrich, is also gratefully acknowledged for his technical help. To speak Swabian is not necessarily a factor of misunderstanding if kindness is present in the relationships. I was hence able to communicate effectively with Magdalene. Carola did the AFM measurements reported in this thesis and was an efficient and nice interlocutor. It is not surprising that Anna is working on DNA. Let us remember that her nice character was designed primarily by a combination of genes in her DNA. Maybe she feels greatly indebted to Mother Nature. I am looking forward to reading the article of Prof. Dr. Musyanovych! Luis is quite small. But he is a huge monument dedicated to good temper and enthusiasm. Blue Membranes Company made a golden deal when they hired you, I want to buy the first stocks! You see, there is a big difference between Baden and Schwaben. If you are not that convinced, take lessons for free with Marissa and Andreas Schatzinger. Some

people stayed with a bad feeling about Indian people after they saw Indiana Jones and the Temple of Doom. If you have the opportunity to meet Anitha, you will discover that there are not so bad and that they can even be very friendly. I am grateful to Clemens to have come downhill from the Allgäu to release some of the freshness of these mountains. Heike is blond, Maria-Verena is brown-haired but they are friend. They seemed to agree to bring an additional sweet touch of femininity to the department. Some of the polymer characterizations were realized by Marlies (DSC and TGA) and Mike (GPC). They conjugate both technical competence with good mood and thus even a non-satisfactory result did not become necessarily a disappointment. Christine and Marianne are the alternative current who power the administrative work of the OC3 department. I am indebted for their help concerning this matter. There is a film directed by Quentin Tarantino called Reservoir Dogs (1992). In this film, the people are named Mister White, Mister Pink, Mister Orange… Nico, you are far better than they are since you are dealing with all sorts of pigments. In this sense, but rather because your character has many colourful good aspects, you should be called Mister Multi-color. I had the privilege to work with a nice fellow countryman in the person of J-B. Courage, je suis sur que tout ira bien pour toi. Je souhaite a toute la famille plein de reussite et de bonheur, du fond du coeur. Omayma you gave birth to a very nice baby. He will be, Inch Allah, as successful and happy as you are. Behind a severe beard is hidden a first-rate STM champion in the person of Christoph. Stefan prefers to hide his ambition to illuminate the world with oligo(poly?)thiophene in his lab. You are both forgiven not to do miniemulsion polymerizations, because you are doing well. Without them, I am nothing. “Them” serves here to describe Elvira who makes the IR measurements, and Prof. Walter, Herr Schmidt and Reinhardt of the Electron Microscopy Department. Thanks to Ulrich, I enjoyed a collaboration with the Solid-state Physics department of Ulm. Alfred and Achim are the living proofs that physicians have also interesting things to do and to say. Jürgen and Thomas were the first Swabian PhD specimen I met. They facilitated my introduction to the very specific world of the University of Ulm. Anne did not stay long in our department but we benefited from her experience and kindness. I wish you a nice academic carrier and good continuation in your life! It was a pleasure to know Eiw, a nice little Thai girl from the other side of the world. Even if they did not come from so long distance, it was also a pleasure to meet Dawid and Pietro. It is possible apparently to have the energy of the Yang-tseu-kiang and the fineness of a Chinese carving. Who have doubts as to this never met Yayun (this could be a Chinese proverb). I would like to express my gratitude to Eyk, Christoph, Michael and Daniela for their excellent work during their Kochknecht time. Special thanks to Jacob Horger

who crossed the Atlantic Ocean to make a training period in our little town. My family is a mark, a foyer whose warmth constantly feed my heart. What you gave me is of inestimable value. Love has a name for me. It is adorned under the form of a very cute funny nice person I met more than three years ago. Marianne, I love you and I am sorry for the moments of stress generated by the thesis.

References

Art poétique

...De la musique encore et toujours !
Que ton vers soit la chose envolée
Qu'on sent qui fuit d'une âme en allée
Vers d'autres cieux à d'autres amours.

Que ton vers soit la bonne aventure
Eparse au vent crispé du matin
Qui va fleurant la menthe et le thym...
Et tout le reste est littérature.

Paul Verlaine (1844-1896)
French poet, from Jadis et naguère **1884**.

[**Amo**_2000]
Amore Bonapasta, A.; Buda, F.; Colombet, P. *Chem. Mater.* **2000**, *12*, 738.
[**Ant**_2002]
Antonietti, M.; Landfester K. *Prog. Polym. Sci.* **2002**, *27*, 689.
[**Ant**_2003]
Antonietti, M.; Tauer, K. *Macromol. Chem. Phys.* **2003**, *204*, 207.
[**Ase**]
Aseyev, V. *What is Light Scattering?*
[**Asu**_1998]
Asua, J. M., Schoonbrood, H. A. S. *Acta Polym.* **1998**, *49*, 671.
[**Bar**_2001]
Barrere, M.; Maitre, C.; Dourges, M. A.; Hemery, P. *Macromolecules*, **2001**, *34*, 7276.
[**Bar2**_2001]
Barrere, M.; Ganachaud, F. ; Bendejacq, D.; Dourges, M.-A. ; Maitre, C.; Hemery, P. *Polymer* **2001**, *42*, 7239.
[**Bar**_2003]
Barrere, M.; Landfester, K. *Macromolecules* **2003**, *36*, 5119.
[**Bar2**_2003]
Barrere, M.; Landfester, K. *Polymer* **2003**, *44*, 2833.
[**Bec**_2000]
Bechtold, N.; Landfester, K. *Macromol. Symp.* **2000**, *151*, 549.
[**Bec2**_2000]
Bechtold, N.; Landfester, K. *Macromolecules* **2000**, *33*, 4682.
[**Boi**_2001]
Boisson F, Uzulina I, Guyot A *Macromol. Rap. Commun.* **2001**, *22,* 1135.
[**Bou**_1998]
Bourgeat-Lami, E.; Lang, J. *J. Colloid Interface Sci.* **1998**, *197*, 293.
[**Bou**_1999]
Bourgeat-Lami, E.; Lang, J. *J. Colloid Interface Sci.* **1999**, *210*, 281.
[**Bou**_2005]
Boutti, S.; Bourgeat-Lami, E.; Zydowicz, N. *Macromol. Rap. Commun.* **2005**, *26*, 1860.
[**Bre**_2003]
Breitenkamp, K. Emrick, T. *J. Am. Chem. Soc.* **2003**, *125*, 12070.

[**Bur**_1997]

Burmeister, F. ; Schäfle, C. ; Matthes, T. ; Böhmisch, M.; Boneberg, J.; Leiderer, P. *Langmuir* **1997**, 2983.

[**Cai**_2005]

Caille, J.-R.; Debuigne, A.; Jerome, R. *Macromolecules* **2005**, *38*, 27.

[**Car**_1998]

Caruso, F.; Caruso, R. A.; Mohwald, H. *Science* **1998**, *282*, 1111.

[**Car**_1999]

Caruso, F.; Caruso, R. A.; Mohwald, H. *Chem. Mater.* **1999**, *11*, 3309.

[**Car**_2001]

Caruso, F. *Adv. Mater.* **2001**, *13*, 11.

[**Car2**_2001]

Caruso, F.; Spasova, M.; Salgueirino-Maceira, V.; Liz-marzan, L. M. *Adv. Mater.* **2001**, *13*, 1090

[**Cau**_2002]

Cauvin, S.; Sadoun, A.; Dos Santos, R.; Belleney, J.; Ganachaud, F.; Hemery, P. *Macromolecules* **2002**, *35*, 7919.

[**Cau**_2004]

Cauvin, S.; Ganachaud, F. *Macromol. Symp.* **2004**, *215*, 179.

[**Cau**_2005]

Cauvin, S. ; Ganachaud, F. ; Moreau, M. ; Hemery, P. *Chem. Commun.* **2005**, *21*, 2713.

[**Ces**_1993]

Cesteros L. C.; Isasi J. R.; Katime I. *Macromolecules* **1993**, *26*, 7256.

[**Che**_2005]

Chemtob, A. ; Gilbert, R. G. *Macromolecules* **2005**, *38*, 6796.

[**Cho**_2005]

Cho, S.- H.; Kim, W.-Y.; Jeong, G.-K.; ee, Y.-S. *Colloids and Surfaces A: Physiochemical and Engineering Aspects* **2005**, *255*, 79.

[**Cla**_2001]

Claverie, J. P. ; Viala, S. ; Maurel, V.; Novat, C. *Macromolecules* **2001**, *34*, 382.

[**CME**]

http://www.cmeba.univ-rennes1.fr/niveau2/PagePrincipeMEB.htm

[**Coc**_1997]

Cochin, D.; Laschewsky, A.; Nallet, F. *Macromolecules* **1997**, *30*, 2278.

[**Cos**_1981]

Costa, G.; Nencioni, M.; Russo, S.; Semeghini, G. *Makromol. Chem.* **1981**, *182*, 1399.

[**Cun**_2002]

Cunningham, M. F.; Xie, M.; McAuley, K. B.; Keoshkerian, B.; Georges, M. K. *Macromolecules* **2002**, *35*, 59.

[**Dav**_1963]

Davies, J. T.; Rideal, E. K. *Interfacial phenomena* **1963**, 2nd Ed.; Acad Press, London

[**DeB**_2000]

De Brouwer, H; Monteiro, M. J.; Tsavalas, J. G.; Schork, F. J. *Macromolecules* **2000**, *33*, 9239.

[**Dua**_2001]

Duan, H.; Chen, D.; Jiang, M.; Gan, W.; Li, S.; Wnag, M. Gong, J. *J. Am. Chem. Soc.* **2001**, *123*, 12097.

[**Duf**_2003]

Dufour, M. G.; Guyot, A. *Coll. Polym. Sci.* **281**, 105.

[**ElG**_2004]

El-Gibaly, I.; Anwar, M. *Int. J. Pharm.* **2004**, *278*, 25.

[**Eli**_2001]

Elias, H.-G. In Makromoleküle Band 2, Wiley-VCH, **2001**

$D_{sphere} = 2*(3M/4\pi\rho N_A)^{1/3}$

[**Flem**_2001]

Fleming, M. S.; Mandal, T. K.; Walt, D. R. *Chem. Mater.* **2001**, *13*, 2210.

[**Gan**_2005]

Ganachaud, F.; Katz, J. L. *ChemPhysChem* **2005**, *6*, 209.

[**Goe**_1998]

Goedel, W. A. ; Heger. R. *Langmuir* **1998**, *14*, 3470.

[**Gri**_1954]

Griffin, W. C. *J. Soc. Cosmetic. Chem.* **1954**, *5*, 249.

[**Guy**_1994]

Guyot, A.; Tauer, K. (1994) Polymer synthesis advances in polymer science **1994**, *111*, 43.

[**Guy**_1996]

Guyot, A. *Curr. Opin. Colloid Interface Sci.* **1996**, *1*, 580.

[**Guy**_2003]

Guyot, A.; Graillat, C.; Favero, C. *CR Chim.* **2003**, *6*, 1319.

[**Ham**_2005]
Ham, H. T.; Choi, Y. S.; Jeong, N.; Chung, I. J. *Polymer* **2005**, *46*, 6308.
[**Han**_1989]
Hanabusa, K.; Higashi, J.; Koyama, T.; Shirai, H. *Makromol. Chem.* **1989**, *190*, 1.
[**Hel**_2002]
Held, A. ; Kolb, L. ; Zuideveld, M. A.; Thomann R.; Mecking, S.; Schmid, M.; Pietruschka, R.; Lindner, E. ; Khanfar, M. ; Sunjuk, M. *Macromolecules* **2002**, *35*, 3342.
[**Hor**_2001]
Horn, D.; Rieger, J. *Angew. Chem. Int. Ed.* **2001**, *40*, 4330.
[**ImJ**_2005]
Im, S.; Jeong, U.; Xia, Y. *Nature Materials* **2005**, *4*, 671.
[**ISI**_2005]
According to ISI Web of Science on the 26/10/05, 91.3 % of the documents published in 2005 with miniemulsion in the title, abstract or keywords contained also the word polymerization in the title, abstract or keywords. 89.2 % of documents in an all years search with miniemulsion in the title, abstract or keywords contained also the word polymerization in the title, abstract or keywords.
[**ISI2**_2005]
According to ISI Web of Science on the 26/10/05, 13.6 % of the documents published in 2005 with miniemulsion in the title, abstract or keywords contained also the word encapsulation polymerization in the title, abstract or keywords. 9.3 % of documents in an all years search with miniemulsion in the title, abstract or keywords contained also the word encapsulation in the title, abstract or keywords.
[**Jan**_2004]
Jang, Y.; Choi, D. S.; Kim, J. G. *Langmuir* **2004**, *20*, 6570.
[**Jia**_2001]
Jiang, P. Bertone, J. F.; Colvin, V. L. *Science* **2001**, *191*, 453.
[**Kam**_2003]
Kamata, K.; Lu, Y.; Xia, Y. *J. Am. Chem. Soc.* **2003**, *125*, 2384.
[**Kaw**_2001]
Kawahara, H.; Goto, T.; Ohnishi, K.; Ogura, H.; Kage, H. *J. Appl. Polym. Sci.* **2001**, *91*, 128.
[**Kaw**_2003]
Kawaguchi, A.; Tsurutani, N. *Macromol. Symposia* **2003**, *202*, 77.

[**Kim**_2003]
Kim, N.; Sudol, E. D.; Dimonie, V. L.; El-Aasser, M. S. *Macromolecules* **2003**, *36*, 5573.
[**Kuc**_2005]
Kuchanov, S. I.; Khokhlov, A. R. *Macromolecules* **2005**, *38*, 2937.
[**Lag**_1997]
Lagaly, G.; Schulz, O.; Zimehl, R. *Dispersionen und Emulsionen* **1997**, Steinkopff (Darmstadt).
[**Lan**_1999]
Landfester, K.; Bechtold, N.; Förster, S.; Antonietti, M. *Macromol. Rapid. Commun.* **1999**, *20*, 81.
[**Lan**_2000]
Landfester, K.; Tiarks, F.; Hentze, H.-P.; Antonietti, M. *Macromol. Chem. Phys.* **2000**, *201*, 1.
[**Lan2**_2000]
Landfester, K. *Macromol. Symp.* **2000**, *150*, 171.
[**Lan3**_2000]
Landfester, K.; Willert, M.; Antonietti, M. *Macromolecules* **2000**, *33*, 2370.
[**Lan**_2001]
Landfester, K. *Macromol. Rapid. Commun.* **2001**, *22*, 896.
[**Lan**_2002]
Landfester, K.; Rothe, R.; Antonietti, M. *Macromolecules* **2002**, *35*, 1658.
[**Lan**_2003]
Landfester K (2003) Top Curr Chem 227:75
[**Lan**_2005]
Landfester, K.; Pawelzik, U; Antonietti, M. Polymer, **2005**, *46*, 9892.
[**Lans**_1999]
Lansalot, M.; Farcet, C.; Charleux, B.; Vairon, J.-P.; Pirri, R. *Macromolecules* **1999**, *32*, 7354.
[**Lans**_2000]
Lansalot, M. ; Farcet, C. ; Charleux, B. ; Vairon, J. P. ; Pirri, R. ; Tordo, P. In *Controlled/ Living Radical Polymerization : Progress in ATRP, NMP, and RAFT* ; Matyjaszewski, K. , Ed.; *ACS Symp. Ser.* **2000**, *768*, 138.
[**Les**_2005]
Lestage, D. J. Urban, M. *Langmuir* **2005**, *21*, 4266.

[**Ley**_2003]
Ley, S. V. ; Ramarao, C. ; Lee, A.-L.; Ostergaard, N.; Smith, S. C.; Shirley, I. M. *Org. Lett.* **2003**, *5*, 185.
[**LiC**_2005]
Li, C.- Y.; Chiu, W.- Y.; Don, T.- M. *J. Polym. Sci. Part A : Polym. Chem.* **2005**, *43*, 4870.
[**Lid**_1991]
Lide, D.R. *In Handbook of Chemistry and Physics*, 72nd ed., CRC Press, 1991-1992; p 16.
[**LiM**_2005]
Li, M.; Daniels, E. S.; Dimonie, V.; Sudol, E. D.; El-Aasser, M. S. *Macromolecules* **2005**, *38*, 4183.
[**Lim**_2003]
Limouzin, C.; Caviggia, A.; Ganachaud, F.; Hemery, P. *Macromolecules* **2003**, *36*, 667.
[**Liu**_2002]
Liu, S.; O'Brien, D. F. *J. Am. Chem. Soc.* **2002**, *124*, 6037.
[**Luo**_2004]
Luo, Y. ; Zhou, X. *J. Polym. Sci. Part A : Polym Chem.* **2004**, *42*, 2145.
[**Mai**_2000]
Maitre, C.; Ganachaud, F.; Ferreira, O.; Lutz, J. F.; Paintoux, Y.; Hemery, P. *Macromolecules* **2000**, *33*, 7730.
[**Man**_2000]
Mandal, T. K.; Fleming, M. S.; Walt, D. R. *Chem. Mater.* **2000**, *12*, 3481.
[**Mar**_1999]
Marinakos, S. M.; Novak, J. P.; Bousseau, L.C., III ; House, A. B. ; Edeki, E. M. ; Feldhaus, J. C. ; Feldheim, D. M. *J. Am. Chem. Soc.* **1999**, *121*, 8518.
[**Mar**_2002]
Marie, E.; Landfester, K.; Antonietti, M. *Biomacromolecules* **2002**, *3*, 475.
[**Mar**_2003]
Marie, E.; Rothe, R.; Antonietti, M.; Landfester, K. *Macromolecules* **2003**, *36*, 3967.
[**Mat**_1995]
Matyjaszewski, K.; Gaynor, S. G.; Wang, J. S. *Macromolecules* **1995**, *28*, 2093.
[**Mat**_2000]
Matyjaszewski, K. *Controlled Radical Polymerization*; ACS Symposium Series 768; American Chemical Society: Washington, DC, 2000.

[**McD**_2000]
McDonald, C. J.; Bouck, K. J.; Chaput, A. B.; Stevens, C. J. *Macromolecules* **2000**, *33*, 1593.
[**Mem**_1996]
Memeger, W., Jr.; Campbell, G. C.; Davidson, F. *Macromolecules* **1996**, *29*, 6475.
[**Min**_2005]
Minami, H.; Okubo, M.; Oshima, Y. *Polymer* **2005**, *46*, 1051-1056.
[**Min2**_2005]
Minami, H.; Kobayashi, H.; Okubo, M. *Langmuir* **2005**, *21*, 5655.
[**Moc**_2002]
Mock, J. J.; Barbic, M.; Smith, D. R.; Schultz, D. A.; Schultz, S. *J. Chem. Phys.* **2002**, *116*, 6755.
[**Mon**_2003]
Montenegro, R; Antonietti, M.; Landfester, K. *J. Phys. Chem. B.* **2003**, *107*, 5088.
[**Mor**_2002]
Mori, H.; Seng, D. C.; Zhang, M.; Muller, A. H. *Langmuir* **2002**, *18*, 3682.
[**Odi**_1991]
Odian, G. in *Principles of Polymerization*, 3rd ed., John Wiley and Sons, Inc., 1991.
[**Oku**_1998]
Okubo, M.; Konishi, Y.; Minami, H. *Coll. Pol. Sci.* **1998**, *276*, 638.
[**Oku**_2000]
Okubo, M.; Konishi, Y; Minami, H. *Coll. Pol. Sci.* **2000**, *278*, 659.
[**Ott**_1995]
Ottewill, R. H.; Satgurunathan, R. *Coll. Pol. Sci.* **1995**, *273*, 379.
[**Pai**_2006]
Paiphansiri, U.; Tangboriboonrat, P.; Landfester, K. *Macromol. Bioscience* **2006**, *6,* 33.
[**Pal**_2006]
Palaprat, G.; Ganachaud, F.; Mauzac, M.; Hemery, P. *Polymer*, in press.
[**Par**_2001]
Park, M.; Xia, C.; Advincula, R. C.; Schutz, P.; Caruso, F. *Langmuir* **2001**, *17*, 7670.
[**Pav**_2001]
Pavlyuchenko, V. N.; Sorochinskaya, O. V.; Irvanche, S. S.; Klubin, V. V.; Kreichman, G. S.; Budto, V. P. Skrifvars, M.; Halme, E.; Koskinen, J. *J. Polym. Sci., Part A: Polym. Chem.* **2001**, *39*, 1435.

[**Pea**_2005]

Pears, D. A.; Smith, S. C. *Aldrichimica Acta* **2005**, *38*, 23.

[**Perr**_2001]

Perruchot, C.; Khan, M. A.; Kamitsi, A.; Armes, S. P.; von Werne, T.; Patten, T. E. *Langmuir* **2001**, *17*, 4479.

[**Pic**_2005]

Pich, A.; Datta, S.; Musyanovych, A.; Adler, H. J. P.; Engelbrecht, L. *Polymer* **2005**, *46*, 1323.

[**Que**_2005]

Quemener, D.; Heroguez, V.; Gnanou, Y. *Macromolecules* **2005**, *38*, 7977.

[**Que2**_2005]

Quemener, D.; Chemtob, A.; Heroguez, V. ; Gnanou, Y. Polymer **2005**, *46*, 1067.

[**Raj**_2003]

Rajot, I.; Bone, S.; Graillat, C.; Hamaide, Th. *Macromolecules* **2003**, *35*, 7484.

[**Ran**_2003]

Ranu, B. C.; Samanta, S. *JOC* **2003**, *68*, 7130.

[**Ric**_1999]

Ricco, L.; Russo, S.; Orefice, G.; Riva, F. *Macromolecules* **1999**, *32*, 7726.

[**Ric**_2002]

Ricco, L.; Monticelli, O.; Russo, S.; Paglianti, A.; Mariani, A. *Macromol. Chem. Phys.* **2002**, *203*, 1436.

[**Rus**_1986]

Ruska, E. The Development of the Electron Microscope and of Electron Microscopy, *Nobel Lecture*, **1986**.

[**Sar**_2005]

Sarkar, A. ; Kapoor, S. ; Mukherjee, T. *J. Phys. Chem. B.* **2005**, *109*, 7698.

[**Sch**_1997]

Schoonbrood, H. A. S.; Asua, J. M. *Macromolecules* **1997**, *30*, 6034.

[**Sch**_2005]

Schreiber, E. *Diplom Thesis*, Universität Ulm, **2005**.

[**Sco**_2005]

Scott, C.; Wu, D.; Ho, C.-C.; Co, C. C. *J. Am. Chem.. Soc.* **2005**, *127*, 4160.

[**SCO**_2005]
The plot of the logarithm base 10 of the cumulative number of documents with miniemulsion in the title, abstract or keywords found with SCOPUS between the 01/01/1986 and the 27/10/2005 could be linearized with a correlation factor of 0.98.
[**Seb**_1976]
Sebenda, J. In *Comprehensive Chemical Kinetics* Bamford C. H.; Tipper C. F., Eds.; Elsevier: Amsterdam, **1976**; *Vol. XV*, Chapter 6.
[**Sel**_1999]
Selvan, S. T.; Haykawa, T.; Nogami, N.; Möller, M. *J. Phys. Chem. B* **1999**, *103*, 7441.
[**Sou**_2002]
Soula, R.; Saillard, B.; Spitz, R.; Claverie, J.; Llaurro, M. F. ; Monnet, C. *Macromolecules* **2002**, *35*, 1513.
[**Sun**_2002]
Sun, Y.; Xia, Y. *Science* **2002**, *298*, 2176.
[**Sun2**_2002]
Sun, Y.; Yin, Y. ; Mayers, B. T.; Herricks, T.; Xia, Y. *Chem. Mater.* **2002**, *14*, 4736.
[**Tad**_2003]
Taden, A.; Antonietti, M.; Landfester, K. *Macromol. Rap. Commun.* **2003**, *24*, 512.
[**Tai**_2006]
Taira, S.; Du, Y.-Z. ; Kodaka, M. *Biotechnology and Bioengineering* **2005**, in press.
[**Tak**_2005]
Takasu, M.; Kawaguchi, H. *Coll. Polym. Sci.* **2005**, *283*, 805.
[**Tia**_2001]
Tiarks, F.; Landfester, K.; Antonietti, M. *J. Polym. Sci. Part A: Polym. Chem.* **2001**, *39*, 2520.
[**Tia2**_2001]
Tiarks, F.; Landfester, K.; Antonietti, M. *Langmuir* **2001**, *17*, 5775.
[**Tia3**_2001]
Tiarks, F.; Landfester, K.; Antonietti, M. *Langmuir* **2001**, *17*, 908.
[**Toj**_1997]
Tojo, C.; Blanco, M. C.; Rivadulla, F.; Lopez-Quintela, M. A. *Langmuir* **1997**, *13*, 1970.
[**Tom**_2000]
Tomov, A.; Broyer, J.-P.; Spitz, R. *Macromol. Symp.* **2000**, *150*, 53.
[**Tor**_2005]
Torini, L.; Argillier, J. F.; Zydowicz, N. *Macromolecules* **2005**, *38*, 3225.

[**Tou**_2004]

Touchard, V.; Graillat, C.; Boisson, C.; D'Agosto, F.; Spitz, R. *Macromolecules* **2004**, *37*, 3136.

[**Uge**_1973]

Ugelstad, J. *Polymer Letters Edition* **1973**, *11*, 503.

[**UNL**]

http://www.unl.edu/CMRAcfem/semoptic.htm

[**USP**_BASF]

US patent 6,117,939 BASF.

[Voi_2000]

Voit, B. *Angewandte Chemie* **2000**, *112*, 3549.

[**Von**_2001]

Von Werne, T.; Patten, T. E. *J. Am. Chem. Soc.* **2001**, *123*, 7497.

[**Wil**_2002]

Willert, M; Landfester, K. *Macromol. Chem. Phys.* **2002**, *203*, 825.

[**Won**_2002]

Wong, M. S.; Cha, J. N.; Choi, K.; Deming, T. J.; Stucky, D. *Nano Lett.* **2002**, *2*, 583.

[**WuX**_2000]

Wu, X. Q.; Schork, F. J. *Ind. Eng. Chem. Res.* **2000**, *39*, 2855.

[**XuX**_2004]

Xu, X.; Asher, S. A. *J. Am. Chem. Soc.* **2004**, *126*, 7940.

[**Yan**_2005]

Yang, M.; Wang, W.; Yuan, F.; Zhang, X.; Liang, F.; He, B.; Minch, B.; Wegner, G. *J. Am. Chem. Soc.* **2005**, *127*, 15107.

[**Zha**_2002]

Zha, L.; Zhang, Y.; Yang, W.; Fu, S. *Adv. Mater.* **2002**, *14*, 1090.

[**Zha**_2003]

Zhang, K.; Chen, H.; Chen, X.; Chen, Z.; Chen, Z.; Cui, Z.; Yang, B. *Macromol. Mater. Eng.* **2003**, *288*, 380.

[**Zho**_2002]

Zhou, Q. Y.; Wang, S. X.; Fan, X. W.; Advincula, R. C. *Langmuir* **2002**, *18*, 3324.

[**Zho**_2005]

Zhou, H.; Jiang, J.; Zhang, K. *J. Polym. Sci. Part A: Polym Chem.* **2005**, *43*, 2567.

Zusammenfassung und Ausblick

Im Rahmen dieser Doktorarbeit wurden neuartige Wege zur Polymerisation in Miniemulsion beschrieben. Diese Arbeit betrifft zwei wichtige Aspekte der Miniemulsionspolymerisation: erstens die Entwicklung von neuen, bisher nicht in Heterophasen durchgeführte Polymerisationsprozessen und zweitens die Synthese von neuen hochwertigen Materialien.

Diese neuen Prozesse besitzen im Vergleich zu den bisher entwickelten Prozessen mehrere Vorteile. Sie ermöglichen nicht nur eine Kosteneinsparung während der Produktion, sondern auch die Synthese neuer Materialien. Außerdem kann aufgrund der Verwendung von Wasser als Dispersionsmittel der Einsatz solcher Materialien in der Industrie zu einem gesteigerten Umweltbewusstsein beitragen. Der zweite Aspekt dieser Arbeit trifft die Materialien selbst. Wenn ein Material interessante, wie z.B. magnetische, thermo-sensitive, licht-emittierende Eigenschaften besitzt, wird sein Wert erhöht. Das gleiche gilt, wenn dieses Material spezielle Verwendungsmöglichkeiten, wie z.B. die Verkapselung einer hydrophilen Substanz bietet. Diese Vorteile wurden durch Regulierung den Dispersionseigenschaften, welche direkt vom Polymer und von der Morphologie des Kolloids abhängen, erreicht.

Es wurden im Rahmen der Arbeit verschiedene Miniemulsionspolymerisationen wie radikalische, anionische Polymerisationen oder Polykondensationen durchgeführt, um verschiedene Funktionalitäten von Nanopartikeln zu erreichen.

Im ersten Teil der Arbeit wurden zunächst verschiedene radikalische Polymerisationen von Styrol und dem Vernetzer Divinylbenzol in wässriger Miniemulsion durchgeführt. Neben den Monomeren wurden in der dispergierten Phase Oktan oder Toluol eingesetzt. Das Verhältnis von Monomer zu dem hydrophoben Lösungsmittel steuerte die Morphologie der Partikel. Mit Erfolg wurden so Kapseln in einer Oktan-enthaltenden dispergierte Phase synthetisiert. Die Rauheit der Partikeloberfläche wurde anhand der eingesetzten Menge an Vernetzter kontrolliert.

Des weiteren wurden Polymer/Metall-Hybridlatexpartikel in direkter wässriger Miniemulsion hergestellt und untersucht. Hydrophobe Platin-Komplexe wurden dazu in Polystyrol-Partikeln verkapselt. Aufgrund ihrer Monodispersität konnten die Partikel hochgeordnet auf Siliziumsubstraten angeordnet werden. Im Rahmen einer Zusammenarbeit mit der Festkörperphysik-Abteilung der Universität Ulm konnten durch Plasma-Ätzen geordnete Metall-Cluster auf einer Silizium-Oberfläche erhalten werden.

Es wurde im Rahmen dieser Arbeit auch gezeigt, dass Änderungen in der Zusammensetzung der dispergierten Phase der Miniemulsions-Polymerisation zu neuen interessanten Materialien führt. Im dritten Teil der Arbeit konnte gezeigt werden, dass Variationen des Initiators zu interessanten Materialien führen. Verschiedene Borohydrid-Salzen wurden als unkonventionelle Initiatoren zur Miniemulsionspolymerisation von Styrol genutzt. Mit Iodomethan als Regler für Übertragungsreaktionen wurden hochmolekulare Polymere in sehr guter Ausbeute synthetisiert.

Im vierten Teil der Arbeit wurde Styrol und Divinylbenzol mit einem polymerisierbaren Tensid copolymerisiert. Stabile Polystyrol- und Poly(styrol-*co*-butylacrylat)-Partikeln sowie Polydivinylbenzol-Kapseln konnten mit dem polymerisierbaren Tensid in der Miniemulsion synthetisiert werden. Mit Hilfe von XPS-Messungen wurde gezeigt, dass das polymerisierbare Tensid auf der Oberfläche des Latex effektiv gepfropft war.

Im fünften Teil der Arbeit wurde die Stabilität inverser Miniemulsionen gegenüber hohen Temperatur untersucht. Versuche bei Temperaturen höher als 150 °C haben gezeigt, dass Miniemulsionen im Regelfall aufgrund von Koaleszenz-Phänomen mit der Zeit unstabil sind. Es wurde daher versucht, Polyvinylpyrrolidon (PVP) als zusätzlichen Stabilisator einzuführen. So konnten inverse Miniemulsionen, die eine DMSO- oder 2-Pyrrolidon-enthaltende dispergierte Phasen besitzen, bei hohen Temperaturen für mehr als zehn Stunden effektiv stabilisiert werden. Bei Temperaturen unterhalb von 170 °C war das lipophobe K_2CO_3 ein osmotischer Stabilisator für Miniemulsionen mit 1-Vinyl-2-pyrrolidon als disperse Phase besonders gut geeignet. Diese Miniemulsionen waren erst bei Temperaturen höher als 170 °C unstabil. Diese bei hohen Temperaturen entwickelte Miniemulsion wurde für zwei verschiedene Anwendungen benutzt, um die Einsatzflexibilität der Methode zu zeigen. So wurden die freie radikalische Polymerisation von 1-Vinyl-2-pyrrolidinon sowie die Reduzierung von Silbernitrat durch Ethylenglycol in den Miniemulsionströpfen durchgeführt. Eine Kombination beider Reaktionen ermöglichte die Synthese hybrider Polymer/Metall-Nanopartikel. Diese Ergebnisse zeigen, dass die Miniemulsionstechnik auch im hohen Temperaturbereich seine Anwendung findet und dass neue Nanomaterialien in Miniemulsionströpfen synthetisieren werden können.

Im sechsten Teil wurde zum ersten Mal gezeigt, dass Polymer-Nanokapseln mit einem hydrophilen Kern mittels der Polymerisation in inverser Miniemulsion synthetisiert werden konnten. Hierzu wurde zunächst N-N´-Dimethylacrylamid in wässriger Phase gelöst. Während die Polymerisation kommt es aufgrund der Phasenseparation zur Bildung von Nanokapseln mit einer Polymerhülle um die wässrigen Tröpfchen.

Declaration of originality

This thesis is my original work and has not been presented for a degree in any other University.